ON THE DYNAMIC CHARACTERISTICS OF BEAMS, PLATES AND SHELLS

A THESIS

Presented to

The Faculty of the Division of Graduate Studies and Research

by

Esam Eldin Nassar

In Partial Fulfillment

of the Requirements for the Degree

Doctor of Philosophy

in the School of Aerospace Engineering

Georgia Institute of Technology

August 1973

ON THE DYNAMIC CHARACTERISTICS

OF BEAMS, PLATES AND SHELLS

Approved:

Chairman

Date Approved by Chairman: 6 Aug 73

ACKNOWLEDGMENTS

My thanks and appreciation are due to my advisor Professor Wilfred H. Horton. Throughout this work his guidance and advice were invaluable. His generous attention and continuous support are greatly appreciated.

I am thankful to Professor M. Stallybrass for his assistance in eliminating several errors and obscurities from this thesis. My appreciation is also due to Professor J. Craig for his helpful hints on instrumentation. My friend and colleague Mr. Mahender K. Singhal generously offered some of his cylindrical shell specimens for my experimentation. His offer is certainly appreciated.

This work was sponsored by various grants from the National Aeronautics and Space Administration to whom my thanks are due.

I am grateful to Mr. K. Elshishini and Mr. A. Heiba at Helwan Aircraft Factories for their early encouragement and support to start my graduate study at Georgia Tech.

Finally to my wife Hanem and my son Ayman I present this work. Their patience and understanding provided the right environment for the completion of a successful study.

TABLE OF CONTENTS

LIST OF TABLES

LIST OF ILLUSTRATIONS

Figure | Page

NOMENCLATURE

A	coefficient of deflection term given in Equation (B-12), also, means acceleration in Chapter III.
a	length of a rectangular plate
a_1, a_2, a_3 and a_4	coefficients in rational function expressions
B	coefficient of deflection term; Equation (B-12)
b	width of rectangular plate
b_1, b_2, b_3 and b_4	coefficients in rational function expressions
C	coefficient of deflection term; Equation (B-12)
$\bar{D}$	plate bending stiffness: $\bar{D} = Eh^3/12(1 - \nu^2)$
D	coefficient of deflection term; Equation (B-12)
E	modulus of elasticity, also coefficient of deflection term; Equation (B-13)
F	coefficient of deflection term given in Equation (B-13), also, denotes excitation force in Chapter III.
F_1 and F_2	quantities given by Equations (B-10) and (B-11)
f	excitation frequency
G	coefficient of deflection term; Equation (B-13)
g	gravitational acceleration
H	coefficient of deflection term; Equation (B-13)
h	plate thickness
I	moment of inertia
I_i	integrals in Appendices C and D; i = 1,2, ...

J_i	integrals in Appendices C and D, i = 1,2, ...
K	linear spring constant
k	torsional spring constant
L	beam length
LVDT	linear variable differential transformer; a displacement transducer
M_D	dynamic mass; ratio of the excitation force to the resulting acceleration (= F/A)
$\bar{m}$	mass per unit length of a beam or mass per unit area of a plate
m and n	number of vibrational modes
P and P_{cr}	axial load and its critical value
Q, Q_1 and Q_2	dummy variables used in Appendices C and D
q	intensity of uniform lateral loading on a beam
q_1 and q_2	quantities defined in Equation (1-26)
R	aspect ratio of a rectangular plate; equals b/a; $0 \leq R \leq 1$
T	kinetic energy of the vibrating plate
U	strain energy of the plate and the associated rotational springs
$U_1, U_2, \ldots, U_9$	energy terms used in Appendices C and D
W	beam or plate deflection function
$W_{0\,0}, W_{\infty\,\infty}, W_{\infty\,0}$ & $W_{0\,\infty}$	beam deflection functions corresponding to combinations of extreme rotational restraint conditions
$W_{ijk\ell}$	where i,j,k and ℓ can take either 0 or ∞. The deflection function of a plate whose edges are subjected to rotational restraints of parameters i,j,k and ℓ

X	nondimentional coordinate axis, $X = x/L$
x, y and z	coordinate axes system
β	nondimensional rotational restraint parameter. For a beam $\beta = kL/EI$. For a plate $\beta = ka/\bar{D}$ on x = constant sides and $\beta = kb/\bar{D}$ on y = constant sides
$\beta_1, \beta_2, \beta_3$ and β_4	rotational restraint parameters at the ends of a beam or restraint parameters per unit length at the edges of a plate.
γ	linear restraint parameter; $\gamma = KL^3/EI$
δ	function given by Equation (2-17). Also lateral deflection of the plate given in Table 22.
ϵ	expression defined in Equation (1-15). Also the bending strain given in Table 20.
θ	cylindrical coordinate used in Chapter III.
λ_m	beam frequency parameter defined in Equation (2-6)
$\mu_{n,12}$	the n^{th} eigenvalue for a vibrating beam subjected to rotational restraints β_1 and β_2; $\mu^2_{n,12} = \omega_{n,12} = \omega^*_{n,12}\sqrt{\bar{m}L^4/EI}$
$\bar{\mu}_1$, $\bar{\mu}_2$ and $\bar{\mu}_3$	the frequency parameters of beams with ends hinged-hinged, clamped-clamped and hinged-clamped, given in Equation (1-26)
$\varphi(R)$	function of R defined by Equation (2-18)
ψ_1 and ψ_2	are deflection functions for the plate, used in the discussion of Chapter II only.

ω_n nondimensional n^{th} frequency parameter

$$\omega_n = \mu_n^2 = \omega_n^* \sqrt{\bar{m}L^4/EI} \quad \text{for beams,}$$

$$\omega_n = \omega_n^* \sqrt{\bar{m}b^4/\bar{D}} \quad \text{for plates}$$

ω_n^* the n^{th} natural frequency of vibration of a beam or a plate

ω_{1234} fundamental frequency parameter for a plate subjected to rotational restraint parameters β_1, β_2, β_3 and β_4 on the sides $x = -a/2$, $x = a/2$, $y = -b/4$ and $y = b/2$ respectively, (see Figure 2)

SUMMARY

The work discussed in this thesis lays the foundations for correlating the vibrational, flexing and buckling characteristics of elastically restrained column and plate structures. It demonstrates that potentially powerful methods for non-destructive evaluation of critical axial loads based upon vibrational characteristics are feasible.

In Chapter I extensive use is made of a rational function technique to develop simple approximate expressions for both the natural frequencies and mode shapes of uniform elastically restrained beams. These developments are of importance both to the practising engineer and to the further research. For the former they provide high accuracy simple and readily usable general formulae. Their significance in the research aspect arises from the fact that the technique enables variable separation to be used. Thus the vibrational characteristics of plates become more tractable. This subject is dealt with in depth in Chapter II. Using a simplified energy solution the vibration of rectangular plates with unequal elastic rotational restraint on the several edges is treated. A simple explicit-relationship is developed. From this relationship numerical results are readily obtained and such results have been used in conjunction with the rational function approach to devise extremely simple general relationships for plates. These relationships are as directly applicable by practising engineers as those derived for columns.

No direct correlation between the flexing and vibration characteristics has either been found or sought. However, in Appendix A a general expression for beam displacement in terms of restraint parameters and behavior under "idealized" conditions is generated. This work gives clear broad implications with regards to non-destructive testing.

The subject of non-destructive testing of columns, plates, and shells is dealt with in Chapter III. Here it is shown that the dynamic mass variation in a compressed structure can effectively be used to determine, non-destructively, the critical load level for the structure. The accuracy with which this can be accomplished is high.

CHAPTER I

APPROXIMATE FORMULAE FOR THE VIBRATIONAL CHARACTERISTICS OF BEAMS WHOSE ENDS ARE SUBJECTED TO ELASTIC RESTRAINTS

Introduction

The analytical determination of the critical frequencies of elastically restrained beams is an eigenvalue problem and the method of solution is well known and straightforward. The characteristic equations which define the various natural frequencies can be established readily. These equations, being transcendental, do not admit a closed form solution. However, graphical and/or numerical methods can be used to determine the roots but, frequently, great amounts of labour are involved.

Standard engineering handbooks, e.g. [1], list natural frequencies only for beams with "extreme" boundary restraints, i.e., boundaries which are either simply supported or clamped. However, for realistic structures, the end conditions are not generally so simple and some degree of elastic restraint always exists. Few attempts have been made to formulate simple solutions when these practical conditions exist. Newmark [2] presented an approximate solution for the case of a beam whose ends were rigidly supported against lateral displacement and elastically restrained against rotation. The formula, which he

derived by numerical calculations from the exact solution*, is accurate to within 4%.

Currently, the specific case referenced is the only one for which a simple formula exists. Thus, in general, for elastically restrained beams solving the transcendental equations is inevitable. Such process has little appeal to the design engineer since it is both lengthly and laborious.

There is no doubt that for practical applications, a simple formula, accurate within engineering limits, is preferable to a tedious rigorous analysis which yields only slightly different answers. Similarly, from an analyst's viewpoint a good approximate solution to a problem often leads the way to deal with the more complex situations. This is particularly true when the approximation process brings concurrent mathematical and conceptual simplicities. These, then, are the fundamental issues which create the need to develop simple approximate solutions.

In the remainder of this chapter a general process for dealing with the vibrational characteristics of elastically restrained beams will be presented. The technique will be applied to a number of specific cases as delinated in Figures 1 (a), (b) and (c). The first case will be treated in detail and the results for the other two will be given in a concise form.

---

* The term "exact" is used to describe the eigenvalues obtained from the characteristic equation by an accurate numerical scheme.

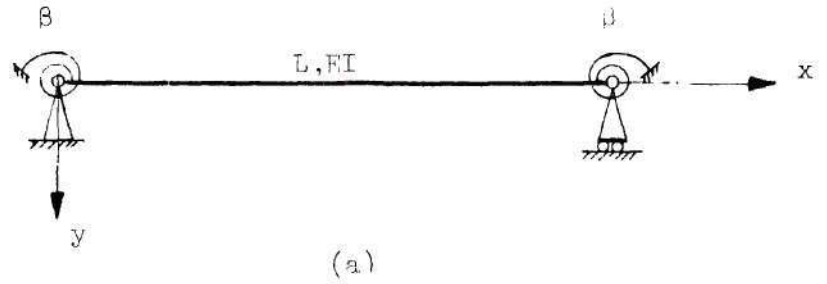

(a)

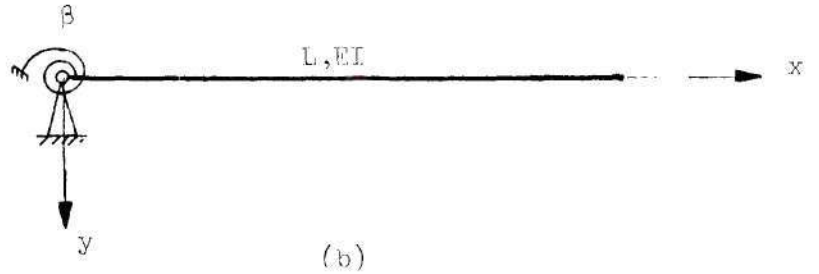

(b)

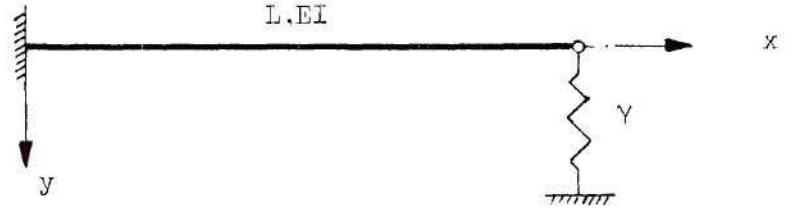

(c)

Figure 1. Beams with Elastic End Restraints.

Method of Solution

The method used in the following work is based on rational functions [3], [4]. Briefly the technique is to represent the frequency parameter as the ratio of two polynomials in the end restraint parameters. For the simplest approximation these polynomials are taken to be of the first degree and in these circumstances the frequency relationship can be expressed as

$$\omega = \frac{a_1\beta + a_2}{b_1\beta + b_2} \tag{1-1}$$

The coefficients a_1, a_2, b_1 and b_2 are then evaluated by forcing this function to match the exact numerical values under a number of conditions. In general, higher approximations can be obtained by considering second order polynomials in the form

$$\omega = \frac{a_1\beta^2 + a_2\beta + a_3}{b_1\beta^2 + b_2\beta + b_3} \tag{1-2}$$

Although the above form of the rational function gives the most direct and convenient expression for the purpose of computation, other non-direct expressions can also be developed. The choice is governed by the purpose for which the approximation is desired. Another useful expression will be developed in the following exponential form

$$\omega = e^{\left(\frac{a_1\beta+a_2}{b_1\beta+b_2}\right)} \tag{1-3}$$

where, as before, the a's and b's are coefficients to be evaluated. This form is particularly of value when formulating relationships between buckling and vibration [5].

Beams with Ends Laterally Supported and Elastically Restrained Against Rotation

Approximate Formulae for the Vibrational Frequencies

We shall begin this section by considering the symmetric case of Figure 1(a). The solution will be taken in the form of Equation (1-2). For simplicity the polynomials will be assumed as complete quadratics in the parameter β thus

$$\omega = \mu^2 = \left(\frac{a_1\beta+a_2}{b_1\beta+b_2}\right)^2$$

For the fundamental frequency compliance with the numerical solution will be forced for three values of end fixity. These will be taken to be at

$$\beta = 0 \quad ; \quad \mu = \pi$$

$$\beta = \infty \quad ; \quad \mu = 4.73 \simeq \frac{3\pi}{2}$$

$$\beta = 5.72^{*} \quad ; \quad \mu = 1.25\pi$$

---

* The question of the choice of the third condition is discussed at the end of this chapter.

Thus, the coefficients are determined and the formula can be written as

$$\mu = \pi \left(\frac{9\beta + 10\pi}{6\beta + 10\pi}\right) \tag{1-4}$$

The error in the frequency given by this formula is shown in Table 1 from which it can be seen that the maximum error is less than 1%.

If we consider the exponential form:

$$\omega = e^{\left(\frac{a_1\beta + a_2}{b_1\beta + b_2}\right)}$$

and force the expression to satisfy the exact frequency at $\beta = 0$, 3* and ∞ (where the frequency parameters are π, 3.71, 4.73 respectively), we obtain

$$\omega = \mu^2 = \pi^2 \, e^{\left(\frac{9\beta}{11\beta + 49}\right)} \tag{1-5}$$

and the error is shown in Table 2.

Higher frequencies can also be obtained in a rational function form. For example, it can be shown that the second and the third frequencies can be expressed in the following forms.

$$\mu_2 = \pi \left(\frac{2.5\beta + 19.65}{\beta + 9.85}\right) \tag{1-6}$$

Table 1. Accuracy of $\omega = \mu^2 = \pi^2\left\{\frac{9\beta + 10\pi}{6\beta + 10\pi}\right\}^2$

β	ω exact	$\pi^2\left(\frac{9\beta+10\pi}{6\beta+10\pi}\right)^2$	% Error
0	9.86959	9.86050	0.000
.1	10.0656	10.0554	-0.102
.2	10.2545	10.2361	-0.180
.5	10.7818	10.7487	-0.307
1	11.5518	11.5157	-0.312
2	12.7937	12.786	-0.060
5	15.1894	15.2794	0.592
10	17.2695	17.4103	0.816
100	21.5418	21.4761	-0.305
1000	22.2844	22.1295	-0.695
100000	22.3643	22.1988	-0.74
	Maximum % Error		
∞	22.3733	22.2066	-0.745
9.7	17.1797	17.32	+0.816

Table 2. Accuracy of $\omega = \mu^2 = \pi^2 e^{\left[\frac{9\beta}{11\beta + 49}\right]}$

β	ω_{exact}	$\pi^2 e^{\left[\frac{9\beta}{11\beta + 49}\right]}$	% Error
0	π^2	π^2	0
.1	10.0656	10.0485	-0.17
.5	10.7817	10.7191	-0.58
1	11.5518	11.4668	-0.73
3	13.7618	13.7183	-0.32
5	15.1893	15.2130	0.16
10	17.2694	17.3831	0.66
100	21.5418	21.6012	0.28
1000	22.2842	22.2872	0.01
10000	22.372	22.2674	-0.02

Maximum % Error is: -0.75 at $\beta = 1.2$ and
0.77 at $\beta = 15$

and

$$\mu_3 = \pi \left(\frac{3.5\beta + 43.9}{\beta + 34.35} \right) \tag{1-7}$$

It is interesting to note that Equations (1-4), (1-6) and (1-7) can be rewritten as follows

$$\mu_1 \simeq \pi \left(1 + \frac{\beta}{2\beta + \pi^2} \right) \tag{1-8}$$

$$\mu_2 \simeq \pi \left(2 + \frac{\beta}{2\beta + 2\pi^2} \right) \tag{1-9}$$

$$\mu_3 \simeq \pi \left(3 + \frac{\beta}{2\beta + 3\pi^2} \right) \tag{1-10}$$

which suggests that one may write

$$\mu_n \simeq \pi \left(n + \frac{\beta}{2\beta + n\pi^2} \right) \tag{1-11}$$

and the accuracy of this expression is shown in Table 3 for $n = 1,2,3$. It is also to be noted that this expression strongly resembles that which Newmark obtained by different analysis [2].

If we consider the nonsymmetric case we should anticipate that Equation (1-2) would be modified by the presence of two restraint parameters and would show no bias with respect to either. Therefore, we may write

Table 3. Percentage Error in $\omega_n = \mu_n^2 = \pi^2 \left(n + \frac{\beta}{2\beta + \pi^2 n}\right)$

β	n		
	1	2	3
0	0	0	-0.0002
.1	-0.0157	-0.0059	-0.0027
.5	0.0506	-0.0249	-0.0152
1	0.2703	-0.0395	-0.314
3	1.1326	-0.0442	-0.0967
5	1.5267	-0.0268	-0.154
10	1.6011	-0.0095	-0.250
100	-0.1604	-0.0233	-0.195
1000	-0.6784	-0.0197	-0.028
10000	-0.7379	-0.0195	-0.0034
	Maximum % Error		
	+ 1.73 at 7.5 - 0.75 at ∞	+ 0.04 at 25 - 0.044 at 3	-0.34 at 30

$$\omega_{12} = \mu_{12}^2 = \frac{a_1\beta_1\beta_2 + a_2(\beta_1 + \beta_2) + a_3}{b_1\beta_1\beta_2 + b_2(\beta_1 + \beta_2) + b_3} \qquad (1\text{-}12)$$

which reduces to the form of Equation (1-2) when $\beta_1 = \beta_2 = \beta$.

To evaluate the coefficients we shall force the expression to satisfy the following five conditions.

$$\beta_1 = \beta_2 = 0 \quad ; \quad \mu = \pi$$

$$\beta_1 = \beta_2 = \infty \quad ; \quad \mu = 4.73$$

$$\beta_1 = 0 \,, \quad \beta_2 = \infty \quad ; \quad \mu = 3.927$$

$$\beta_1 = 0 \,, \quad \beta_2 = 1 \quad ; \quad \mu = 3.2733$$

$$\beta_1 = 1 \,, \quad \beta_2 = 2 \quad ; \quad \mu = 3.5768$$

Hence we obtain the formula

$$\mu_{12}^2 = \pi^2 + \frac{12.5\,\beta_1\beta_2 + 36.7(\beta_1 + \beta_2)}{\beta_1\beta_2 + 6.6(\beta_1 + \beta_2) + 36.9} \qquad (1\text{-}13)$$

which is accurate to within 0.15% as shown in Table 4.

It is worthwhile to note that by further algebraic manipulation Equation (1-13) may be reduced to

$$\mu_{12}^2 = \pi^2 \left[\frac{(1.505\,\beta_1 + 6.07)(1.505\,\beta_2 + 6.07) + 1.2(\beta_1 + \beta_2)}{(\beta_1 + 6.07)(\beta_2 + 6.07) + .53(\beta_1 + \beta_2)}\right]$$

Table 4. Accuracy of $\omega_{12} = \mu_{12}^2 = \pi^2 - \dfrac{12.5\,\beta_1\beta_2 + 36.7(\beta_1+\beta_2)}{\beta_1\beta_2 + 6.6(\beta_1+\beta_2) + 36.9}$

Error %

β_1 \ β_2	0	.1	.5	1	3	5	10	100	1000	10000
0	0	.002	.012	.009	-.02	-.04	-.05	-.07	-.08	-.08
.1		.007	.015	.011	-.02	-.04	-.04	-.06	-.07	-.07
.5			.017	.014	-.01	-.02	-.03	-.05	-.06	-.06
1				.010	-.01	-.01	-.01	-.03	-.04	-.04
3					.007	.020	.044	.029	.010	.008
5						.046	.080	.067	.045	.043
10							.125	.114	.087	.084
100								.090	.059	.055
1000		Max. error $\simeq$ 0.15 %							.024	.021
10000		at $(\beta_1,\beta_2) = (20, 50)$								.017

thus,

$$\mu_{12}^2 = \pi^2 \frac{\left(1.505\ \beta_1 + 6.07\right)\left(1.505\ \beta_2 + 6.07\right)}{\left(\beta_1 + 6.07\right)\left(\beta_2 + 6.07\right)} \times \tag{1-14}$$

$$\left\{ \frac{1 + \dfrac{1.2\left(\beta_1 + \beta_2\right)}{\left(1.505\ \beta_1 + 6.07\right)\left(1.505\ \beta_2 + 6.07\right)}}{1 + \dfrac{.53\left(\beta_1 + \beta_2\right)}{\left(\beta_1 + 6.07\right)\left(\beta_2 + 6.07\right)}} \right\}$$

For all values of β_1 and β_2 in the ranges $0 \le \beta_1 \le \infty$ and $0 \le \beta_2 \le \infty$, the quantities between the square brackets are small compared to unity. Therefore by use of the binomial theorem, the quantity in the brace bracket can be approximated as follows

$$\left\{\ \right\} \simeq 1 + \frac{1.2\left(\beta_1 + \beta_2\right)}{\left(1.505\ \beta_1 + 6.07\right)\left(1.505\ \beta_2 + 6.07\right)} \tag{1-15}$$

$$- \frac{.53\left(\beta_1 + \beta_2\right)}{\left(\beta_1 + 6.07\right)\left(\beta_2 + 6.07\right)} = 1 + \varepsilon$$

where

$$\varepsilon < \frac{\left(\beta_1 + \beta_2\right)\left(1.2 - .53\right)}{\left(1.505\ \beta_1 + 6.07\right)\left(1.505\ \beta_2 + 6.07\right)}$$

i.e.,

$$\epsilon < \frac{.67\left(\beta_1 + \beta_2\right)}{2.26\ \beta_1\beta_2 + 9.1\left(\beta_1 + \beta_2\right) + 36.8}$$

hence

$$\frac{1}{\epsilon} > 13.6 + \frac{2.26\ \beta_1\beta_2}{.67\left(\beta_1 + \beta_2\right)} + \frac{36.8}{.67\left(\beta_1 + \beta_2\right)}$$

Since the second and third terms are always positive,

$$\frac{1}{\epsilon} > 13.6$$

i.e.,

$$\epsilon < \frac{1}{13.6}\ \left(= .0735\right)$$

Thus, as a first approximation ϵ may be neglected compared to unity and hence Equation (1-14) reduces to

$$\omega_{12} = \mu_{12}^2 \simeq \pi^2\ \frac{\left(1.505\ \beta_1 + 6.07\right)\left(1.505\ \beta_2 + 6.07\right)}{\left(\beta_1 + 6.07\right)\left(\beta_2 + 6.07\right)} \qquad (1\text{-}16)$$

The accuracy of this formula as determined by numerical calculation and comparison is within 4% as shown in Table 5.

It is clear from the above expression that the critical frequency for a beam with end restraint parameters β_1 and β_2 is very nearly the geometric mean of the frequencies of the two symmetric beams with restraint parameters β_1 and β_2 respectively, i.e.,

Table 5. Accuracy of $\omega_{12} = \mu_{12}^2 = \pi^2 \left(\frac{1.505\ \beta_1 + 6.07}{\beta_1 + 6.07}\right)\left(\frac{1.505\ \beta_2 + 6.07}{\beta_2 + 6.07}\right)$

	Error %									
	β_2									
β_1	0	.1	.5	1	3	5	10	100	1000	10000
0	0	-0.17	-0.76	-1.30	-2.46	-2.35	-3.41	-3.68	-3.66	-3.66
.1		-0.34	-0.88	-1.39	-2.46	-2.92	-3.33	-3.55	-3.53	-3.52
.5			-1.29	-1.67	-2.45	-2.77	-3.05	-3.10	-3.05	-3.05
1				-1.92	-2.43	-2.63	-2.76	-2.65	-2.59	-2.58
3					-2.32	-2.23	-2.06	-1.62	-1.52	-1.51
5						-2.00	-1.70	-1.13	-1.03	-1.02
10							-1.29	-0.65	-0.55	-0.54
100								-0.17	-0.12	-0.12
1000									-0.09	-0.08
10000										-0.08

$$\omega_{12} = \mu_{12}^2 \simeq \mu_{11}\,\mu_{22} \tag{1-17}$$

This relation can also be verified if we use the expression for μ_{11} (and μ_{22}) as that given by Equation (1-4), thus

$$\omega_{12} = \mu_{12}^2 = \pi^2 \left(\frac{9\beta_1 + 10\pi}{6\beta_1 + 10\pi}\right)\left(\frac{9\beta_2 + 10\pi}{6\beta_2 + 10\pi}\right) \tag{1-18}$$

The error in this formula is, again, not more than 4% as shown in Table 6.

It is interesting to note that, although the constant terms in Equations (1-16) and (1-18) are different (being 36.4 and 27.5 respectively) the accuracy of both formulae is almost equal. This suggests that a further simplification might be considered, namely

$$\mu = \pi \left(\frac{3\beta + 11}{2\beta + 11}\right) \tag{1-19}$$

which has a maximum error of -1%. For the nonsymmetric case this yields

$$\mu_{12}^2 = \pi^2 \left(\frac{3\beta_1 + 11}{2\beta_1 + 11}\right)\left(\frac{3\beta_2 + 11}{2\beta_2 + 11}\right) \tag{1-20}$$

in which the maximum error is -4%.

Other approximations of higher accuracy can be obtained if the

Table 6. Accuracy of $\omega_{12} = \mu_{12}^2 = \pi^2 \left(\frac{9\beta_1 + 10\pi}{6\beta_1 + 10\pi}\right)\left(\frac{9\beta_2 + 10\pi}{6\beta_2 + 10\pi}\right)$

	Error %									
	β_2									
β	0	.1	.5	1	3	5	10	100	1000	10000
.0	0	-0.18	-0.26	-0.32	-1.06	-1.52	-2.31	-3.68	-3.89	-3.99
.1		-0.1	-0.27	-0.47	-1.08	-1.52	-2.19	-3.50	-3.71	-3.73
.5			-0.31	-0.37	-0.70	-1.0	-1.54	-2.68	-2.87	-2.89
1				-0.31	-0.36	-0.54	-0.93	-1.92	-2.09	-2.11
3					0.22	0.34	0.25	-0.41	-0.55	-0.56
5						0.59	0.64	0.10	-0.03	-0.05
10							0.82	0.33	0.20	0.18
100								-0.30	-0.49	-0.51
1000									-0.69	-0.72
10000										-0.74

arithmetic mean of the square root of the frequencies $\mu_{n,11}$ and $\mu_{n,22}$ is considered, viz

$$\mu_{n,12} = \frac{\mu_{n,11} + \mu_{n,22}}{2} \tag{1-21}$$

If Equation (1-4) is substituted into Equation (1-21) we obtain

$$\mu_{12} = \frac{\pi}{2}\left[\frac{9\beta_1 + 10\pi}{6\beta_1 + 10\pi} + \frac{9\beta_2 + 10\pi}{6\beta_2 + 10\pi}\right] \tag{1-22}$$

which is accurate to within 1% as shown in Table 7.

Similarly if Equation (1-19) is substituted into Equation (1-21) we get

$$\mu_{12} = \frac{\pi}{2}\left(\frac{3\beta_1 + 11}{2\beta_1 + 11} + \frac{3\beta_2 + 11}{2\beta_2 + 11}\right) \tag{1-23}$$

and the maximum error in this case is -1%.

By use of the arithemetic mean law an expression for the higher natural frequencies of vibration can also be obtained, viz

$$\mu_{n,12} = \frac{\pi}{2}\left[2n + \frac{\beta_1}{2\beta_1 + \pi^2 n} + \frac{\beta_2}{2\beta_2 + \pi^2 n}\right] \tag{1-24}$$

and the maximum errors in the frequencies obtained by this formula are

Table 7. Accuracy of $\omega_{12} = \mu_{12}^2 = \frac{\pi^2}{4}\left(\frac{9\beta_1 + 10\pi}{6\beta_1 + 10\pi} + \frac{9\beta_2 + 10\pi}{6\beta_2 + 10\pi}\right)^2$

	Error %									
	β_2									
β_1	0	.1	.5	1	3	5	10	100	1000	10000
0	0	-0.05	-0.22	-0.35	-0.51	-0.5	-0.41	-0.06	0.01	0.02
.1		-0.10	-0.24	-0.35	-0.47	-0.44	-0.34	0.01	0.08	0.09
.5			-0.31	-0.34	-0.31	-0.24	-0.10	0.26	0.33	-0.34
1				-0.31	-0.16	-0.04	0.13	0.48	0.54	0.55
3					0.22	0.41	0.59	0.82	0.85	0.85
5						0.59	0.75	0.83	0.83	0.83
10							0.82	0.61	0.56	0.55
100								-0.30	-0.49	-0.51
1000									-0.69	-0.72
10000										-0.74

as follows

1.85%	at	(5,10)	for	n = 1
0.42%	at	(5, ∞)	for	n = 2
-0.21%	at	(0,10)	for	n = 3
-0.23%	at	(100,100)	for	n = 4
-0.26%	at	(100,100)	for	n = 5

Although Equation (1-24) does not have the accuracy that was attained in Equation (1-13) for n = 1, it has the great virtues of simplicity and generality.

The several formulae which have been derived by expressing the nonsymmetric case in terms of the two corresponding symmetric cases are fully consistent with prior observations on nonsymmetric boundary conditions. Newmark [2,6], in both of his studies of the instability and vibration of columns derived geometric mean laws. Ludquist [7] and Stowell [8] developed similar expressions in their studies on plates. They however considered arithmetic mean laws as well as geometric.

Approximate Formula for the Mode Shape

In Appendix (A) an exact general formula for the deflection of elastically restrained laterally loaded beams is derived by use of a rational function technique. This formula expresses the condition for specific restraint parameters in terms of the behaviors when the end fixities are zero or infinity or combinations thereof. The expression therein described satisfies exactly the pertinent differential equation

and the appropriate boundary conditions. The generality of the result suggests strongly that a similar situation might well be true for both of the buckling and vibrational shapes of columns.

In view of this we investigate in the following paragraphs the applicability of the concept. To begin with we take the deflection function in the form

$$W = \frac{a_1 + a_2\,\beta_1\,\beta_2 + a_3\,\beta_1 + a_4\,\beta_2}{b_1 + b_2\,\beta_1\,\beta_2 + b_3\,\beta_1 + b_4\,\beta_2} \tag{1-25}$$

As the rotational restraint parameters β_1 and β_2 reach their extreme values, i.e., zero or infinity, the mode shape takes the corresponding form as given below

$$\left.\begin{aligned} W_{0\,0} &= \sin \bar{\mu}_1 X \\ W_{\infty\,\infty} &= 0.63\left[\cosh \bar{\mu}_2 X - \cos \bar{\mu}_2 X + q_1\left(\sin \bar{\mu}_2 X - \sinh \bar{\mu}_2 X\right)\right] \\ W_{\infty\,0} &= 0.69\left[\cosh \bar{\mu}_3 X - \cos \bar{\mu}_3 X + \sin \bar{\mu}_3 X - \sinh \bar{\mu}_3 X\right] \\ W_{0\,\infty} &= 0.98\left[\sin \bar{\mu}_3 X - q_2 \sinh \bar{\mu}_3 X\right] \end{aligned}\right\} \tag{1-26}$$

where

$$0 \le X \le 1, \quad X = \frac{x}{L}$$

$$\bar{\mu}_1 = \pi \ , \qquad \bar{\mu}_2 = 4.73 \ , \qquad \bar{\mu}_3 = 3.927 \ ,$$

$$q_1 = \frac{\cosh \bar{\mu}_2 - \cos \bar{\mu}_2}{\sinh \bar{\mu}_2 - \sin \bar{\mu}_2} \qquad \left(= 0.9825 \text{ for the first mode}\right)$$

$$q_2 = \frac{\sin \bar{\mu}_3 + \cos \bar{\mu}_3}{\cosh \bar{\mu}_3 + \sinh \bar{\mu}_3} \qquad \left(= - 0.0278635 \text{ for the first mode}\right)$$

The above shapes were obtained by use of the classical methods for solving the differential equation as given in standard text books [9,10]. These shapes were normalized such that the mid-span deflection is unity.

Substituting the shapes pertinent to the extreme values of β_1 and β_2 in Equation (1-25) we obtain relations between the a's and b's and hence Equation (1-25) reduces to

$$W = \frac{b_1 W_{0\,0} + b_2 \beta_1 \beta_2 W_{\infty\,\infty} + b_3 \beta_1 W_{\infty\,0} + b_4 \beta_2 W_{0\,\infty}}{b_1 + b_2 \beta_1 \beta_2 + b_3 \beta_1 + b_4 \beta_2} \qquad (1\text{-}27)$$

To determine the ratios between b_1, b_2, b_3 and b_4 one resorts to the three conditions that have been outlined in Appendix (A), namely, the symmetry of the mode shape when $\beta_1 = \beta_2 = \beta$ and the relationships between the bending moment and the slope at both ends.

By following a similar argument as that developed in the appendix the symmetry condition leads to

$$b_3 = b_4 \tag{1-28}$$

and the bending moment-slope relations give

$$b_1 = \left[\frac{W''_{\infty\ 0}}{W'_{0\ 0}} \right]_{x=0} \cdot b_4 \tag{1-29}$$

and

$$b_2 = \left[\frac{W'_{0\ \infty}}{W''_{\infty\ \infty}} \right]_{x=0} \cdot b_4 \tag{1-30}$$

The results are grouped and summarized in Table 8.

The approximate mode was compared to the exact shape which was derived in Appendix (B). The magnitude of the deflection and the error percentage in the approximate shape were evaluated at steps of one tenth the beam length. Towards the ends of the beam the exact deflection tends to zero and therefore the error calculated becomes meaningless. However, if we restrict our computation, arbitrarily, to the range between one tenth and nine tenth of the span, the maximum errors are found to be -1.25% at $\beta_1 = 0$ and $\beta_2 = 20$ and $x = 0.9L$; and 0.75% at $\beta_1 = 0$, $\beta_2 = 5$ and $x = 0.1L$.

Table 8. Summary of Approximate Formulae for the Vibrational Characteristics of Beams with Elastic End Restraints

Case (a) Equal Restraint

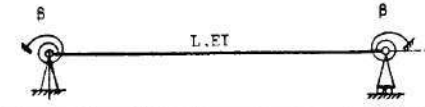

Characteristic Equations and Approximate Formulae	Matching Points	Maximum % Error in ω $(= \mu^2)$
$2\mu^2 \sin\mu \sinh\mu + 2\mu\beta(\sin\mu\cosh\mu - \cos\mu\sinh\mu) + \beta^2(1 - \cos\mu\cosh\mu) = 0$		
$\mu = \pi\left(\frac{9\beta + 10\pi}{6\beta + 10\pi}\right)$	0, 5.72, ∞	0.82 at $\beta = 9.7$ -0.75 at $\beta = \infty$
$\mu = \pi\, e^{\left(\frac{9\beta}{11\beta + 49}\right)}$	0, 3, ∞	-0.75 at $\beta = 1.2$ +0.76 at $\beta = 15$
$\mu_n = \pi\left(n + \frac{\beta}{2\beta + \pi^2 n}\right)$		n = 1: 1.73 at $\beta = 7.5$ n = 2: -0.04 at $\beta = 3$ n = 3: -0.34 at $\beta = 30$

Table 3. (continued)

Case (a) Unequal Restraint	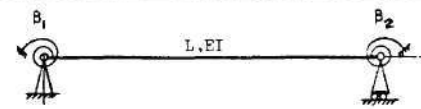	
Characteristic Equations and Approximate Formulae	Matching Points	Miximum % Error in $\omega(=\mu^2)$
$2\mu^2 \sin\mu \sinh\mu$ $+ \mu(\beta_1 + \beta_2)(\sin\mu\cosh\mu - \cos\mu\sinh\mu)$ $+ \beta_1\beta_2(1 - \cos\mu\cosh\mu) = 0$		
$\omega = \mu^2 = \pi^2 + \dfrac{12.5\,\beta_1\beta_2 + 36.7(\beta_1 + \beta_2)}{\beta_1\beta_2 + 6.6(\beta_1 + \beta_2) + 36.9}$	(0, 0) (∞, ∞) (0, ∞) (0, 1) (1, 2)	0.15 at (20, 50) -0.08 at (0, ∞)
$\omega = \mu^2 = \pi^2 \left(\dfrac{9\beta_1 + 10\pi}{6\beta_1 + 10\pi}\right)\left(\dfrac{9\beta_2 + 10\pi}{6\beta_2 + 10\pi}\right)$	geometric mean	0.82 at (10, 10) -1.0 at (0, ∞)

Table 8. (continued)

Case (a) Unequal Restraint

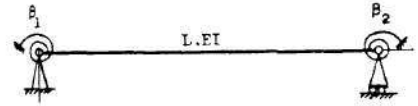

Characteristic Equations and Approximate Formulae	Matching Points	Maximum % Error in $w(= \mu^2)$
$\mu = \frac{\pi}{2}\left(\frac{9\beta_1 + 10\pi}{6\beta_1 + 10\pi} + \frac{9\beta_2 + 10\pi}{6\beta_2 + 10\pi}\right)$	arithmetic	0.85 at (1, ∞)
	mean	-0.75 at (∞, ∞)
$\mu_{n,12} = \frac{\pi}{2}\left(2n + \frac{\beta_1}{2\beta_1 + \pi^2 n} + \frac{\beta_2}{2\beta_2 + \pi^2 n}\right)$	arithmetic	1.85 at 5, 10 & n = 1
	mean	.42 at 5, ∞ & n = 2
		- .21 at 0, 10 & n = 3
		- .23 at 100, 100 & n = 4
		- .26 at 100, 100 & n = 5

Table 8. (continued)

Case (a) Unequal Restraint	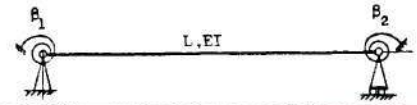

Characteristic Equations and Approximate Formulae	Maximum % Error in W

Mode Shape

$$W = \frac{b_1 W_{0\,0} + b_2 \beta_1 \beta_2 W_{\infty\,\infty} + \beta_1 W_{\infty\,0} + \beta_2 W_{0\,\infty}}{b_1 + b_2 \beta_1 \beta_2 + \beta_1 + \beta_2}$$

-1.25 at (0, 20)
and x = 0.9L
+0.75 at (0, 5)
and x = 0.1L

where

$$b_1 = \left[\frac{W''_{\infty\,0}}{W'_{0\,0}}\right]_{x=0} \quad \left(= 6.774 \text{ for first mode}\right)$$

$$b_2 = \left[\frac{W'_{0\,\infty}}{W''_{\infty\,\infty}}\right]_{x=0} \quad \left(= 0.1403 \text{ for first mode}\right)$$

and $W_{0\,0}$, $W_{\infty\,\infty}$, $W_{\infty\,0}$ and $W_{0\,\infty}$ are given in Equation (1.26)

Table 8. (continued)

Case (l)

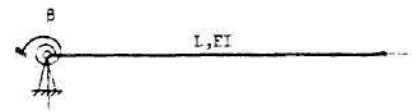

Characteristic Equations and Approximate Formulae	Matching Points	Maximum % Error in $\omega(=\mu^2)$
$\mu\left(\sin\mu\cosh\mu - \cos\mu\sinh\mu\right) = \beta\left(1+\cos\mu\cosh\mu\right)$		
$\mu = \left(\frac{1.875\beta + 1.52}{\beta + 1.722}\right)$, $\beta \geq 1$	β = 1, 3, ∞	0.74 at β = 10 -0.22 at β = 1
$\mu = \left(\frac{1.875\beta^2 - 0.675\beta - 2.67}{\beta^2 + 0.615\beta - 2.769}\right)$, $\beta \geq 1$	β = 1, 3, 5, 10, ∞	0.09 at β = 20 -0.17 at β = 5
$\mu = e^{\left(\frac{1.057 + 1.038\beta}{\beta + 1.59}\right)} - 1$, $\beta \geq 1$	β = 1, 5, ∞	0.31 at β = 50 -1.7 at β = 2.5

Table 8. (continued)

Case (c) 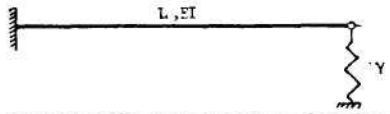		
Characteristic Equations and Approximate Formulae	Matching Points	Maximum % Error in $\omega(=\mu^2)$
$\gamma\left[\cosh\mu\sin\mu-\sinh\mu\cos\mu\right]$ $=-\mu^3\left[1+\cosh\mu\cos\mu\right]$		
$\mu=\dfrac{4.01\gamma+30}{1.02\gamma+16}$	$\gamma=0,\ 5,\ \infty$	3.8 at $\gamma=20$
$\omega=\mu^2=e^{\left(\frac{125\gamma+620}{46\gamma+490}\right)}$	$\gamma=0,\ 5,\ \infty$	3.56 at $\gamma=20$

Beams with Other End Fixities

Rational function approximations were derived for two more cases of elastic end fixities; Figures 1 (b) and (c). For both cases direct expressions as well as exponential forms were developed. Since the method of analysis is the same as previously outlined, detailed derivations will be ommitted and the final results only will be presented. Table 8 lists the results pertinent to all the cases that have been considered in this chapter.

Discussion

The intent outlined at the beginning of this chapter has been achieved. Simple, accurate approximate expressions for the vibrational characteristics of elastically restrained beams have been obtained. Such formulae are demanded for practical applications and they are equally of interest in analytical studies. In the next chapter it will be demonstrated how such solutions can play an important role in dealing with more complex situations. Specifically they will be used as the basis to vastly simplify the solutions for the more complex problems of vibration of rectangular plates with elastic boundary restraints.

With regard to the question of the "matching points", it is obvious that the choice of these points determines the error involved in the final formula. Therefore it would be desirable to find a simple mathematical procedure with which one can determine the best matching conditions for optimum accuracy. However, for the type of problems with which we have been concerned, compliance with the extreme conditions is desirable. For best accuracy, the "third point" can

clearly be determined by a trial and error process, and the utility of the final result amply justifies this expenditure. Nevertheless, in most cases of buckling and vibration approximations of accuracies within engineering limits were obtained if the mean value of the dependent variable was chosen.

CHAPTER II

APPROXIMATE SOLUTIONS FOR THE NATURAL FREQUENCIES OF VIBRATION OF RECTANGULAR PLATES WHOSE EDGES ARE SUBJECTED TO ELASTIC ROTATIONAL RESTRAINTS

Introduction

Except for the case of simply supported edges, exact solutions for the vibrational characteristics of rectangular plates are difficult to obtain [11,12]. Approximate solutions for plates with the edges subjected to various combinations of extreme fixities are available in the literature. Warburton [13] developed solutions for the frequency of transverse vibration of a rectangular plate with several combinations of free, simply supported and clamped edges. He used a Rayleigh-Ritz type solution and generated his displacement function from the products of the waveforms of elastically restrained beams. Janish [14] obtained the fundamental frequencies for 18 combinations of extreme boundary conditions. He used a Rayleigh quotient and assumed the waveforms to be simple trigonometric functions which satisfied only the geometric boundary conditions. Iguchi [15] dealt with the square plate with two opposite edges simply supported and the other two clamped. By solving the characteristic equation, (see Ref. 16, p. 47), which results from substituting the boundary conditions into the general solution, he obtained the first six frequency parameters. Ödman [17] solved the same characteristic equation with less accuracy than did

Iguchi and extracted 36 of its roots.

Several other approximate solutions for the cases of extreme edge fixities have been developed. A comprehensive survey of such approximations is presented in reference [16]. However, there are few solutions for the problem of the plate vibration when the edges are elastically restrained against rotation.

One of the earliest attempts to deal with such a problem was made for the purpose of investigating the mechanical vibration of a chassis used for electronic equipment [18]. Typically such a chassis is formed by bending the edges of a plate down. In the reference cited the chassis was treated as a plate with elastic edge supports. The Rayleigh-Ritz method was used and a trial function was assumed to be an arithmetic average of the eigenfunctions for plates with simply supported edges and those having clamped edges. Theoretical and experimental results were obtained for a particular chassis.

Solutions to the vibration of elastically restrained rectangular plates have been developed also by two other investigators [19,20]. Neither of these considered the general case of unequal restraints. Moreover, the solutions they introduced require elaborate and lengthly calculations for the determination of the natural frequencies, a situation which renders their approach inconvenient for practical applications.

It is most clear from the preceding review that the calculation of the vibrational frequencies of elastically restrained plates is a complicated problem. In many respects the situation is similar to the problem of the beam vibration which has been treated in the previous chapter. In addition there are many cases in which exact solutions

cannot be derived even for the extreme boundary restraint conditions. In fact we may state that in all cases of practical edge restraint the determination of the critical frequencies is a most involved computational question. Thus, there is, even more so, in the case of plates, a sound reason to attempt to develop more readily, usable approximate solutions for direct applications.

In this chapter we treat the general case when the elastic edge restraint parameters $\beta_1, \beta_2, \beta_3$ and β_4 are unequal. As before, our aim is to obtain simple convenient solutions for the natural frequencies of vibration in as broad a context as possible.

Two approaches are utilized; a Rayleigh-Ritz type solution and, a rational function representation. These are introduced in detail in the remaining of this chapter.

A Rayleigh-Ritz Solution to the Problem

In studies of structural dynamics approximate solutions for the fundamental frequencies of vibration can be derived from Rayleigh's principle [11,21]. In such a method it is necessary to begin with displacement functions which satisfy the geometric boundary conditions of the problem.

Considering the problem of the free vibration of a plate whose edges are rigidly supported against lateral displacement and elastically restrained against rotation an approximation for the fundamental frequency will be given by equating the strain energy to the kinetic energy, that is

$$U = T \tag{2-1}$$

where

U is the strain energy of the plate

$$U = \frac{\bar{D}}{2} \int_{-b/2}^{b/2} \int_{-a/2}^{a/2} \left[\left(\frac{\partial^2 W}{\partial x^2} \right)^2 + \left(\frac{\partial^2 W}{\partial y^2} \right)^2 + 2 \frac{\partial^2 W}{\partial x^2} \frac{\partial^2 W}{\partial y^2} \right] dx\, dy \qquad (2\text{-}2)$$

$$+ \frac{1}{2} \left\{ \int_{-b/2}^{b/2} \left[k_1 \left(\frac{\partial W}{\partial x} \right)^2_{x = -a/2} + k_2 \left(\frac{\partial W}{\partial x} \right)^2_{x = a/2} \right] dy \right.$$

$$\left. + \int_{-a/2}^{a/2} \left[k_3 \left(\frac{\partial W}{\partial y} \right)^2_{y = -b/2} + k_4 \left(\frac{\partial W}{\partial y} \right)_{y = b/2} \right] dx \right\}$$

T is the kinetic energy

$$T = \frac{\bar{m}\omega^2}{2} \int_{-b/2}^{b/2} \int_{-a/2}^{a/2} W^2 \, dxdy \qquad (2\text{-}3)$$

W is the assumed trial function

$W \equiv W(x,y)$

ω is the natural frequency of vibration

x & y are coordinate axes as shown in Figure 2.

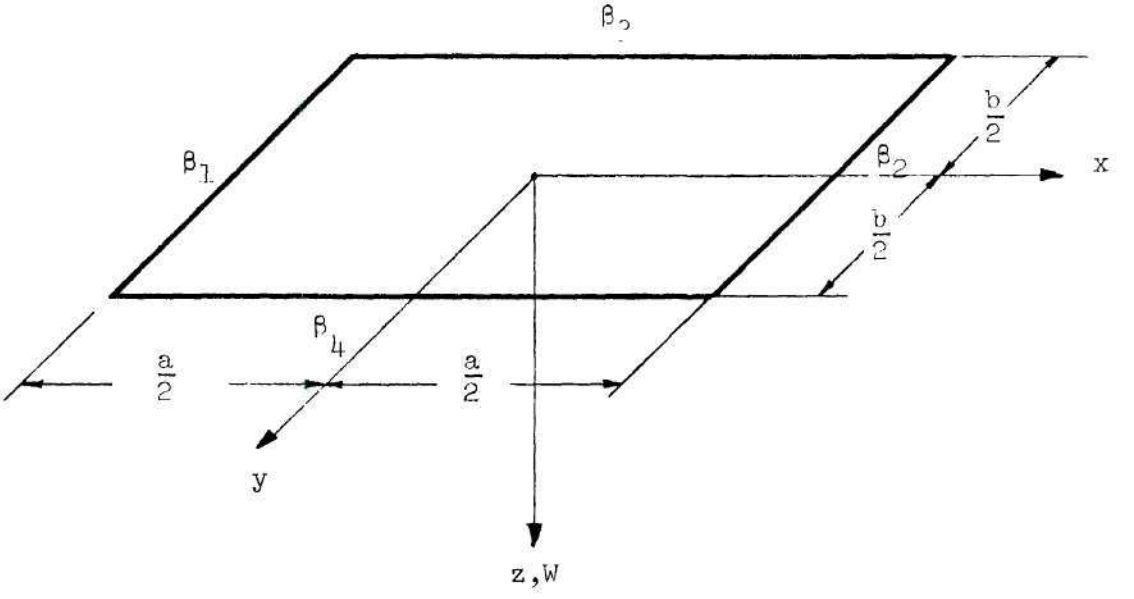

Figure 2. Elastically Restrained Rectangular Plate.

The Ritz method is an extension of Rayleigh's principle which permits simultaneous approximate determination of the first n characteristic frequencies of the vibrating system. In such a method a trial function is assumed in the form

$$W(x,y) = \sum_{m=1}^{n} a_m W_m(x,y) \tag{2-4}$$

where, $W_1(x,y)$, $W_2(x,y),\ldots,$ $W_n(x,y)$ are linearly independent functions each of which satisfies the essential boundary conditions of the problem. The $a_m (m = 1,2,\ldots,n)$ are parameters with respect to which Equation (2-1) will be differentiated. This results in a system of n homogeneous linear equations in the a_m. The coefficients of these parameters are known functions of the, as yet undetermined, frequencies ω_m. For a non-trivial solution of the above system of equations the determinant of the coefficients of the parameters a_m is set equal to zero. The roots of this determinant give approximations to the first n characteristic frequencies of the plate. This method was first used by Ritz [22] in the study of the vibration of a square plate with free edges. He assumed the generating function to be in the series form

$$W(x,y) = \sum_{n=1}^{N} \sum_{m=1}^{M} a_{mn} W_m(x) W_n(y) \tag{2-5}$$

where $W_m(x)$ and $W_n(y)$ are the m^{th} and n^{th} modes of vibration of a beam whose ends are supported in a manner similar to that of the

corresponding edges of the plate.

Later, investigators used the Ritz method, together with the same waveform given by Equation (2-5), in dealing with the vibration of plates with various other boundary conditions.

For the elastically restrained plates, Carmichael [20] considered the case of equal elastic restraints on opposite edges of the plate. He took the mode shape to be a 36 term series of the form given by Equation (2-5), (where M = N = 6). He minimized the energy Equation (2-1) with respect to the coefficients, but due to the great amount of work involved, he did not expand the resulting determinant. Instead, by observing that the diagonal terms were much greater than the off-diagonal terms he formulated an approximate solution in which the mn^{th} mode was represented by the mn^{th} term only.

Even with such simplification the problem is involved because knowledge of the mode shape and the natural frequencies of vibration of the elastically restrained beams are still a necessity.

There is strong evidence that, if a good choice of a generating function is made, a one term representation of the mode shape can be used without great loss in the accuracy of the resulting solution. Carmichael's observation of the heavily weighted characteristic determinant along the diagonal is supported by Young's results [23]. Young considered a square plate with several edge conditions. His trial function consisted of 36-terms series of the type given by Equation (2-5). He obtained the natural frequencies of vibration and calculated the relative magnitudes of the coefficients of each term

in the series. For an mn^{th} mode the predominant coefficient is shown to be that of the mn^{th} term, the relative magnitudes of the majority of the coefficients of the other terms are no more than one percent of that of the mn^{th} term. Some of the coefficients could be as high as 15% depending on how far the nodal lines deviate from straight lines or from being parallel to the plate edges. In fact for those vibrational modes which could be described as $mn \pm nm$ modes, the nodal lines are no longer straight lines parallel to the edges of the plate and in such cases the relative magnitudes of the coefficients of the mn^{th} and nm^{th} terms become of the same order of magnitude.

Warburton [13] studied this issue in detail. His trial functions consisted of the principal terms only; namely the mn^{th} and tne nm^{th} modes. He concluded that a good estimate of the natural frequency of vibration corresponding to the combined mode shapes can be obtained using functions consisting of the mn^{th} term only. His conclusion is also verified in the present analysis for the elastically restrained plates.

There is no doubt that the application of the Rayleigh-Ritz procedure is a straightforward process. The conditions which govern the choice of the displacement function are also readily defined, however, the process of choosing a pertinent function or combinations of functions is not so easily delineated. The choice of the generating function is fundamental to the issue since this function determines the final form of the solution, its accuracy and its conveneince. It totally controls the amount of work involved in deriving the solution and even determines whether or not a convenient final solution can be

obtained. This situation was clearly observed in the above cited reference [20], where the increasing complexity of the analysis became prohibitive and a complete solution was impractical to obtain.

In this section certain useful formulations are adopted in the choice of the waveform. These are based upon the rational function approach which was successfully used in the previous chapter. They bring considerable simplification at the expense of little change of accuracy.

A literature search indicated that a solution for the general case of unequal elastic restraints is not known. In order to be able to assess the accuracy of our intended approximate solutions, the first task undertaken was the development of a general solution based on a well established method. A concurrent requirement was of course, that this solution should not involve an unreasonable amount of computation. That solution will be designated as solution No. 1. Solution No. 2 is then obtained by modifying solution No. 1 by inclusion of certain simplified expressions which were derived in Chapter I. As a result we are able to effect a considerable saving in computational time at the expense of little or no change in the accuracy.

The final solution, designated solution No. 3, was made by using a broader approximation than that adopted for No. 2. This in essence consisted of taking a simplified waveform developed from the more exact by a rational function approach.

Solution No. 1

The mode shape was taken in the form

$$W_{mn}(x,y) = W_m(x)\, W_n(y) \tag{2-6}$$

where

$$W_m(x) = A_m \cosh \frac{\lambda_m x}{a} + B_m \sinh \frac{\lambda_m x}{a} + C_m \cos \frac{\lambda_m x}{a} + D_m \sin \frac{\lambda_m x}{a}$$

$$W_n(y) = E_n \cosh \frac{\mu_n y}{b} + F_n \sinh \frac{\mu_n y}{b} + G_n \cos \frac{\mu_n y}{b} + H_n \sin \frac{\mu_n y}{b}$$

λ_m is the m^{th} frequency parameter for a beam whose ends are subjected to elastic rotational restraints defined by the parameters β_1 and β_2.

μ_n is the n^{th} frequency parameter for a beam whose ends are subjected to elastic rotational restraints defined by the parameters β_3 and β_4.

$A_m, \ldots, D_m$ and $E_n, \ldots, H_n$

are given by either Equation (B-12) or (B-13) in Appendix B, and

$-\frac{a}{2} \leq x \leq \frac{a}{2}$ and $-\frac{b}{2} \leq y \leq \frac{b}{2}$, see Figure 2.

Equation (2-6) is used to evaluate the energy terms given by Equations (2-2) and (2-3), and the frequency is obtained from Equation (2-1). Details of the computation are given in Appendix C.

In Table 9 the above solution is compared to that which

Table 9. Comparison of Solutions No. 1 and 2 to the Series Solution of Ref. [20] at $\beta_1 = \beta_2 = \beta_3 = \beta_4 = 20$

Solution	R	Mode Number and Shape					
		1	2	3	4	5	6
	1	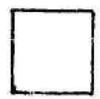		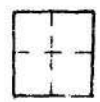	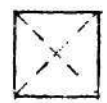		
Reference [20]		31.09	64.31	95.85	117.3	116.8	147.6
Solution No. 1		31.159 (.22)	64.523 (.33)	96.167 (.33)	117.404 (.09)	117.404 (.52)	148.02 (.28)
Solution No. 2		31.153 (.20)	64.51 (.31)	96.125 (.28)			147.95 (.24)
	.8		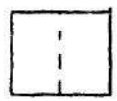	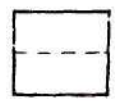	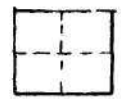	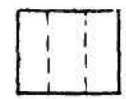	
Reference [20]		25.80	46.02	59.98	79.06	79.24	111.2
Solution No. 1		25.86 (.23)	46.17 (.32)	60.16 (.3)	79.33 (.34)	79.5 (.33)	111.48 (.25)
Solution No. 2		25.856(.22)	46.15 (.29)	60.15 (.29)	79.29 (.29)	79.49(.32)	111.43 (.2)

Note: The quantities between crackets are percentage error as compared to the series solution of reference 20.

-continued-

Table 9. (continued)

Solution	$\frac{b}{a}$	Mode Number and Shape					
		1	2	3	4	5	6
	.6			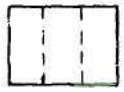	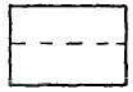	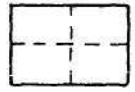	
Reference [20]		22.30	32.58	50.48	56.97	66.96	
Solution No. 1		22.348 (.22)	32.68 (.31)	50.64 (.31)	57.11 (.24)	67.17 (.31)	
Solution No. 2		22.344 (.2)	32.67 (.28)	50.62 (.28)	57.1 (.23)	67.15 (.28)	
	.4	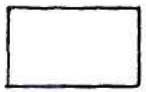					
Reference [20]		20.30	24.15	31.2			
Solution No. 1		20.336 (.18)	24.2 (.21)	31.26(.19)			
Solution No. 2		20.335 (.17)	24.19(.18)	31.25(.15)			
	.2	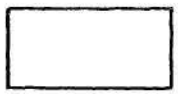		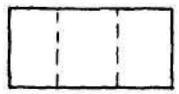			
Reference [20]		19.38	20.15	21.52			
Solution No. 1		19.393 (.07)	20.175 (.12)	21.539 (.09)			
Solution No. 2		19.393 (.07)	20.173 (.11)	21.534 (.07)			

Carmichael [20] obtained using a generating function consisting of a 36-term series. The only available numerical values are those corresponding to a rectangular plate with rotational restraint parameters equal to 20 on all edges. It is seen that the discrepancy is less than 0.5%. It is also clear from Table 9 that for higher frequencies where the nodal lines may no longer be parallel to the plate edges a solution obtained by use of a one generating function (i.e., solution No. 1) still results in excellent frequency estimates even though the assumed mode shape is appreciably different from the exact one. The solution is compared to Iguchi's exact solution [15] for a specific case of extreme edge conditions. This comparison is shown in Table 10.

Solution No. 2

In the solution developed in the preceding paragraphs the numerical determination of the plate frequency depended upon a knowledge of the analogous frequency for the elastically restrained beam which defined the assumed waveform.

The frequencies of vibration of such elastically restrained beams are obtained by numerically searching for the roots of the pertinent characteristic equation. This is generally an iterative process. The work involved in this part of the numerical analysis is far greater than that required for the remaining computations needed to calculate the plate frequency. This difficulty is experienced due to the fact that the beam eigenvalues are implicit functions of the restraint parameter "β". A considerable amount of computational time can be saved if those eigenvalues were expressed as explicit functions

Table 10. Comparison of Solution No. 1 vs. Solution of Reference [15]

	Solution	Frequency Parameter ω		
		R = 1	R = 1/2	R = 1/3
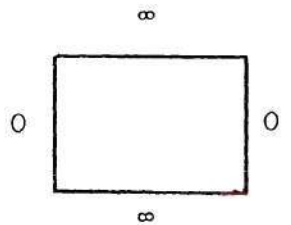	Reference [15]	28.946	23.814	22.985
	No. 1	28.998 (0.18)*	23.82 (.025)*	22.995 (.04)*
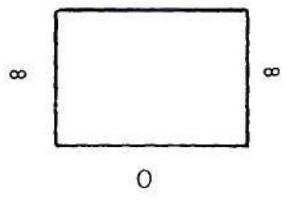	Reference [15]	28.946	13.688	11.359
	No. 1	28.998 (0.18)*	13.762 (0.54)*	11.427 (0.6)*

* Denotes the percentage discrepancy as compared to Solution of Reference [15]

of β, a situation which can be achieved by use of the approximate formulae that were developed in Chapter I by a rational function technique and which are given by Equations (1-13) and (1-24)(for the fundamental and higher frequencies respectively).

Those approximate frequency parameters when introduced into solution No. 1 result in trivial changes in the accuracy as seen in Tables 9 and 11 where solutions Nos. 1 and 2 are compared over large intervals of the elastic restraints and the aspect ratio.

Due to the excellent agreement of the two solutions either one can be used as the reference solution.

Solution No. 3

This third solution fully demonstrates the importance of rational function approximations when dealing with the relatively involved problem of the determination of the vibrational frequencies for elastically restrained rectangular plates.

The Rayleigh-Ritz approach, as previously outlined, is used. The waveform is taken in the form of Equation (2-6). However, W(x) and W(y) are substituted for by the approximate formula for the mode shape of the beam which is given in Equation (1-27).

In essence this substitution makes the mode shape an explicit function of the edge restraint parameters, and in fact simultaneously "separates" the variables.

The analysis becomes most straightforward and is given in Appendix D. The expression obtained for the frequency is clearly seen to be an explicit function of the elastic restraint parameters $\beta_1,\ldots,\beta_4$

Table 11. Comparison Between Solutions No. 1, 2 and 3

(R = 1.0)

Restraint Parameters				Frequency Parameters				
				Solution	Solution No. 2		Solution No. 3	
β_1	β_2	β_3	β_4	No. 1	ω	Error %	ω	Error %
0	1	1	5	22.1815	22.1815	0.00	22.1799	-0.04
0	0	5	1000	25.6479	25.6478	0.00	25.6399	-0.03
0	0	1000	1000	28.9118	28.911	0.00	28.8625	-0.17
0	5	5	5	24.3329	24.3326	0.00	24.3132	-0.08
1	5	1	5	23.6385	23.6386	0.00	23.632	-0.03
1	5	5	1000	27.2564	27.2563	0.00	27.2459	-0.04
5	1000	5	1000	30.4926	30.4924	0.00	30.476	-0.05
5	5	1000	1000	31.2327	31.2317	0.00	31.1603	-0.23
5	1000	1000	1000	33.3264	33.3255	0.00	33.2691	-0.17
10	1	5	10	26.0751	26.0744	0.00	26.0034	-0.27
1000	0	1000	0	27.1584	27.1569	-0.01	26.9516	-0.76
1000	0	0	10	25.6254	25.6246	0.00	25.5351	-0.35
1000	10	10	5	29.6738	29.6722	-0.01	29.5506	-0.42
1000	1000	1000	1000	35.9655	35.9639	0.00	35.8675	-0.27

- continued -

Table 11. Comparison Between Solutions No. 1, 2 and 3 (continued)

(R = 0.8)

Restraint Parameters				Solution	Frequency Parameters			
					Solution No. 2		Solution No. 3	
β_1	β_2	β_3	β_4	No. 1	ω	Error %	ω	Error %
0	1	1	5	18.7743	18.7743	0.00	18.7712	-0.02
0	0	5	1000	22.8115	22.8114	0.00	22.808	-0.02
0	0	1000	1000	26.2926	26.2922	0.00	26.2583	-0.13
0	5	5	5	20.641	20.6408	0.00	20.6176	-0.11
1	5	1	5	19.5108	19.5108	0.00	19.5051	-0.03
1	5	5	1000	23.5857	23.5857	0.00	23.5811	-0.02
5	1000	5	1000	25.2769	25.2767	0.00	25.2648	-0.05
5	5	1000	1000	27.3848	27.3842	0.00	27.3362	-0.18
5	1000	1000	1000	28.4892	28.4887	0.00	28.4454	-0.15
10	1	5	10	21.9687	21.9682	0.00	21.9169	-0.24
1000	0	1000	0	22.4218	22.4206	-0.01	22.2522	-0.76
1000	0	0	10	20.7518	20.7512	0.00	20.6992	-0.25
1000	10	10	5	23.8678	23.8665	-0.01	23.7706	-0.41
1000	1000	1000	1000	29.8698	29.8687	0.00	29.7944	-0.25

- continued -

Table 11. Comparison Between Solutions No. 1, 2 and 3 (continued)

(R = 0.6)

Restraint Parameters				Frequency Parameters				
				Solution	Solution No. 2		Solution No. 3	
β_1	β_2	β_3	β_4	No. 1	ω	Error %	ω	Error %
0	1	1	5	16.2639	16.2639	0.00	16.2591	-0.03
0	0	5	1000	20.7584	20.7584	0.00	20.7593	0.00
0	0	1000	1000	24.4192	24.4192	0.00	24.3988	-0.08
0	5	5	5	18.0241	18.024 .	0.00	17.9973	-0.15
1	5	1	5	16.5534	16.5535	0.00	16.5476	-0.04
1	5	5	1000	21.0478	21.0478	0.00	21.0483	0.00
5	1000	5	1000	21.7558	21.7557	0.00	21.7501	-0.03
5	5	1000	1000	24.8161	24.8159	0.00	24.7882	-0.11
5	1000	1000	1000	25.2923	25.2921	0.00	25.2644	-0.11
10	1	5	10	19.1255	19.1252	0.00	19.0881	-0.20
1000	0	1000	0	19.0398	19.039	0.00	18.8989	-0.74
1000	0	0	10	17.2416	17.2412	0.00	17.2168	-0.14
1000	10	10	5	19.9163	19.9154	0.00	19.8408	-0.38
1000	1000	1000	1000	25.8664	25.8658	0.00	25.8177	-0.19

- continued -

Table 11. Comparison Between Solutions No. 1, 2 and 3 (continued)

(R = 0.4)

Restraint Parameters				Frequency Parameters				
				Solution	Solution No. 2		Solution No. 3	
β_1	β_2	β_3	β_4	No. 1	ω	Error %	ω	Error %
0	1	1	5	14.5844	14.5844	0.00	14.5783	-0.04
0	0	5	1000	19.4003	19.4002	0.00	19.4048	0.02
0	0	1000	1000	23.1903	23.1905	0.00	23.1813	-0.04
0	5	5	5	16.3576	16.3575	0.00	16.3284	-0.18
1	5	1	5	14.6598	14.6598	0.00	14.6534	-0.04
1	5	5	1000	19.4723	19.4723	0.00	19.4769	0.02
5	1000	5	1000	19.6852	19.6851	0.00	19.6862	0.01
5	5	1000	1000	23.2854	23.2855	0.00	23.2734	-0.05
5	1000	1000	1000	23.4387	23.4388	0.00	23.4256	-0.06
10	1	5	10	17.3764	17.3763	0.00	17.3481	-0.16
1000	0	1000	0	16.8844	16.884	0.00	16.7639	-0.71
1000	0	0	10	14.9914	14.9912	0.00	14.9841	-0.05
1000	10	10	5	17.6045	17.6041	0.00	17.5453	-0.34
1000	1000	1000	1000	23.6085	23.6084	0.00	23.5853	-0.10

- continued -

Table 11. Comparison Between Solutions No. 1, 2 and 3 (continued)

(R = 0.2)

Restraint Parameters				Solution	Frequency Parameters			
					Solution No. 2		Solution No. 3	
β_1	β_2	β_3	β_4	No. 1	ω	Error %	ω	Error %
0	1	1	5	13.6392	13.6392	0.00	13.6321	-0.05
0	0	5	1000	18.6383	18.6383	0.00	18.6453	0.04
0	0	1000	1000	22.504	22.5043	0.00	22.5024	-0.01
0	5	5	5	15.4655	15.4655	0.00	15.4349	-0.20
1	5	1	5	13.6483	13.6483	0.00	13.6412	-0.05
1	5	5	1000	18.6467	18.6467	0.00	18.6537	0.04
5	1000	5	1000	18.6819	18.6819	0.00	18.6879	0.03
5	5	1000	1000	22.5143	22.5146	0.00	22.512	-0.01
5	1000	1000	1000	22.5426	22.5429	0.00	22.5399	-0.01
10	1	5	10	16.4766	16.4766	0.00	16.453	-0.14
1000	0	1000	0	15.739	15.7389	0.00	15.6305	-0.69
1000	0	0	10	13.7955	13.7954	0.00	13.797	0.01
1000	10	10	5	16.5109	16.5108	0.00	16.4617	-0.30
1000	1000	1000	1000	22.57	22.5702	0.00	22.5646	-0.02

only. Moreover, its accuracy is extremely high as seen in Table 11.

Although that expression is relatively long it is by far the simplest formula available for the frequency of such a plate problem. Computing the plate frequencies from this formula is not, by any means, more laborious than many calculations that are frequently performed by the practical engineer.

A Rational Function Approach to the Problem

In the foregoing analysis approximate solutions for the frequencies of vibration were obtained for the general case of unequal edge restraints. These solutions are highly accurate and yet do not require a great amount of work for the numerical evaluation of the frequency parameters. Once a series of such results exists, the solution can be expressed in a simple algebraic formula by the use of a rational function technique. The resulting expressions are not only useful for practical applications but they prove valuable for further analytical investigations.

As before we shall start with the simpler cases and then build up to the more general.

Plates with Equal Restraints on all Edges

The vibrations of a square plate subjected to equal elastic rotational restraint on all edges is considered first. Defining β as the restraint parameter and $\omega_{\beta\beta\beta\beta}$ as the frequency parameter, then in view of our previous experience, we write

$$\omega_{\beta\beta\beta\beta} = \frac{a\ \omega_{0000} + \beta\ \omega_{\infty\ \infty\ \infty\ \infty}}{a + \beta} \tag{2-7}$$

This formula clearly satisfies the extreme conditions and the value of β which gives the best general fit is determined by numerical analysis. When $\beta = 1$, $\omega_{1111} = 21.5$, and when these conditions are met the value of 'a' is determined to be 8.25 and thus Equation (2-7) becomes

$$\omega_{\beta\beta\beta\beta} = \frac{8.25\ \omega_{0000} + \beta\ \omega_{\infty\ \infty\ \infty\ \infty}}{8.25 + \beta} \tag{2-8}$$

in which the error in the frequency does not exceed 0.5% over the whole range of β(0 to ∞).

We recognize that the solution for the rectangular plate must degenerate to the solution for the square plate. Thus we assume that the solution for the general case of the aspect ratio other than unity can be written as

$$\omega_{\beta\beta\beta\beta}(R) = \frac{a(R)\ \omega_{0000}(R) + \beta\ \omega_{\infty\ \infty\ \infty\ \infty}(R)}{a(R) + \beta} \tag{2-9}$$

where

$a(R)$ is a coefficient, function of R which has the value 8.25 when R = 1

$\omega_{0000}(R)$ and $\omega_{\infty\ \infty\ \infty\ \infty}(R)$ are the values of the extreme frequency parameters at the appropriate R.

Table 12 summarizes all the appropriate data obtained from and used in the evaluation of Equation (2-9). It is clearly seen that the result is well within normal acceptable tolerances under all conditions.

Equation (2-9) in the form now established opens the way to further generalisation. Each of the functions $a(R)$, $\omega_{0000}(R)$ and $\omega_{\infty\infty\infty\infty}(R)$ can undoubtly be expressed as explicit functions of R. The pertinent formulae are

$$a(R) = 7.35 + 0.9 \sin \pi \left(R - \frac{1}{2}\right) \tag{2-10}$$

$$\omega_{0000}(R) = \pi^2 (1 + R^2) \tag{2-11}$$

$$\omega_{\infty\infty\infty\infty}(R) = 22.4 + 13.6R^{2.645} \tag{2-12}$$

Equation (2-10) is in good agreement with the values of $a(R)$ given in Table 12. The errors in Equations (2-11) and (2-12) are given in Table 13 where it is clear that both formulae are virtually exact.

By substituting Equations (2-10), (2-11) and (2-12) into (2-9) we obtain a general approximate expression for the frequency of the rectangular plate with edges subjected to equal elastic rotational restraints, viz,

$$\omega_{\beta\beta\beta\beta}(R) = \frac{a(R)\ \pi^2(1 + R^2) + \beta(22.4 + 13.6R^{2.645})}{a(R) + \beta} \tag{2-13}$$

Table 12. Data Related to Equation (2-9)

R	$\omega(R)_{0\,0\,0\,0}$	$\omega(R)_{\infty\,\infty\,\infty\,\infty}$	a(R)	Maximum Error %* in ω as Obtained by Equation (2.9)
1.0	19.74	35.99	8.25	0.43 at $\beta = 10$
0.8	16.19	29.9	8.14	0.42 at $\beta = 10$
0.6	13.42	25.9	7.64	0.39 at $\beta = 5$
0.4	11.45	23.65	7.04	0.75 at $\beta = 10$
0.2	10.26	22.64	6.59	1.00 at $\beta = 10$

* Error obtained by comparison to Solution No. 1.

Table 13. Errors in Equations (2-11) and (2-12)

R	ERROR %	
	$\omega_{0000}(R) = \pi^2(1 + R^2)$	$\omega_{\infty\infty\infty\infty}(R) = 22.4 + 13.6R^{2.645}$
1.0	0.00	0.00
0.8	0.00	0.20
0.6	0.00	0.08
0.4	0.00	-0.19
0.2	0.00	-0.21
0.0	0.00	0.0

where a(R) is given by Equation (2-10). The accuracy of the formula (2-13) is given in Table 14 and it is seen that for the practical range of R($0.2 \leq R \leq 1$) the error is nowhere greater than 1% and in most cases a good deal less.

Table 14. Percentage Error in Equation (2-13)

β	R					
	1	0.8	0.6	0.4	0.2	0
0	0.00	0.00	0.00	0.00	0.00	0.00
.5	-0.04	-0.02	-0.03	-0.11	-0.15	-0.1
1	-0.03	0.01	0.00	-0.10	0.11	0.00
2	0.03	0.11	0.13	0.05	0.12	0.32
5	0.23	0.37	0.46	0.42	0.64	1.00
10	0.35	0.52	0.62	0.58	0.84	1.26
100	-0.06	0.08	0.1	-0.1	0.04	0.46
1000	-0.27	-0.14	-0.15	-0.38	-0.26	0.16

Plates with Equal Restraints on Opposite Edges

Analogous to the arithmetic and geometrical mean relations which were successfully used for the beam with unequal end restraints, it seems likely that some form of averaging might be pertinent to the plate problem.

For the square plate a geometric mean relation such as

$$\omega_{1122} = \sqrt{\omega_{1111}\ \omega_{2222}}$$

can be demonstrated to yield errors as high as 9%. On the other hand if we chose an arithemetic mean law viz

$$\omega_{1122} = \frac{\omega_{1111} + \omega_{2222}}{2}$$

we obtain results of 4% error. However, simple manipulation shows that for the square plate the frequency is accurately obtained by using a root mean square law which can be written as

$$\omega_{1122} = \sqrt{\frac{\omega_{1111}^2 + \omega_{2222}^2}{2}} \qquad (2\text{-}14)$$

By using Equation (2-13) to evaluate ω_{1111} and ω_{2222}, the error in the above formula was calculated for all the range of β_1 and β_2 and given in Table 15. It is seen that the maximum error is less than 0.5%.

It is obvious that for a square plate $\omega_{1122} = \omega_{2211}$. Therefore we conclude that

$$\omega_{1122}^2 + \omega_{2211}^2 = \omega_{1111}^2 + \omega_{2222}^2 \qquad (2\text{-}15)$$

Table 15. Accuracy of Equation (2-14)

	Error %							
	β_2							
β_1	0	.5	1	2	5	10	100	1000
0	0.00	-0.02	-0.02	0.02	0.15	0.27	0.21	0.13
.5		-0.04	-0.04	0.00	0.13	0.24	0.19	0.17
1			-0.03	0.00	0.13	0.24	0.18	0.11
2				0.03	0.14	0.25	0.18	0.11
5					0.29	0.30	0.2	0.13
10						0.35	0.2	0.12
100							-0.06	-0.16
1000								-0.27

By referring to the numerical values of the frequencies which can be obtained by use of the solutions developed in the previous sections, one can verify that the same relation (2-15) equally applies to the rectangular plate. Therefore, for a plate with any aspect ratio R one may write the relation

$$\omega_{1122} = \sqrt{\frac{\omega_{1111}^2 + \omega_{2222}^2}{2} + \delta} \qquad (2\text{-}16)$$

and its conjugate

$$\omega_{2211} = \sqrt{\frac{\omega_{1111}^2 + \omega_{2222}^2}{2} - \delta}$$

where δ is obviously equal to zero when R = 1, and thus in general, it ought to be a function of R. For Equation (2-16) to be dimensionally correct δ must have the dimensions of frequency squared. Since there is no known unique way to express δ as a function of both R and ω^2, one may choose the following form

$$\delta = f(\omega^2) \cdot \varphi(R)$$

For any aspect ratio, the magnitude of ω_{1122} falls between ω_{1111} and ω_{2222}. Thus, referring to Equation (2-16) one may write δ in the form

$$\delta = \frac{\omega_{2222}^2 - \omega_{1111}^2}{2} \cdot \varphi(R) \qquad (2\text{-}17)$$

and adjust $\varphi(R)$ accordingly.

Obviously for $R = 1$, $\varphi(R)$ equals zero, and for $R = 0$ $\omega_{1122}^2 = \omega_{2222}^2$ thus $\varphi(R) = 1$. However to completely define $\varphi(R)$ over the whole range of $0 \leq R \leq 1$ we need to resort to specific values of β_1 and β_2. Considering $\beta_1 = 0$ and $\beta_2 = 1000$, $\varphi(R)$ can be evaluated at $R = .8$, $.6$, $.4$ and $.2$ as given in Table 16.

Table 16. Numerical Values of $\varphi(R)$

R	1	.8	.6	.4	.2	0
$\varphi(R)$	0	.372	.702	.909	.995	1.0

Those numerical values can be represented by the following simple relation.

$$\varphi(R) = 1 - R^{2.5} \qquad (2\text{-}18)$$

and therefore substituting Equations (2-17) and (2-18) into (2-16) we get

$$\omega_{1122}(R)=\sqrt{\frac{\omega_{1111}^2(R)+\omega_{2222}^2(R)}{2}+\left(\frac{\omega_{2222}^2(R)-\omega_{1111}^2(R)}{2}\right)\left(1-R^{2.5}\right)} \qquad (2\text{-}19)$$

Although the function $\varphi(R)$ as given by Equation (2-18) was fitted to specific values of the edge restraint parameters β_1 and β_2, it is numerically verified to be a good approximation for all other values of the equal and opposite restraints. This is shown in Table 17 where the frequencies obtained by Equation (2-19) are compared to the more accurate values. It is clear that the error over all the ranges of R, β_1 and β_2 is less than 2%.

Plates with Unequal Restraints on All Edges

In order to deal with the general case of unequal restraints on all edges it is feasible first to consider the situation when the restraints are equal on two opposite edges and unequal on the other two. In such a situation one would expect the plate to follow the law pertinent to the beam with unsymmetric end conditions. Thus

$$\sqrt{\omega_{1233}} = \frac{\sqrt{\omega_{1133}} + \sqrt{\omega_{2233}}}{2}$$

and

$$\sqrt{\omega_{1244}} = \frac{\sqrt{\omega_{1144}} + \sqrt{\omega_{2244}}}{2}$$

and consequently

Table 17. Percentage Error in Equation (2-19)

R	β_1	β_2							
		0	.5	1	2	5	10	100	1000
.8	0.0	0.00	0.01	0.06	0.2	0.58	0.94	1.34	1.35
	0.5	-0.03	-0.02	0.03	0.17	0.55	0.90	1.31	1.32
	1.0	-0.05	-0.04	0.01	0.15	0.53	0.86	1.29	1.29
	2.0	-0.09	-0.07	-0.02	0.11	0.48	0.83	1.24	1.24
	5.0	-0.19	-0.17	-0.12	0.01	0.37	0.70	1.10	1.11
	10.0	-0.37	-0.34	-0.29	-0.16	0.19	0.52	0.91	0.91
	100.0	-1.3	-1.22	-1.15	-1.00	-0.63	-0.3	0.08	0.08
	1000.0	-1.54	-1.47	-1.4	-1.23	-0.85	-0.52	-0.14	-0.14
.6	0.0	0.00	-0.15	-0.21	-0.19	0.04	0.27	0.31	0.24
	0.5	0.13	-0.03	-0.09	-0.09	0.12	0.33	0.35	0.28
	1.0	0.25	0.08	0.00	0.00	0.19	0.38	0.39	0.31
	2.0	0.43	0.24	0.16	0.13	0.29	0.47	0.44	0.36
	5.0	0.71	0.51	0.41	0.36	0.46	0.59	0.51	0.43
	10.0	0.80	0.6	0.5	0.43	0.51	0.62	0.51	0.42
	100.0	0.12	-0.01	-0.06	-0.07	-0.06	0.2	0.10	0.00
	1000.0	-0.16	-0.26	-0.3	-0.29	-0.12	0.03	-0.03	-0.15

Table 17. Percentage Error in Equation (2-19) - continued

R	β_1	β_2							
		0	.5	1	2	5	10	100	1000
	0.0	0.00	-0.27	-0.36	-0.35	-0.11	0.04	-0.34	-0.56
	0.5	0.18	-0.11	-0.22	-0.23	-0.02	0.11	-0.33	-0.51
	1.0	0.33	0.03	-0.10	-0.13	0.05	0.17	-0.29	-0.48
	2.0	0.59	0.26	0.11	0.05	0.18	0.27	-0.22	-0.41
.4	5.0	1.06	0.68	0.49	0.37	0.42	0.46	-0.1	-0.3
	10.0	1.38	0.96	0.75	0.59	0.58	0.58	-0.03	-0.24
	100.0	1.35	0.96	0.75	0.6	0.57	0.55	-0.1	-0.32
	1000.0	1.21	0.84	0.65	0.50	0.50	0.49	-0.16	-0.38
	0.0	0.00	-0.20	-0.19	-0.01	0.48	0.67	-0.05	-0.32
	0.5	0.06	-0.15	-0.15	0.03	0.50	0.69	-0.04	-0.31
	1.0	0.12	-0.10	-0.11	0.06	0.53	0.71	-0.03	-0.30
	2.0	0.21	-0.02	-0.04	0.12	0.57	0.74	-0.01	-0.28
.2	5.0	0.38	0.13	0.09	0.23	0.64	0.80	0.03	-0.25
	10.0	0.5	0.23	0.18	0.30	0.69	0.84	0.05	-0.23
	100.0	0.54	0.26	0.21	0.32	0.70	0.84	0.04	-0.24
	1000.0	0.50	0.23	0.18	0.29	0.68	0.82	0.02	-0.26

$$\sqrt{\omega_{1234}} = \frac{\sqrt{\omega_{1133}} + \sqrt{\omega_{2233}} + \sqrt{\omega_{1144}} + \sqrt{\omega_{2244}}}{4} \qquad (2\text{-}20)$$

The error in the frequency obtained by this formula is shown in Table 18 for wide ranges of the restraint parameters and at several values of the plate aspect ratio. It is concluded that the maximum error is approximately 3.5% and occurs when the plate is square and the edge restraint parameters are (0, ∞, 0, ∞).

Discussion

The solution designated as No. 1 was developed to fill in a gap which existed in literature with regard to the frequency of vibration of the rectangular plate whose edges are unequally restrained. The solution was then used as a basis for comparing the much simpler approximate formulae which were developed throughout the chapter. The question of the accuracy of that solution cannot be handled without having to resort to rigorous analysis and elaborate computations. There are means of assessing the accuracy of the frequency as obtained by solution No. 1 [24,25]. However, such analysis is obviously beyond the scope of the present work.

We have compared solution No. 1 to other solutions which were obtained by more elaborate and lengthy calculations. The comparison was held at specific values of the restraint parameters and geometric ratio which are published in literature. It was shown that by using a one term generating function, estimates of the frequency can be obtained which differ only by less than 1% from those obtained by

Table 18. Error in Formula (2-20)

Restraint Serial Number	Restraint Parameters				R = 1		
					ω_{1234}		
	β_1	β_2	β_3	β_4	Exact*	Approx.	Error %
1	0	1	0	1	20.6234	20.6228	.00
2	0	1	1	5	22.1815	22.2162	.16
3	0	1	5	10	24.1127	24.1742	.26
4	0	0	5	1000	25.6479	25.8957	.97
5	0	0	1000	1000	28.9118	28.9489	.13
6	0	5	5	5	24.3329	24.423	.37
7	0	10	0	10	24.0419	24.2932	1.05
8	1	5	1	5	23.6385	23.7113	.31
9	1	5	5	1000	27.2564	27.5464	1.06
10	1	5	10	1000	28.1149	28.3215	.73
11	5	1000	5	1000	30.4926	30.9695	1.56
12	5	5	1000	1000	31.2327	31.2728	.13
13	5	1000	1000	1000	33.3264	33.5305	.61
14	10	0	5	1000	27.4449	27.8245	1.38
15	1000	0	0	10	25.6254	26.2158	2.3
16	1000	10	5	1	28.1149	28.3215	.73
17	1000	10	10	5	29.6738	29.8846	.71
18	1000	0	1000	0	27.1584	28.0704	3.36
19	1000	1000	1000	1000	35.9655	35.867	-.27

* Solution No. 1

Table 18. (continued)

Restraint Serial Number	R = .8 ω_{1234}			R = .6 ω_{1234}		
	Exact*	Approx.	Error %	Exact*	Approx.	Error %
1	16.9436	16.9454	.01	14.147	14.1444	-.02
2	18.7743	18.85	.40	16.2639	16.2732	.06
3	20.9811	21.1476	.79	18.7335	18.7854	.28
4	22.8115	23.247	1.91	20.7584	20.9868	1.1
5	26.2926	26.6459	1.34	24.4192	24.4776	.24
6	20.641	20.756	.56	18.0241	18.0667	.24
7	19.8318	20.0293	1.00	16.7916	16.9175	.75
8	19.5108	19.5822	.37	16.5534	16.6086	.33
9	23.5857	24.016	1.82	21.0478	21.3244	1.31
10	24.5573	24.9379	1.55	22.1176	22.3286	.96
11	25.2769	25.6733	1.57	21.7558	22.0561	1.38
12	27.3848	27.688	1.11	24.8161	24.9217	.43
13	28.4892	28.7476	.91	25.2923	25.3724	.32
14	23.7132	24.1618	1.89	21.1222	21.3911	1.27
15	20.7518	21.0495	1.43	17.2416	17.4038	.94
16	21.9431	21.9186	-.11	17.6062	17.6879	.46
17	23.8678	23.9189	.21	19.9163	20.016	.50
18	22.4218	23.114	3.09	19.0398	19.4962	2.4
19	29.8698	29.827	-.14	25.8664	25.8271	-.15

Table 18. (continued)

Restraint Serial Number	R = .4 ω_{1234}			R = .2 ω_{1234}		
	Exact*	Approx.	Error %	Exact*	Approx.	Erro %
1	12.2087	12.1935	-1.3	11.082	11.0591	-.21
2	14.5844	14.5579	- .18	13.6392	13.6432	.03
3	17.2687	17.2835	.09	16.4613	16.567	.64
4	19.4003	19.5159	.60	18.6383	18.8221	.99
5	23.1904	23.0612	- .56	22.504	22.4317	-.32
6	16.3576	16.3749	.11	15.4655	15.5486	.54
7	14.8236	14.8594	.24	13.7599	13.7366	-.17
8	14.6598	14.6816	.15	13.6483	13.6663	.13
9	19.4723	19.6356	.84	18.6467	18.8436	1.06
10	20.6138	20.7097	.47	19.8293	19.9778	.75
11	19.6852	19.8918	1.05	18.6819	18.8891	1.11
12	23.2854	23.2149	- .3	22.5143	22.459	-.25
13	23.4387	23.367	- .31	22.5426	22.4853	-.25
14	19.5061	19.6594	.79	18.6552	18.8479	1.03
15	14.9914	15.043	.34	13.7955	13.7715	-.17
16.	14.9768	15.0774	.67	13.698	13.7393	.30
17	17.6045	17.7177	.64	16.5109	16.6446	.81
18	16.8844	17.1173	1.38	15.739	15.8313	.59
19	23.6085	23.5196	- .38	22.57	22.5116	-.26

using generating functions consisting of 36 term series.

It is known that in such a solution the errors in the frequency estimate depend to the second order on the deviation of the assumed mode function from the exact form. Therefore, one expects that the maximum errors in solution No. 1 would take place when the assumed mode shape is at its maximum disagreement with the actual shape. This happens when the plate vibrates in a mode in which the nodal lines are no longer straight lines parallel to the edges. This kind of a mode was met before in conjunction with the fourth and fifth modes of a square plate as shown in Table 9. The error was seen to be within 0.5%.

A second case was investigated, namely the case of the plate with two adjacent sides simply supported and the other two clamped. The mode shape was taken as a combination of the two principal terms, namely

$$W = a_1 W_2(x) W_1(y) + a_2 W_1(x) W_2(y)$$

$$= a_1 \psi_1 + a_2 \psi_2$$

where

$W_1(x)$, $W_2(x)$, $W_1(y)$ and $W_2(y)$ are the 1st and 2nd mode shapes of a beam along the x and y directions respectively.

a_1 and a_2 are parameters to be adjusted

$\psi_1 = W_2(x) \quad W_1(y)$

$\psi_2 = W_1(x) \quad W_2(y)$

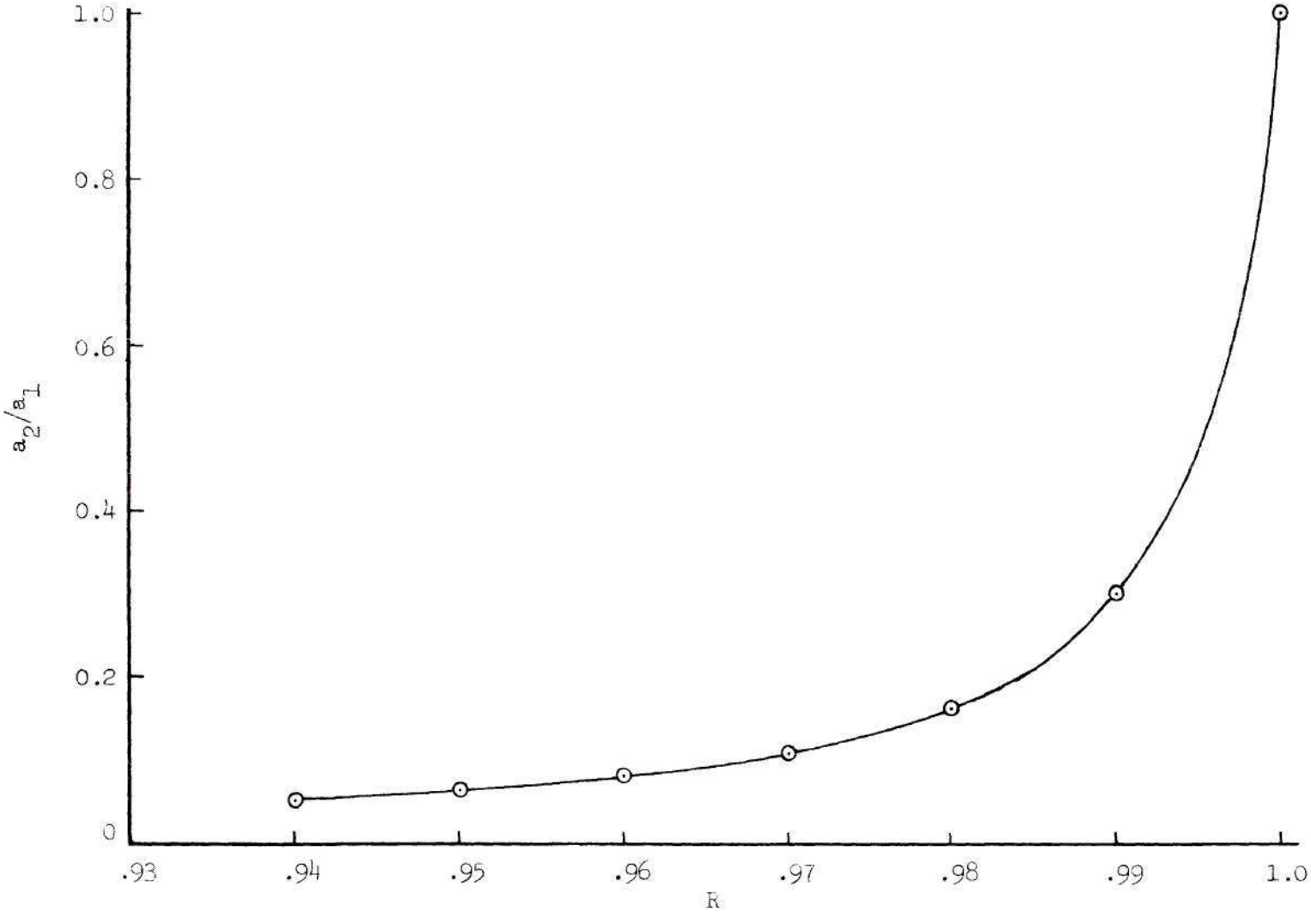

Figure 3. Ratio of the Coefficients a_1 & a_2.

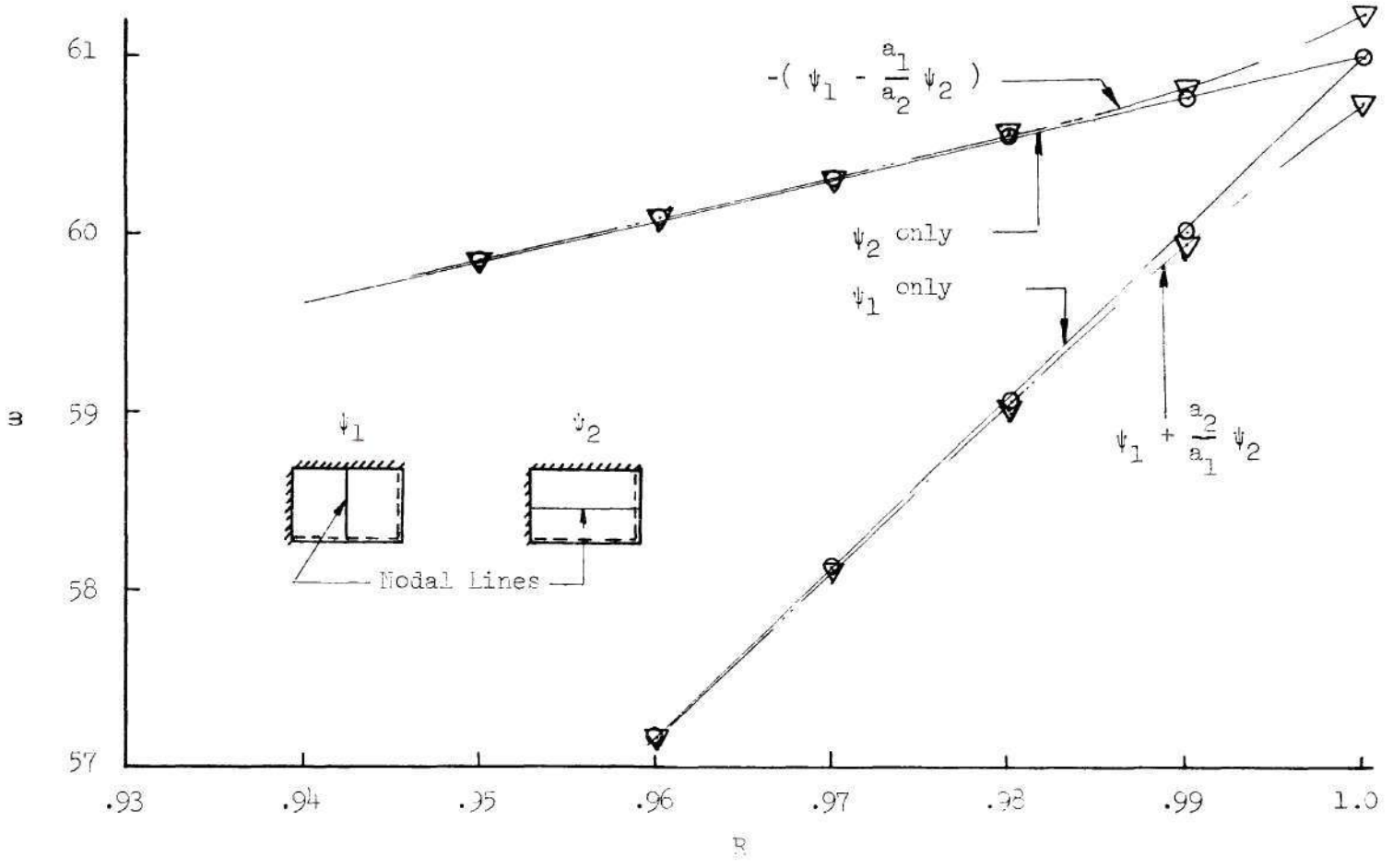

Figure 4. Comparison Between the Frequencies Corresponding to $a_1\psi_1 \pm a_2\psi_2$ Modes and those Corresponding to ψ_1 & ψ_2 Modes.

A typical Rayleigh-Ritz solution was carried out. The determinant of the coefficients of a_1 and a_2 was expanded and the frequency parameters were obtained at several geometric ratios. The corresponding ratios of a_1 and a_2 were also determined as shown in Figure 3. In Figure 4 the frequency results are plotted and compared to the results obtained by use of generating functions consisting of one term only, namely

$$W = W_2(x) \quad W_1(y)$$

and

$$W = W_1(x) \quad W_2(y)$$

Obviously the maximum error occurs when the plate is square in which case we have either $a_2/a_1 = -1$ and $\omega = 61.2519$ or $a_2/a_1 = 1$ and $\omega = 60.7594$. The frequency obtained by the one-term solution was 61.0062 which is within $\pm$ 0.4% from the above values respectively.

Conclusion

In this chapter simple approximate formulae are developed for the frequencies of vibration of rectangular plates with unequal elastic rotational restraints at the edges. The accuracies of the formulae are extremely suitable for engineering applications.

CHAPTER III

THE USE OF THE DYNAMIC RESPONSES FOR THE DETERMINATION OF THE CRITICAL AXIAL LOADS OF STRUCTURES

Introduction

In the preceding chapters the vibrational characteristics of elastically restrained structures were formulated in a simple approximate manner. The work of Singhal [35] shows that for the case of axially loaded beams similar simple formulations are obtained for the buckling loads. A situation which strongly suggests a direct correlation between the vibrational and instability parameters.

In this chapter the relationship between the dynamic characteristics and the instability behavior of axially loaded structures will be studied. The investigation aims at developing a nondestructive testing method for the determination of the actual buckling loads. The problem of nondestructive testing is of upmost interest to both experimental as well as analytical engineers especially those dealing with shell structures. The issue is not new and a variety of techniques and concepts have been developed in dealing therewith.

Such techniques included methods of analyzing the prebuckle deformations, processes for restricting the lateral displacements so as to avoid sudden catastrophic collapses and techniques for associating the instability load with the vibrational characteristics. In more recent times there has been some attention paid to the variation of

the lateral stiffness with the axial load.

The analysis of prebuckle deformations is, generally speaking, made using the so called "Southwell Plot," or some extension thereto [26]. This subject has been extensively reviewed and discussed in the literature. The application to problems of columns and plates is treated in depth in reference [27], while the applicability to shell structures is considered in detail in reference [28]. The method was applied to shells under combined loading [29] and to stiffened shells in axial compression [30]. It is abundantly clear from these works that there is considerable difficulty in the application of the method when the structure is highly sensitive under the considered loading conditions. This is, of course, especially true for cylindrical shells under axial compression. As indicated by Flügge [31], the prime difficulties experienced are the determination of the relevant observation point and the high magnitude of the applied axial force needed to generate meaningful data. This was also apparent in Ford's work [30].

The idea of using a physical restraint, a mandrel, to limit the lateral deflections associated with buckling was developed in references [32] and [33] and was used in testing small scale shell specimens. Such a method however became increasingly difficult to apply as the scale increased.

A recent concept in the non-destructive testing of structural elements is based on associating the buckling loads with the variation in the lateral stiffness. For a column, the idea that normal stiffness tends to zero as the load tends to the critical was known before, e.g.,

reference [34]. Physical intuition suggests that, for other structures of more complex nature the lateral static stiffness variation with destabilizing loads should be related to the critical conditions in a rational manner. Bank [5] has demonstrated experimentally that this is so and Singhal [35] has studied the issue in more detail. The results of their researches on cylindrical shells show that one can determine the buckling region and predict the critical load with good accuracy from the changes in wall stiffness.

The concept of relating vibrational characteristics with instability load levels extends back at least to the early years of this century when Sommerfeld [36] tested a clamped-free column, vertically mounted, with a variable mass attached to the free end. He observed that the natural frequency of the system decreased as the mass increased; ultimately approaching zero as the tip mass reached the level necessary to produce column instability. The buckling-vibration question was extensively investigated by Massonnett [37]. He analysed the behavior of uniform beams, plates and cylindrical as well as spherical shells and showed that in all cases the critical axial load and the square of the natural frequency were very nearly linearly related and that, the linear relationship becomes exact if the mode of free vibration is identical to the buckling mode. His work is amply supported by that of Lurie [38] who demonstrated that for a column with both ends simply supported, where buckling and vibration modes take the same shape, the linear law is exact. However, for other end fixities (between simply supported and clamped) he showed that the deviation

from linearity is small and can be ignored compared to ordinary experimental errors.

Lurie also verified experimentally the nearly straight line relation for a column whose ends were elastically restrained against rotation and was able to determine its buckling load from the vibrational data. His test specimen was a vertically mounted rectangular frame to which the axial load was applied on the two vertical sides and the horizontal members acted as elastic rotational restraints. He also tested stiffened and unstiffened panels and concluded from his work that the vibration method does not have practical application to flat plates. He considered that the technique failed because of non-linearities caused by large initial geometric imperfections. Massonet [39] derived the theoretical relationship between the square of the frequency and the edge thrust for a circular plate with initial curvature. He showed that the greater this curvature the greater the deviation from linearity. A result which gave substance to Lurie's conclusion with regard to plate structures.

The conclusions of the researches referenced were regarded as so substantial that no further efforts were made to use vibrational characteristics as criteria for the determination of instability. The failure to extend from the column to the plate stultified any research on shell bodies. But the concept of static stiffness variation cannot be differentiated from the concept of dynamic stiffness variation and it would therefore appear that by concentrating upon such a parameter a solution could be found.

Development of a Vibrational Method

As indicated in the prior section there are sound reasons to investigate the buckling-vibration relationship by considering dynamic properties other than the natural frequencies of vibration. For shell bodies which are most frequently liable to local rather than overall instability failure the dynamic stiffness, which clearly varies from point to point, is a more attractive correlation parameter than the natural frequency which has a more gross character.

The method investigated is thus directly related to the variation in the lateral dynamic stiffness with axial loading. Briefly the procedure is to pointwise excite the structure with a lateral shaking force at several levels of the axial loading. The dynamic response at the particular excitation points is measured for each load level and a plot is produced for the "Dynamic mass" vs. the applied axial load. The relationship is found to be linear and hence its intersection point with the axial load-axis determines the critical value.

The choice of the dynamic mass as a response parameter is due to the fact that it is directly proportional to the "dynamic stiffness" for a sinusoidal excitation at a fixed frequency. Besides it is defined to be the ratio of the shaking force to the resulting acceleration and both quantities are sensed directly by use of a single unit.

To demonstrate the method three basic structural elements were tested: a column, a flat panel and a cylindrical shell. The testing equipment, procedures and results are explained in detail in the remaining of this chapter.

Equipment and Instrumentation

Loading Arrangements

The tests were conducted in a 120,000 pound capacity Baldwin screwjack universal test machine. The shaking force was provided by MB Vibramate Exciter model PM25. This was driven by a PAR oscillator model 110 of sinusoidal output through a MB power amplifier model 2125. To ensure good positional control the shaker was mounted on a micrometer plate which in turn was seated on a vertically adjustable platform. Figure 5 is a general picture of the test site and Figure 6 shows a typical set up.

Measuring Circuit

The shaking force and the resulting acceleration of the test subject were measured at the excitation point. A B&K Impedance Head type 8001 was used as a force and acceleration transducer. A sketch of the head is shown in Figure 7. The output signals were conditioned by using MB Line Drivers and MB N400 signal amplifying units. The units provided an output voltage of 1 V RMS per full scale input. By proper calibration they permitted analog readout of either the peak or RMS values of the transducer signals directly in terms of force or acceleration units. The conditioned outputs were fed into a SD 101B Dynamic Analyser/Tracking Filter of 1.5 Hz bandwidth which was tuned to the excitation frequency. A two way switch was used to pass one signal at a time into the unit. The Dynamic Analyser provided a DC output proportional to the filtered signal. This output was then available for recording and/or direct reading. The excitation and measuring circuits are shown in Figure 8.

Figure 5. General View of the Test Site.

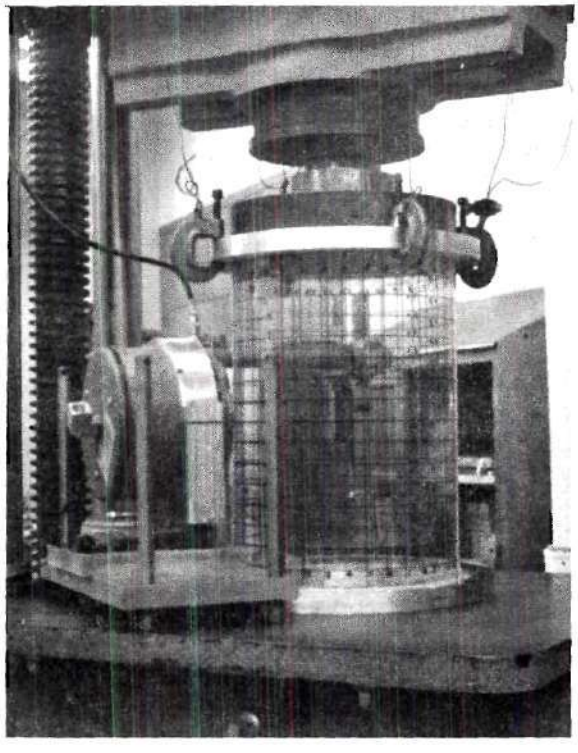

Figure 6. Typical Testing Setup.

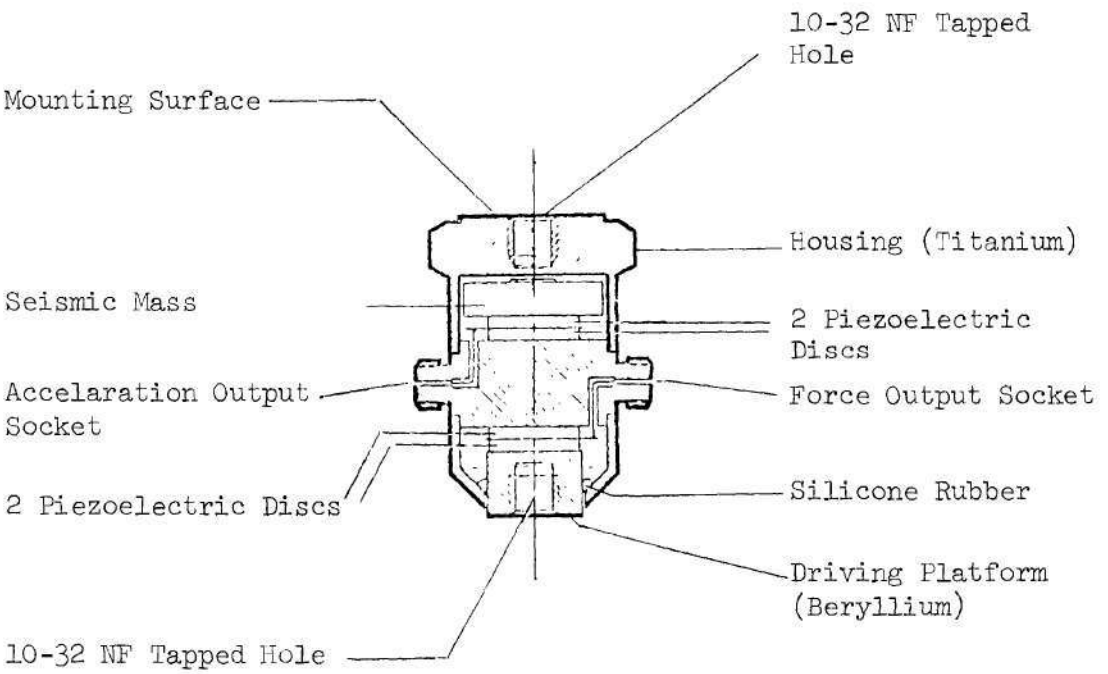

Figure 7. Schematic Drawing of the Impedance Head.

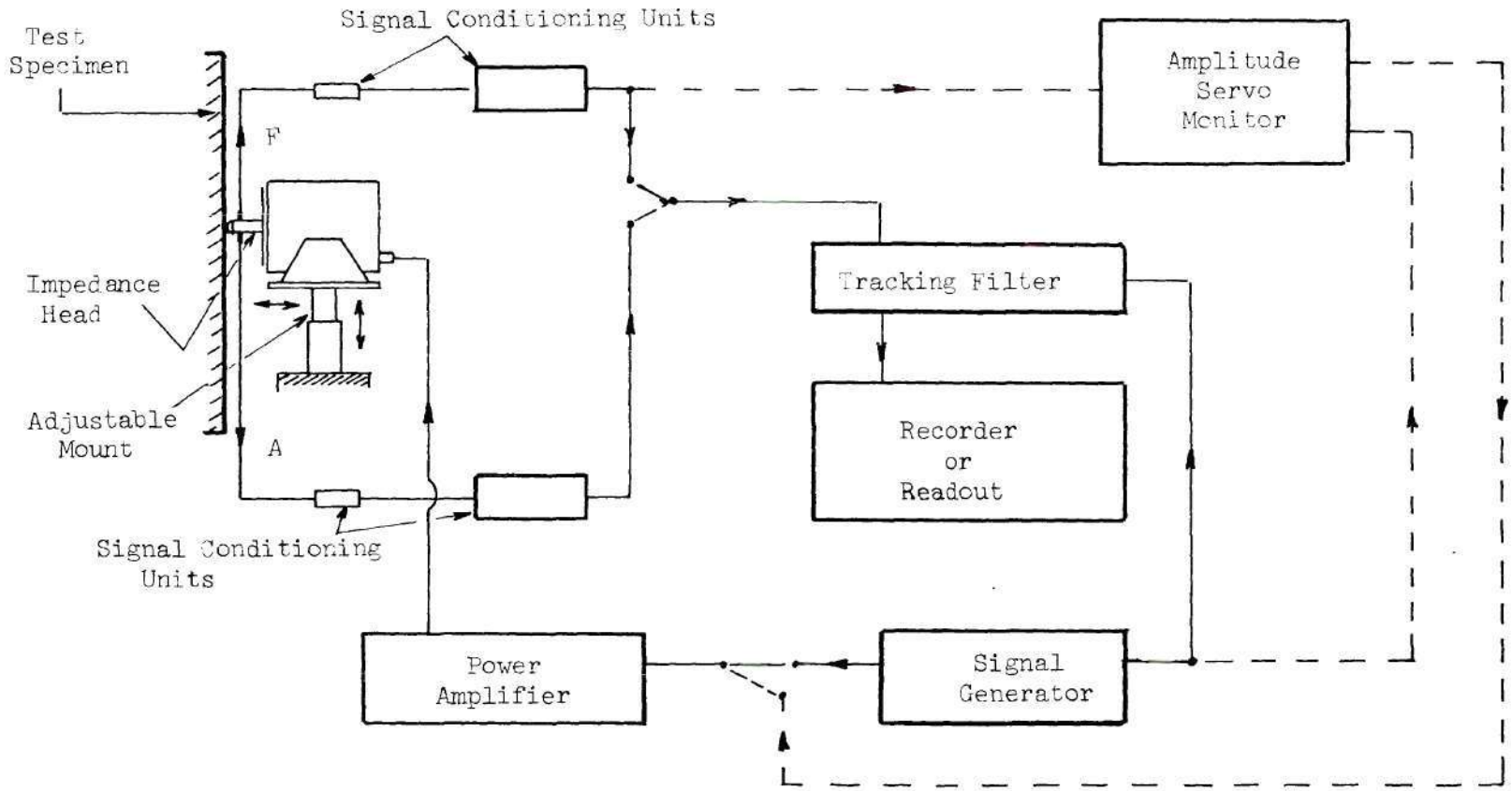

Figure 8. Excitation and Measuring Circuits

In some cases (in conjunction with the panel and shell testing), it was necessary to maintain the shaking force at a constant level. This was done by means of a SD105B Amplitude Servo Monitor. The appropriate circuitry is shown by the dashed lines in Figure 8. The SD105B monitored the force signal and provided the necessary adjusted excitation voltage to keep the shaking force at the desired level.

Data Acquisition and Processing

Recording and processing of the data was extremely simple. The tracking filter enabled direct readout of the filtered signal on its meter. The magnitude of the dynamic mass was obtained directly from the filtered force and acceleration signals.

In order to speed the testing process and to minimize errors the data acquisition and processing were partially automated. This was achieved by using a crossbar scanner and a HP 2402A integrating digital voltmeter interfaced with HP 2115A computer. The computer was programmed to control the operation of the crossbar scanner and the voltmeter and to process the measured signals. The execution of the program was partially controlled by the computer switch registers which were operated via a remote switch located at the test site. This permitted the operator to initiate the data acquisition whenever desired. The system is shown in Figure 9.

Column Testing

The test specimen used was fabricated from 2024 aluminum alloy rod 20-3/4" long of 1/2" x 1/2" square cross section with sloped edges milled on both ends.

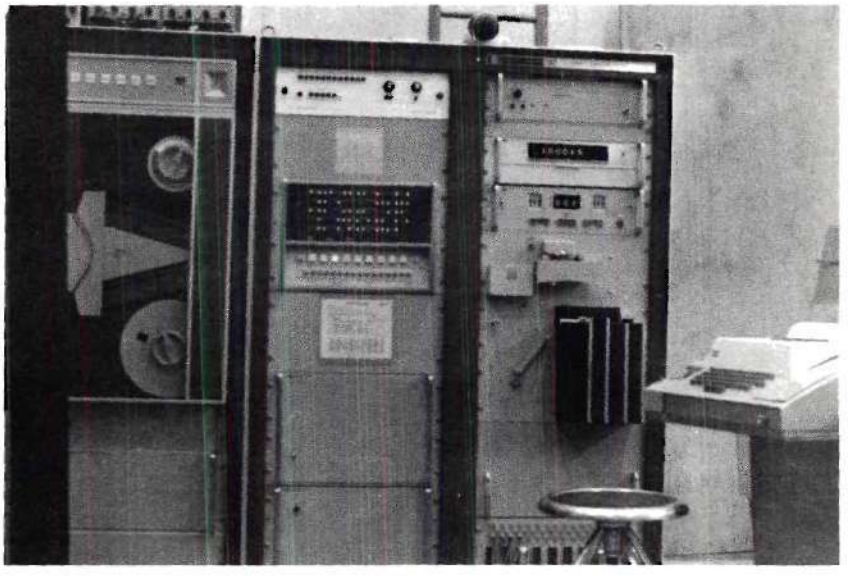

Figure 9. The Data Acquisition System.

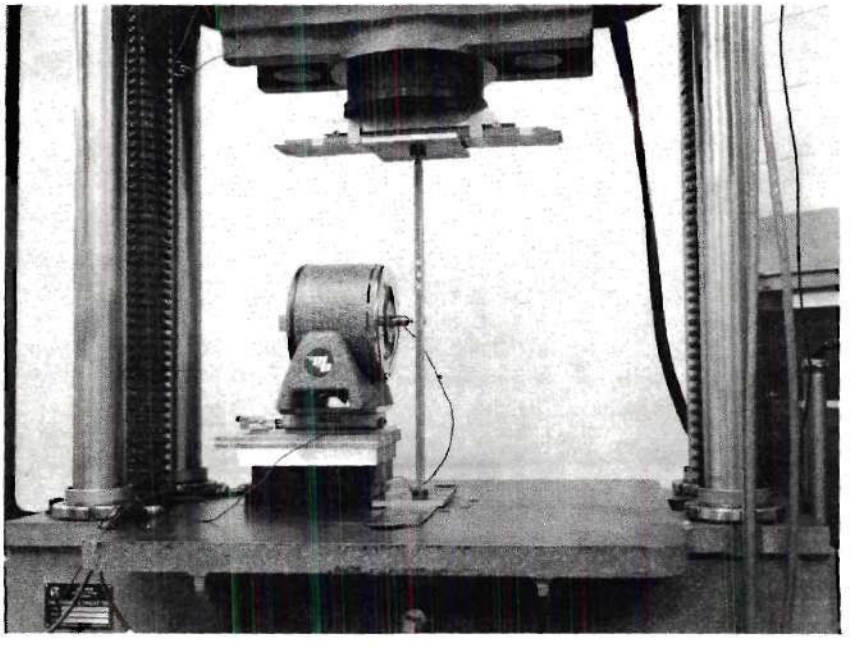

Figure 10. Setup for Column Testing.

The column was mounted in the test machine with its edges supported in hardened steel V-blocks to prevent end lateral displacement, Figure 10. Each block was mounted on a leaf spring which was built up of several steel strips. The use of such a spring was a precaution against possible fluctuation in the axial load during the vibration test.

The first step in the testing process was to determine the excitation levels of the frequency and force parameters. The natural frequency of vibration was roughly determined to be 110 Hz. Therefore, an operational range was chosen between 30 - 100 Hz. The force was determined such that the resulting deflection remains within small limits.

Readings of the shaking force and the resulting acceleration at the excitation point were then recorded for a broad spectrum of axial loads and shaking frequencies.

Results

Table 19 gives typical results obtained for the described column with the shaking force applied at the center. Plots of the dynamic mass M_D vs. the axial load P for several excitation frequencies are presented in Figure 11. For all frequencies the relationships are seen to be linear. As the axial load increases, the dynamic mass decreases until it reaches a minimum (nearly zero). This occurs when the loading level is such that the excitation frequency is the critical frequency. Therefore, from Figure 11 one can determine the natural frequencies of vibration of the column at several axial loading levels and thus one can construct the relationship between the axial load and the square of the natural frequency of vibration as

Table 19. Column Test Results

f		P										
Hz		100	200	300	400	500	600	700	800	900	1000	1100
	F(lb)	.056	.070	.04	.071	.022	.014	.004	.005	.013	.018	.015
70	A(g)	.308	.31	.311	.309	.305	.297	.289	.28	.27	.261	.266
	M_D(lb/g)	.181	.225	.129	.231	.073	.046	.014	.017	.047	.071	.055
	F(lb)	.033	.025	.018	.01	.003	.005	.011	.017	.023	.027	.024
80	A(g)	.349	.34	.33	.319	.308	.295	.282	.269	.257	.248	.253
	M_D(lb/g)	.095	.074	.054	.031	.01	.015	.039	.063	.088	.107	.094
	F(lb)	.012	.006	.002	.005	.01	.015	.02	.024	.028	.03	.028
90	A(g)	.333	.32	.307	.294	.282	.27	.258	.248	.237	.23	.234
	M_D(lb/g)	.037	.019	.005	.018	.036	.056	.076	.096	.117	.131	.121

- continued -

Table 19. (continued)

f		P										
Hz		100	200	300	400	500	600	700	800	900	1000	1100
	F(lb)	.003	.007	.01	.014	.017	.021	.024	.027	.03	.032	.031
100	A(g)	.298	.285	.274	.263	.253	.244	.235	.226	.217	.211	.215
	M_D(lb/g)	.01	.024	.038	.054	.069	.087	.103	.12	.139	.15	.143

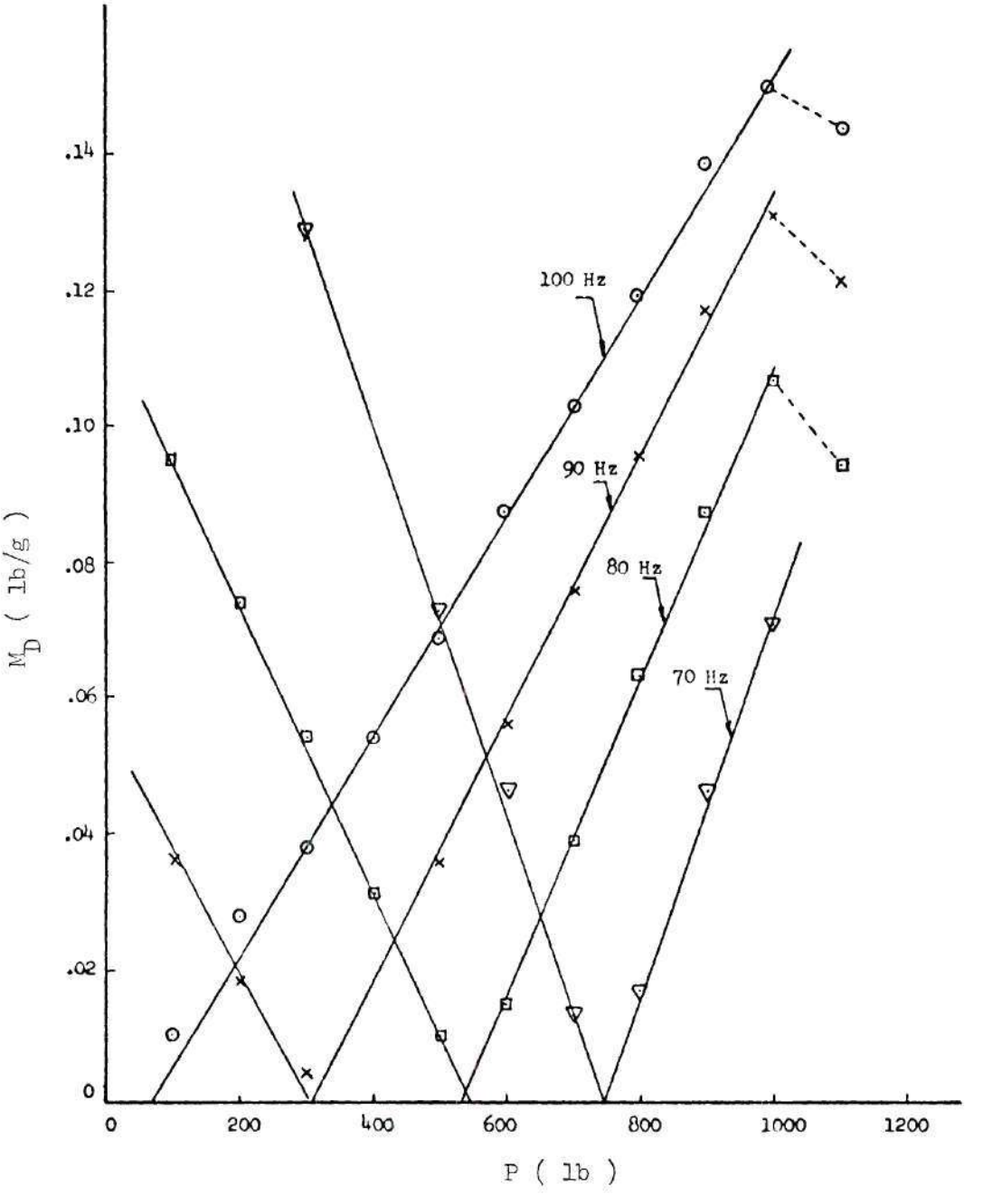

Figure 11. Column - M_D vs. P.

shown in Figure 12. It is clear that the relationship is linear, a result which agrees with the conclusions of Massonett [37] and Lurie [38]. This line cuts the f^2-axis at 10450 which indicates that the critical frequency is 102 Hz approximately. On the other hand the intersection of the line with the P-axis determines the buckling load as 1390 pounds.

The buckling load was also determined experimentally by the Southwell method. Using two strain gages mounted opposite to each other on the tensile and compression sides respectively the bending strains were determined at several levels of the axial loading. These are given in Table 20 and the Southwell Plot is shown in Figure 13. The critical load determined by this method was 1320 pounds. No attempt was made to calculate the theoretical critical load because the end conditions of the column were not exactly defined.

Table 20. Column Testing - Bending Strains

P (lb)	ϵ Micro in/in.	ϵ/P
10	0	0
100	21	.21
200	45	.225
300	74	.247
400	110	.275
500	154	.308
600	212	.353
700	293	.418
800	403	.504
900	580	.644
1000	886	.886

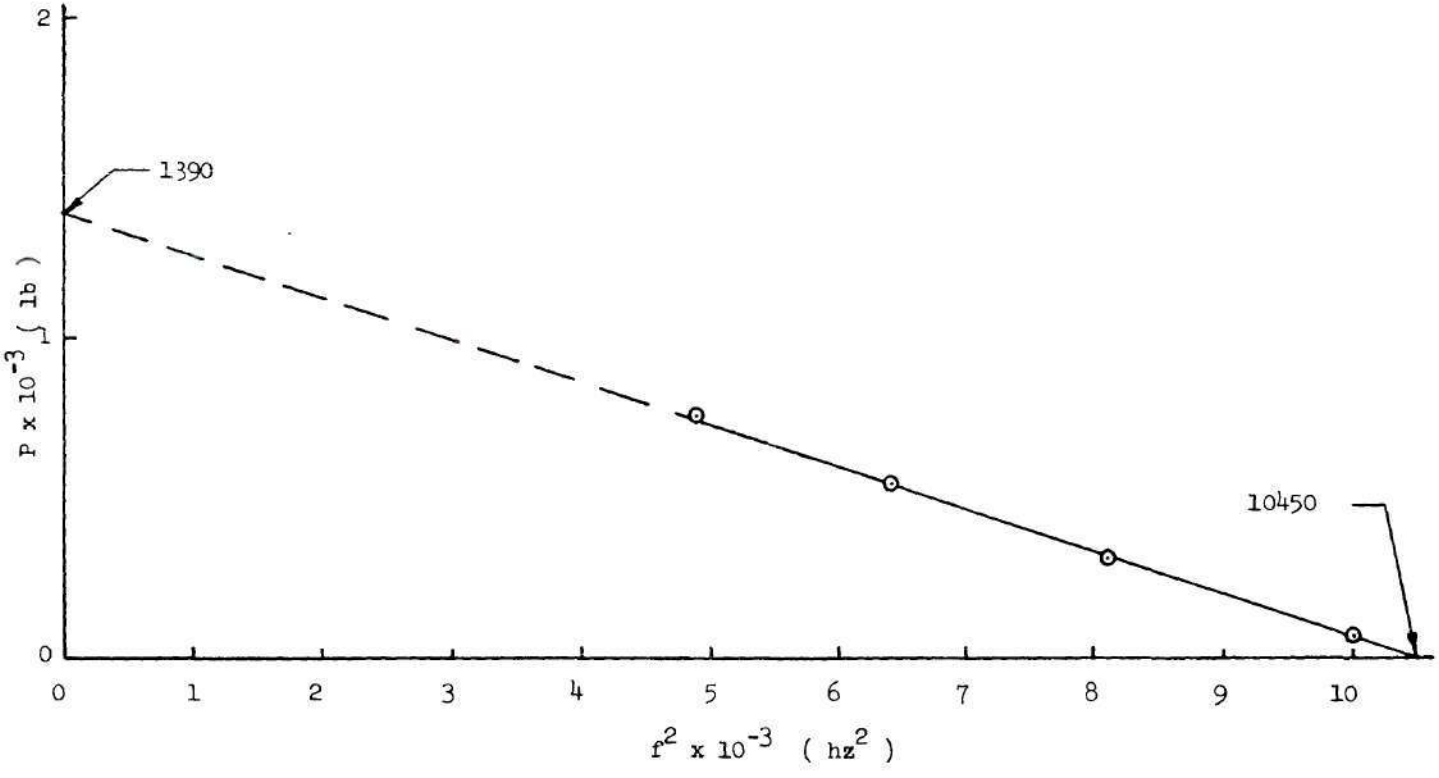

Figure 12. Column - P vs. f^2

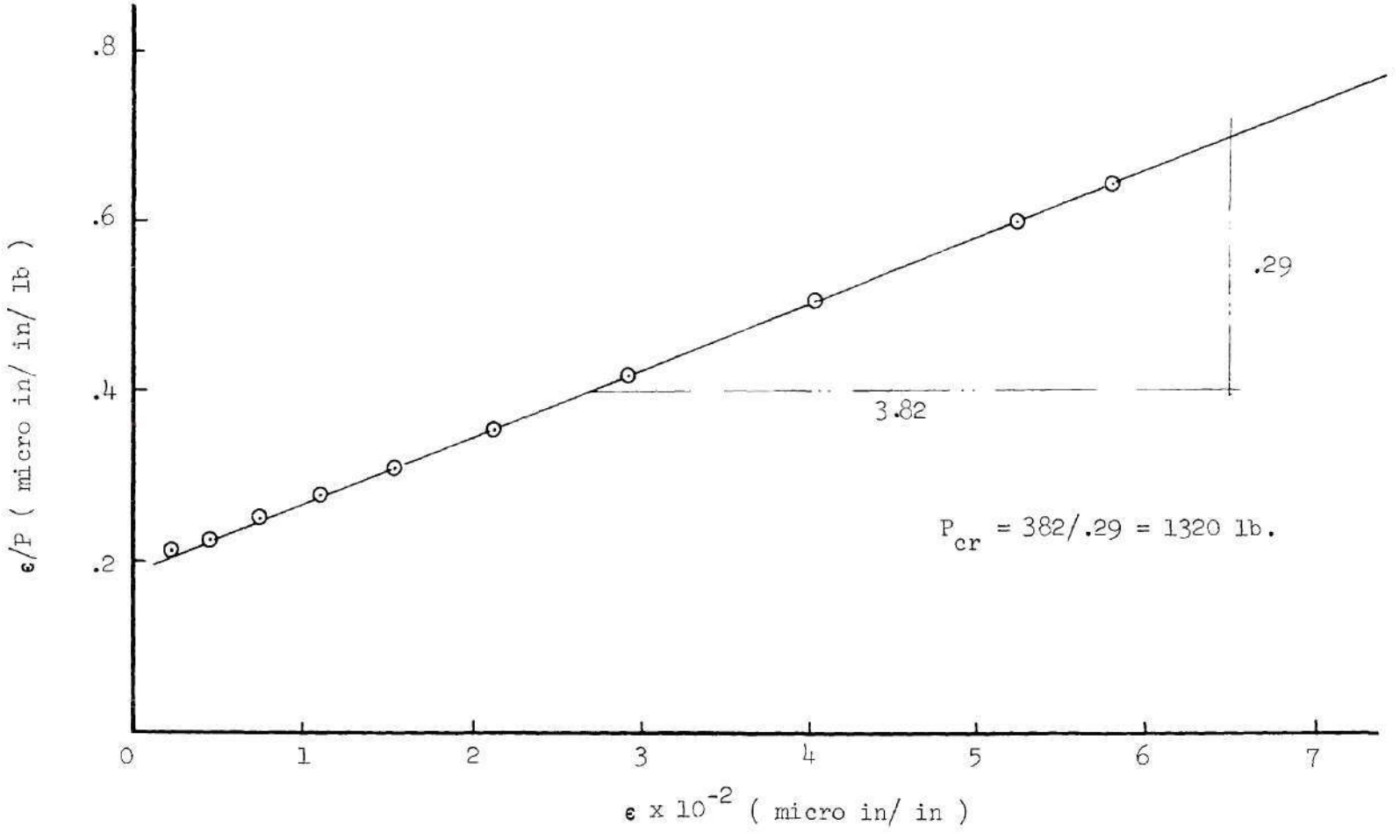

Figure 13. Column - Southwell Plot.

It should be emphasized that the purpose of testing the column was not to verify the results of references [37] and [38] but it was meant to investigate the relationship between dynamic responses, other than the natural frequency of vibration, and the axial load.

The linear variation of the dynamic mass with the increase in the axial load is of significance particularly if a similar variation could be obtained for the more complex structures. This would enable experimentally, to generate data leading to the determination of the critical loading conditions by only applying low levels of the axial force. That kind of reasoning is investigated in the remaining of this chapter.

Shell and Panel Testing

Testing Technique

In essence the philosophy underlying the testing of the shell and panel specimens is similar to that for the column. Basically we are seeking the relationship that describes the variation of the dynamic mass with the increase in the axial load. The aim is to utilize such a correlation in the determination of the critical buckling load. However, the testing technique for the shell and panel differs from that for the column in several respects. In the following we shall discuss these differences and present the method that will be used.

Location of the Observation Point. For shell and panel structures the dynamic mass will obviously go to "zero" when the axial load reaches the critical, only at the location where buckling is going to occur. In the case of the column it was clear that buckling would

take place in such a way that there would be only one half wave with the maximum deflection nearly at the column midpoint. However, for shell structures the situation is different; the location of the buckling is not known and therefore it is not readily obvious where to apply the shaking force.

Thus, the first task is to determine the region in which buckling would occur. For this purpose a complete scan of the shell surface has to be carried out in order to map the initial distribution of the dynamic mass and to determine the location of the minimum.

Method of Shaker - Structure Attachment. The method of attaching the impedance head to the structure is of practical importance. The nut and screw attachment as used in the case of the column becomes impractical in dealing with shell structures especially if a complete scan of the surface is to be done. Therefore it was necessary to search for a different technique which allows the impedance head-shaker combination to be attached to and detached from the structure in a relatively easy and efficient way. It was finally decided that the simpliest way is to apply an inward static deflection to the skin of the shell by the impedance head such that the elastic forces of the skin maintain continuous contact during the shaking movement. The continuity of such a "joint" can be monitored by observing an analog display of either of the force or the acceleration signals or both. Any noticed deviation from being smooth continuous curves would indicate a discontinuity in the follow-up of the structure to the shaker movement.

Testing Procedure. The procedure adopted for shell testing was developed from the test conducted on the column. It can be

summarized as follows:

1. One determines the area in which buckling is likely to occur first. This is done by carrying out a complete scan of the dynamic mass distribution around the surface of the shell and determining the area of the least. The level of the excitation force must be kept constant throughout the scan and this is achieved by introducing an amplitude monitor into the excitation circuit as shown in Figure 8. The location of the least M_D might be confirmed by repeated scans at additional increments of the axial load.

2. Having determined the expected location of the buckle, its center is marked on the shell and the shaking force is applied thereat.

Unlike the case of the column it is found that at a single excitation frequency, the variation of the dynamic mass with the increase in the axial loading is not in general linear. On the other hand measurements of the dynamic mass are found to be sensitive to the level of the excitation force F.

By studying the variation of the M_D with the increase in F one reveals the following relationship. For a fixed excitation frequency and axial load, if F is increased from zero, the dynamic mass is observed to decrease smoothly until it reaches a minimum and then increases again.

The relation is consistently similar for other axial loads and shaking frequencies. The magnitude of the minimum M_D and the corresponding shaking force obviously depend on the axial load and the excitation frequency. Typical relations as obtained for the elliptic and circular shells are shown later (e.g., Figures 21 through 25).

It is to be noted that, for columns the changes in M_D caused by variations in F do not exhibit the same characteristics as in the case of shells.

3. The last step is to determine the magnitude of the minimum M_D for each axial load level at a single excitation frequency. By plotting these minima against the corresponding axial loads one obtains a linear relationship which intersects the P-axis at the critical value.

The location of the intersection could be confirmed by plotting the results at other excitation frequencies.

Specimens

The shell and panel specimens were fabricated from plexiglass sheets of 0.030" nominal thickness. The ends were stiffened by 1/4" square cross-section rings of the same material. The method of manufacture was similar to that described by Ford [30]. The suitability of the material for the manufacture of models to simulate metallic structures was also verified in the above reference.

Three different configurations were tested, namely,

1. Unstiffened elliptic cylindrical shell with a cutout on one of the sides of minimum curvature.

2. Unstiffened circular cylindrical shell.

3. Unstiffened rectangular panel.

The dimensions and the geometric properties of each are given in Table 21.

The panel model was fabricated as a square cylindrical shell. Three of its sides were rigidly stiffened by 1" thick Styrene foam sheets thus leaving the fourth side to represent the test panel.

Table 21. Geometric Properties of Test Specimens

(a)

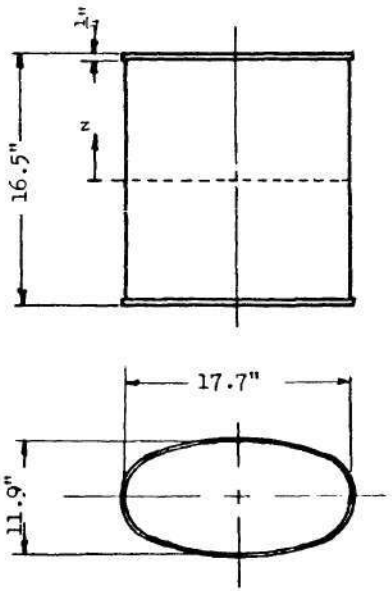

Elliptic Shell	
Circumference	47.1"
Major Axis	17.7"
Minor Axis	11.9"
Height	16.5"
Skin Thickness	0.030"

(b)

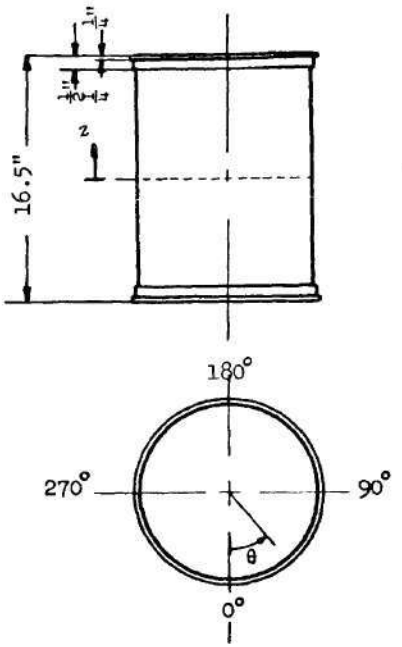

Circular Shell	
Diameter	11.46"
Height	16.5"
Skin Thickness	0.030"

(c)

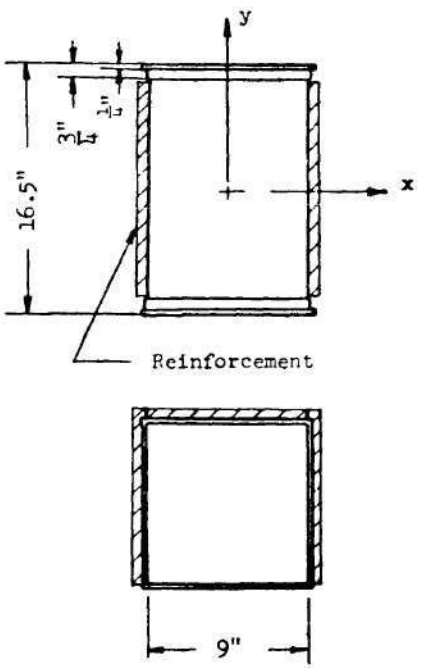

Rectangular Panel	
Width	9"
Height	16.5"
Skin Thickness	0.030"

Results

Elliptic Shell. This was the first shell body to which the vibration method was applied. The model was used by another colleague for a different research program which was going on at that time. Since the shell was already mounted in the testing machine, it was feasible to utilize the set up to initiate the vibration testing during the idling periods of the other research activity.

The shell had a cutout in one of the minimum curvature sides and thus buckling was expected to occur first on that side. Since our interest was mainly to develop the vibrational technique, there was no point in introducing any type of structural complexity into the issue at such an early stage. Therefore it was decided to force the buckle to occur on the side opposite to the cutout. This was done by eccentrically applying the axial loading closer to the side where failure was planned.

The area of minimum curvature was scanned in order to obtain the dynamic mass distribution. The shaking force was maintained constant at 0.078 pounds throughout the scan. The results were plotted and the region of the least M_D was determined as shown in Figure 14. The scan was repeated at higher axial loads and the region of the least M_D was observed to be at the same location. This region was later confirmed to be within the buckling area when the axial load was carried high enough to cause failure.

Having determined the point of least dynamic mass, the shaking force was applied at that location. The dynamic mass was recorded while the excitation force was increased from zero until a definite minimum of

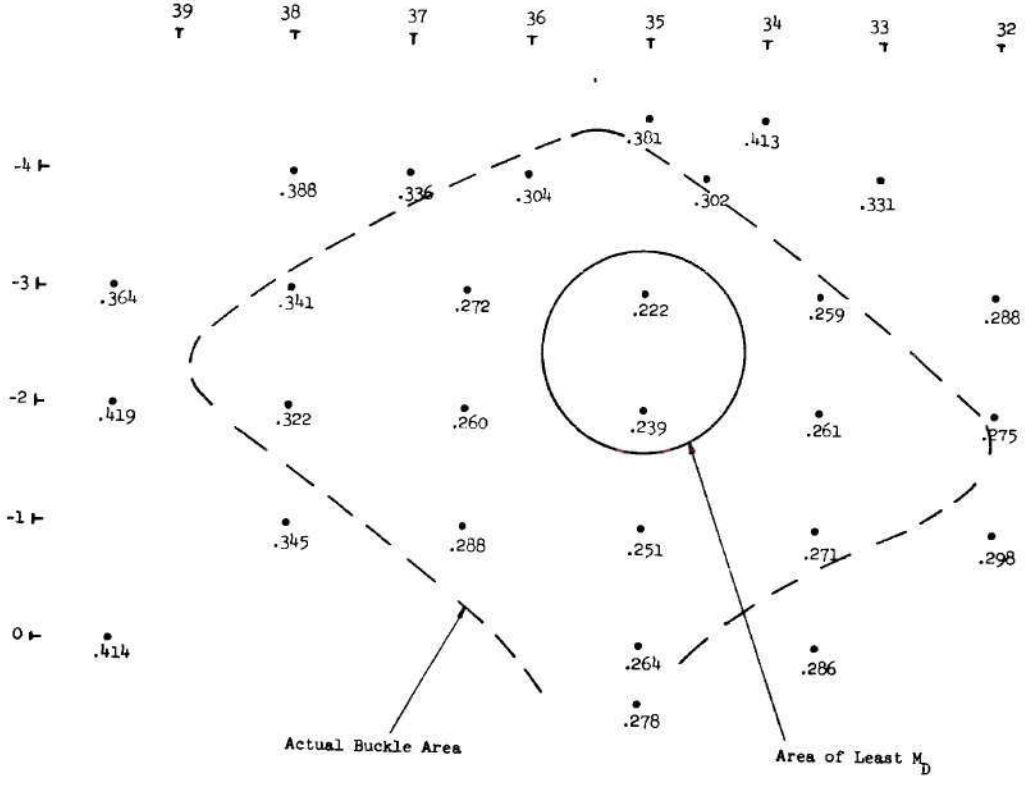

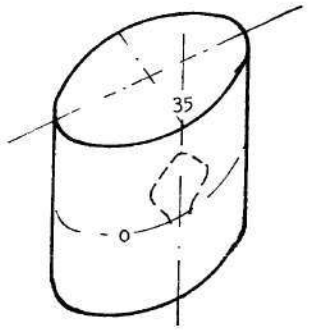

Figure 14. Elliptic Shell - M_D Distribution
(P = 0, f = 20 Hz & F = 0.078 lb)

M_D was obtained. The axial load was then stepwise increased and for each level the shaking force and the corresponding dynamic mass were recorded. The procedure was carried out for excitation frequencies of 5, 10, 20 and 40 Hz and the results are plotted in Figures 15, 16, 17 and 18 respectively. The minimum M_D is determined for each curve and those minima are plotted vs. the corresponding axial load as shown in Figure 19. For each excitation frequency the relationship between M_D and P is a straight line which, if extended, cuts the P-axis at the critical buckling load of the shell. It is clear that for all excitation frequencies, the resulting straight lines intersect the P-axis virtually at the same point. Thus the critical load was determined to be between 310 pounds and 315 pounds. The shell was later buckled and the observed buckling load was 335 pounds.

Circular Cylindrical Shell. The dynamic mass distribution was determined over a large portion of the shell at no axial load. The readings were taken at 1" intervals around the circumference and at 11 vertical locations between and including -4" and +6" from the mid-height of the shell. The scan was carried out at an excitation frequency of 40 Hz. The excitation force was maintained at 0.0783 pounds within ± 0.4%. Typical plots of the circumferential distribution are shown in Figure 20 for the zero vertical station (shell mid-height) and +6" station. The minimum M_D of the whole scan was determined to be at location $(z,\theta) = (1", 40^\circ)$.

Measurements of the dynamic mass were then taken at that location at various shaking forces and over a wide range of excitation frequencies and axial loading. The data is plotted in Figures 21 to 25

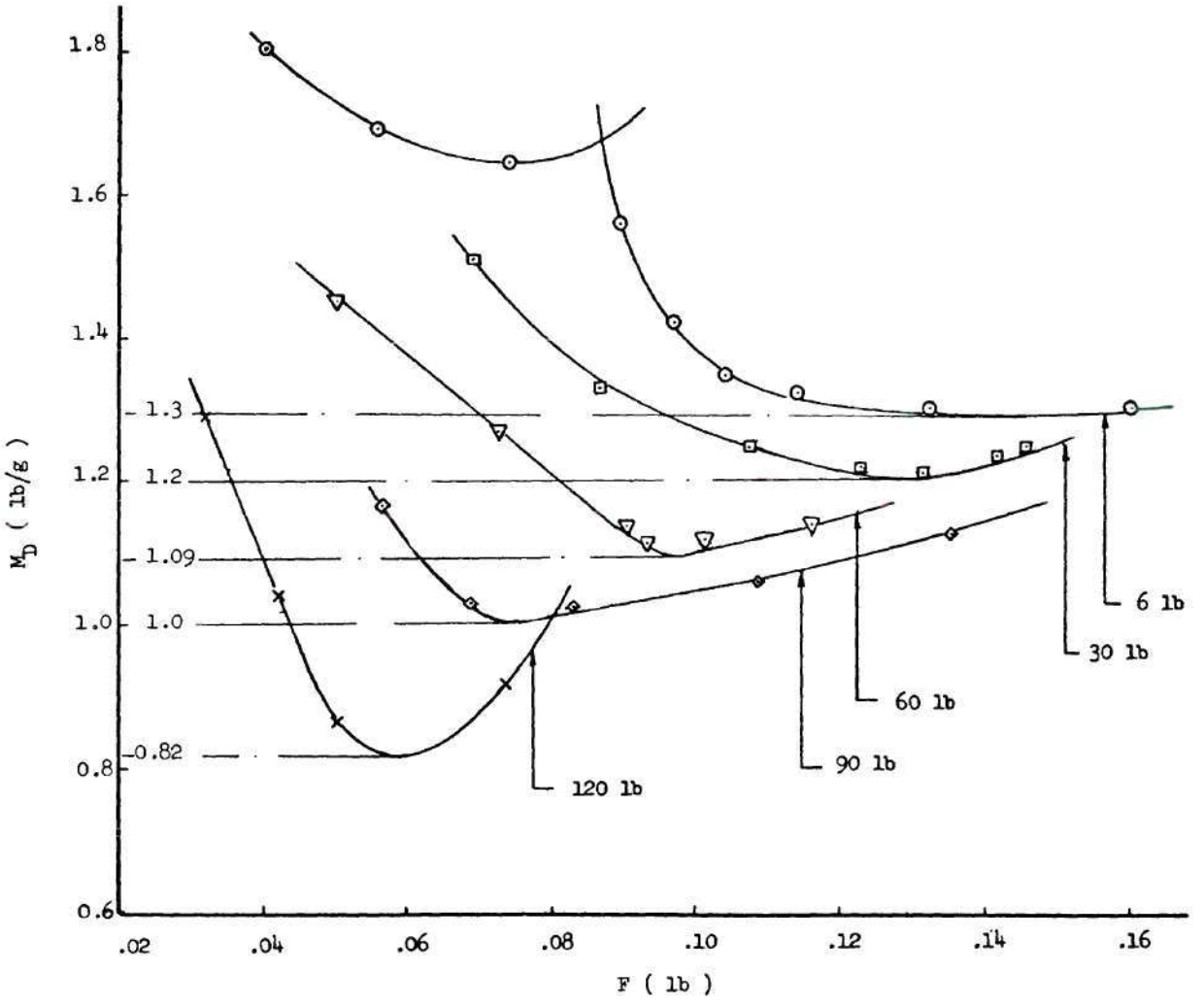

Figure 15. Elliptic Shell - M_D vs. F at 5 Hz.

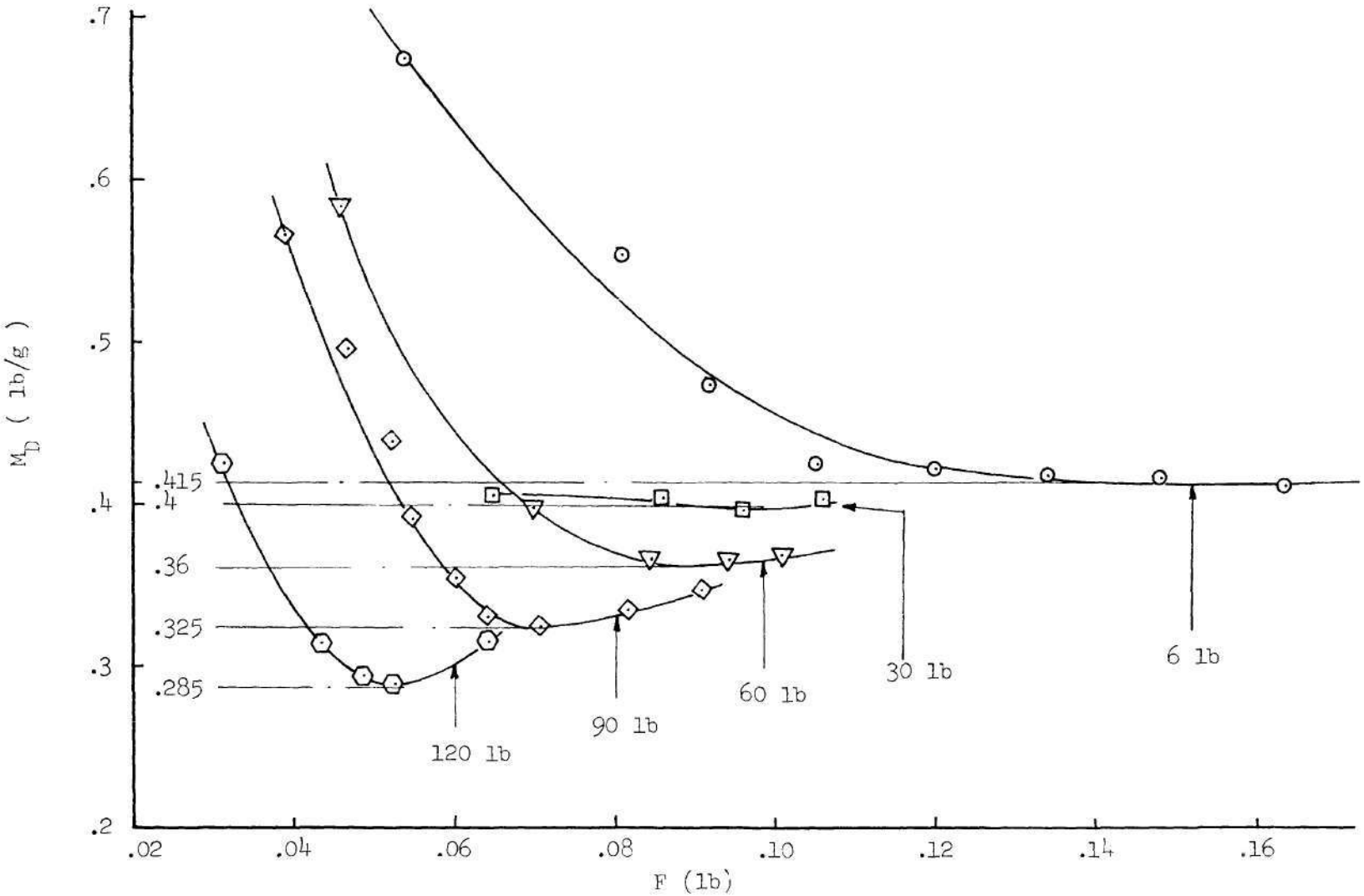

Figure 16. Elliptic Shell - M_D vs. F at 10 Hz.

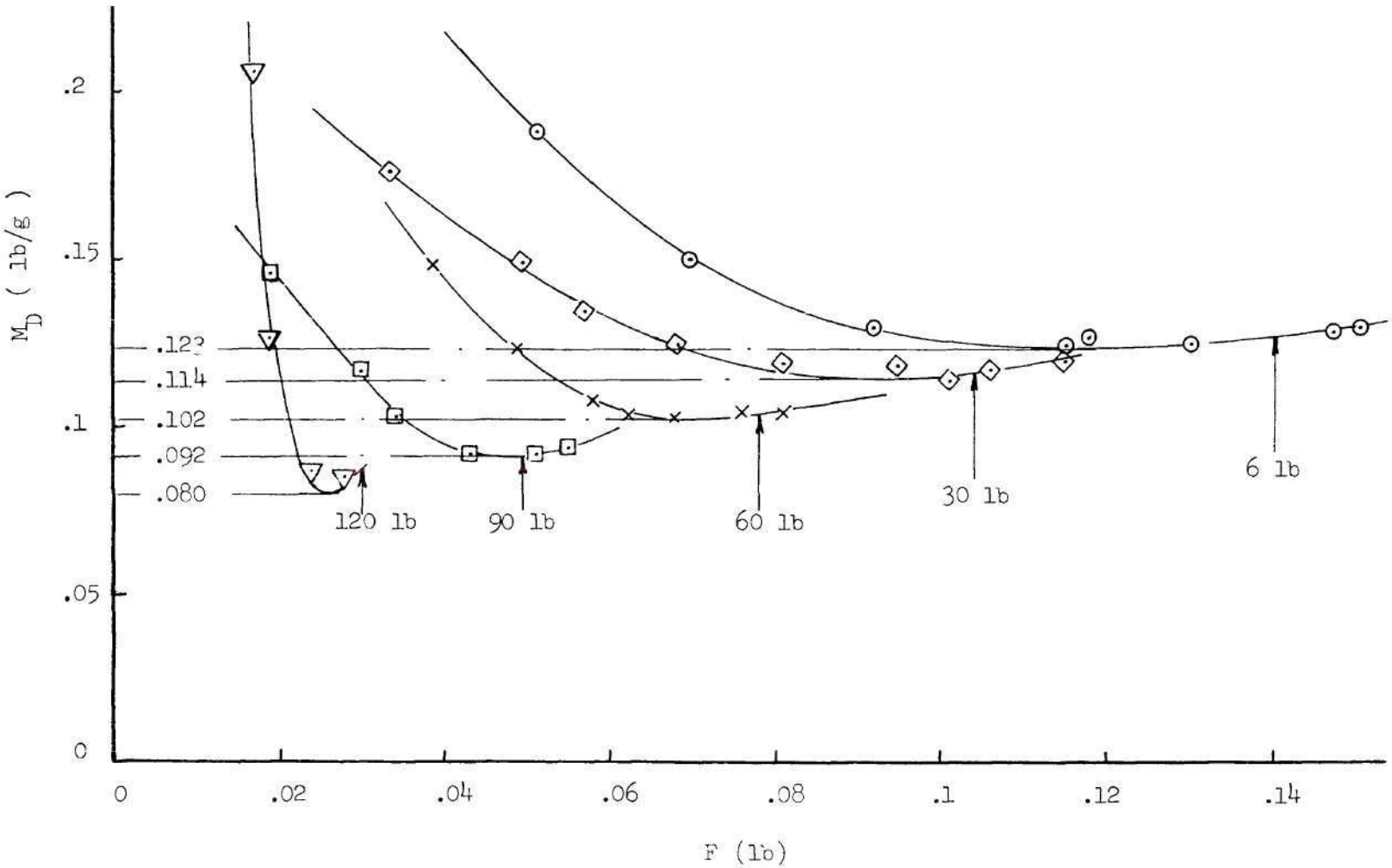

Figure 17. Elliptic Shell - M_D vs. F at 20 Hz.

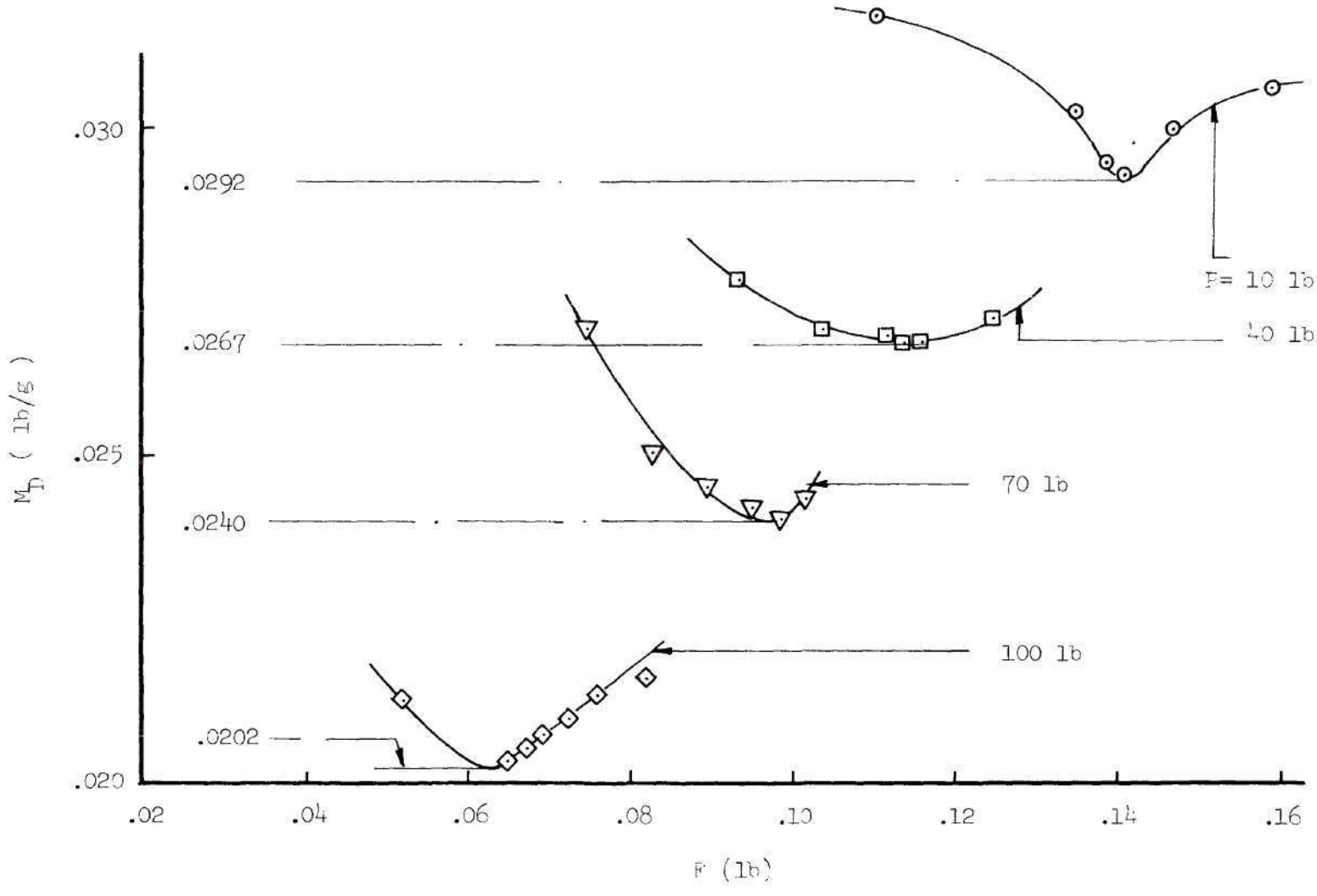

Figure 18. Ellip[illegible] Shell - M_D vs. F at 40 Hz.

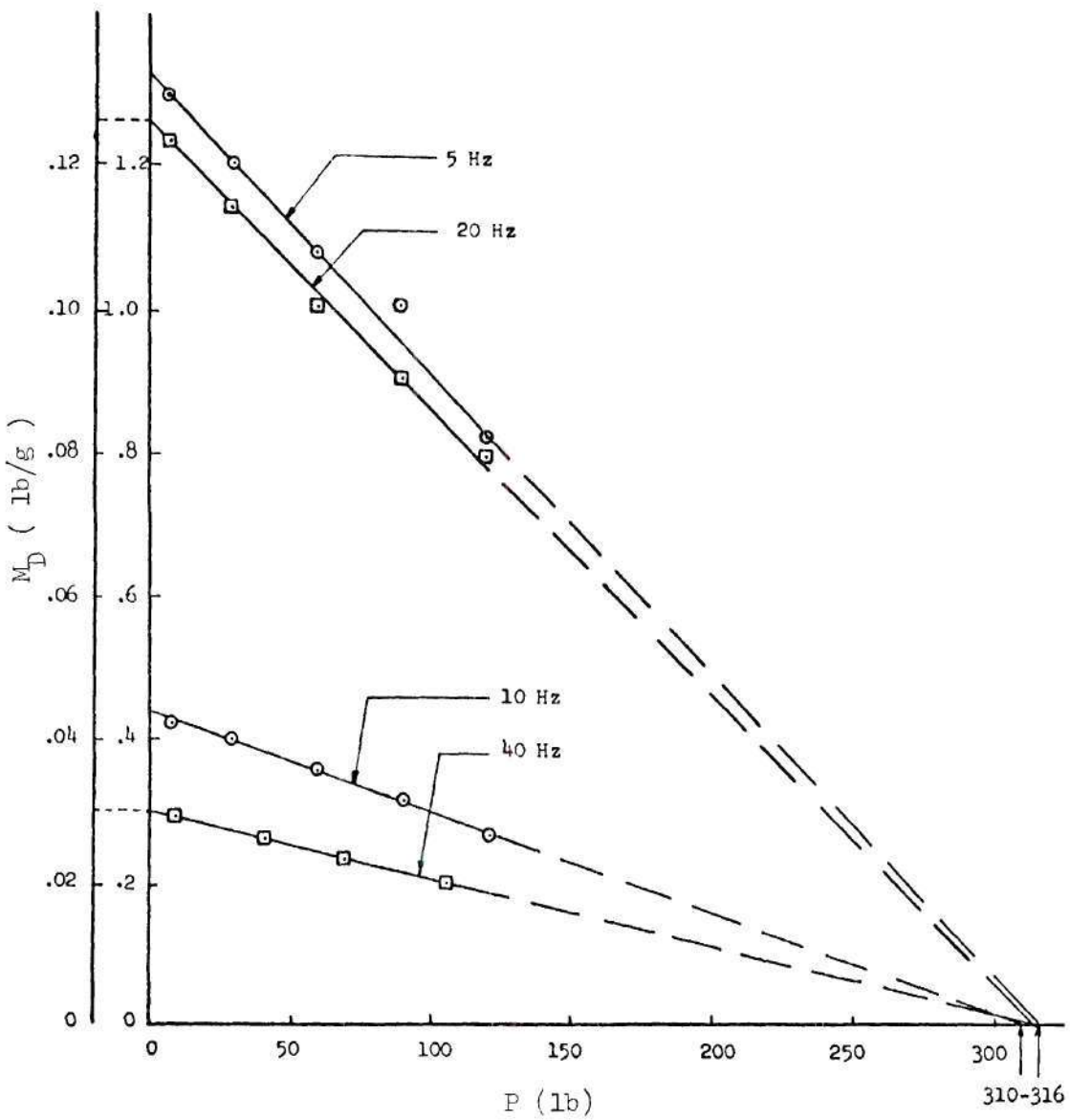

Figure 19. Elliptic Shell - Minimum M_D vs. Corresponding P.

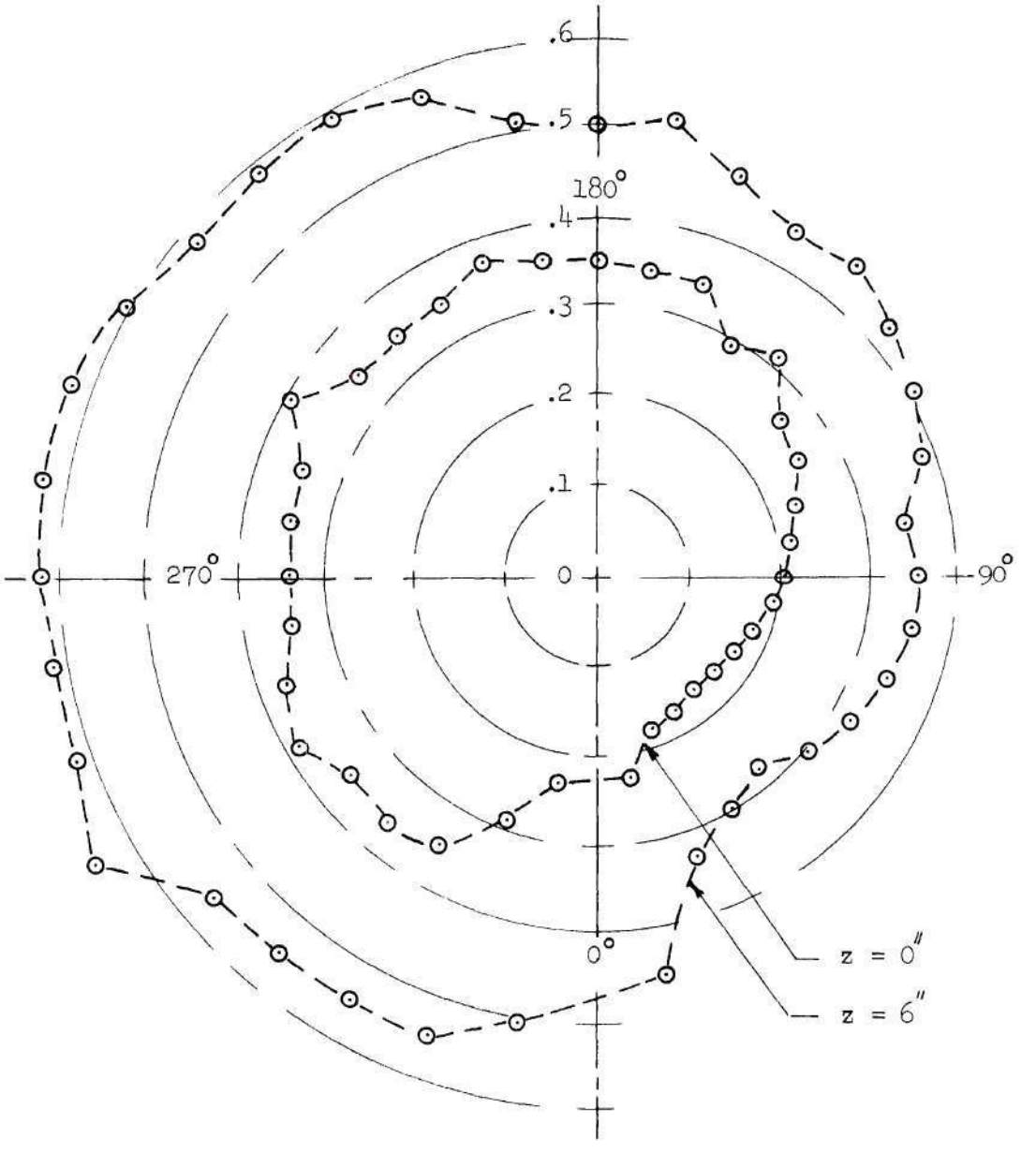

Figure 20. Circular Shell - Typical Circumferential Plot of M_D (P = 0, f = 40 Hz and F = 0.0783 lb)

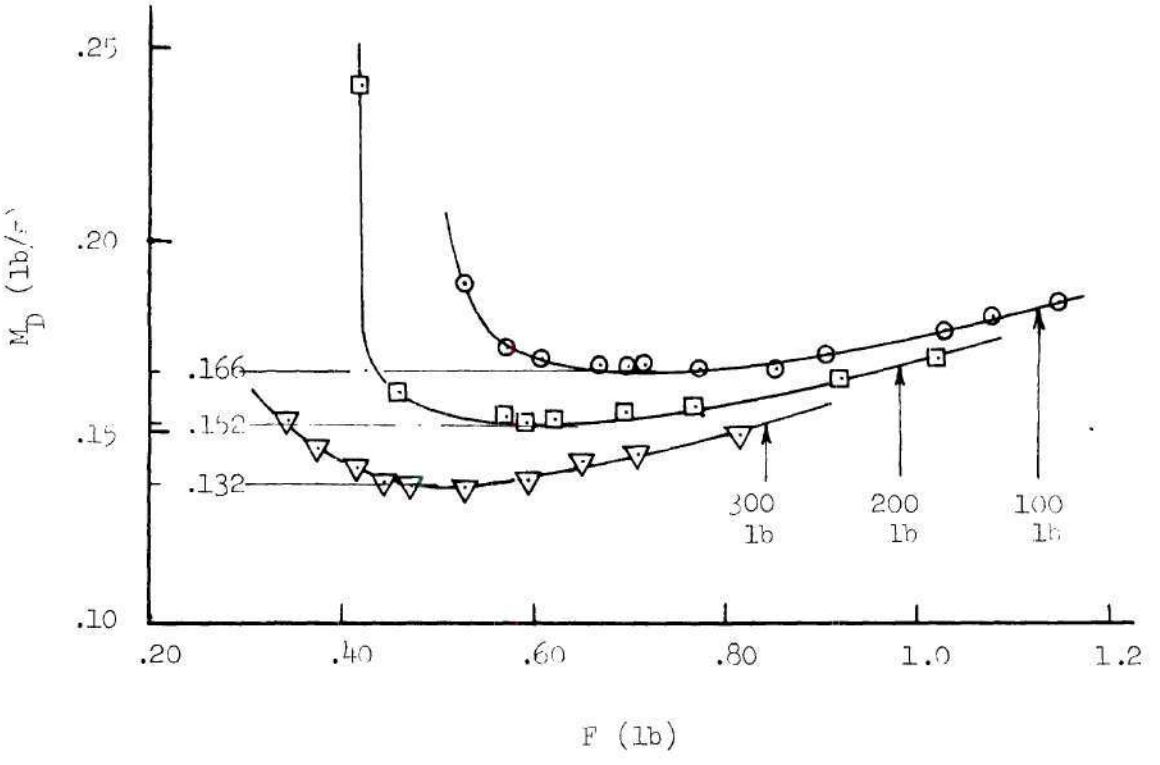

Figure 21. Circular Shell - M_D vs. F at 30 Hz.

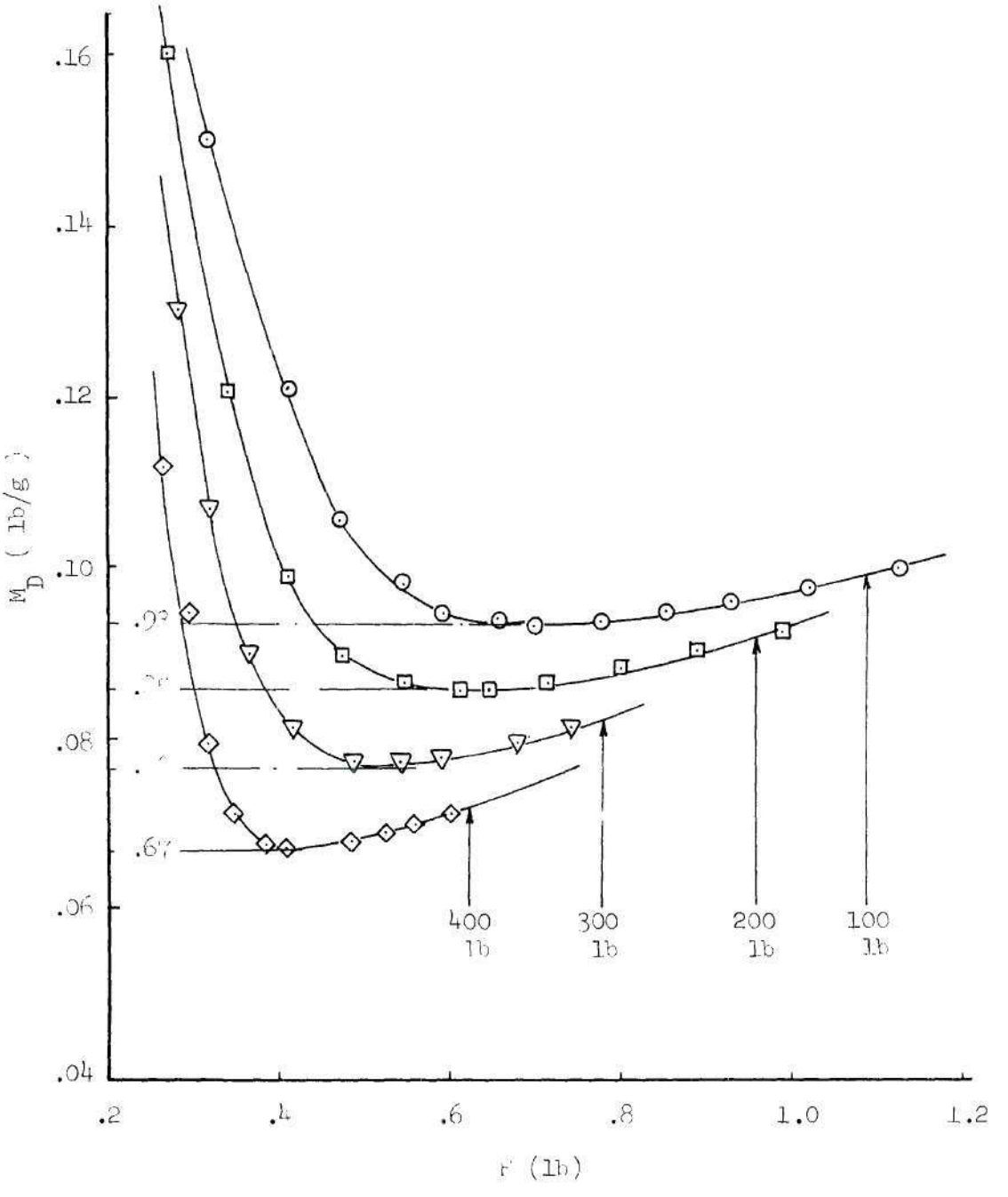

Figure 22. Circular Shell - M_D vs. F at 40 Hz.

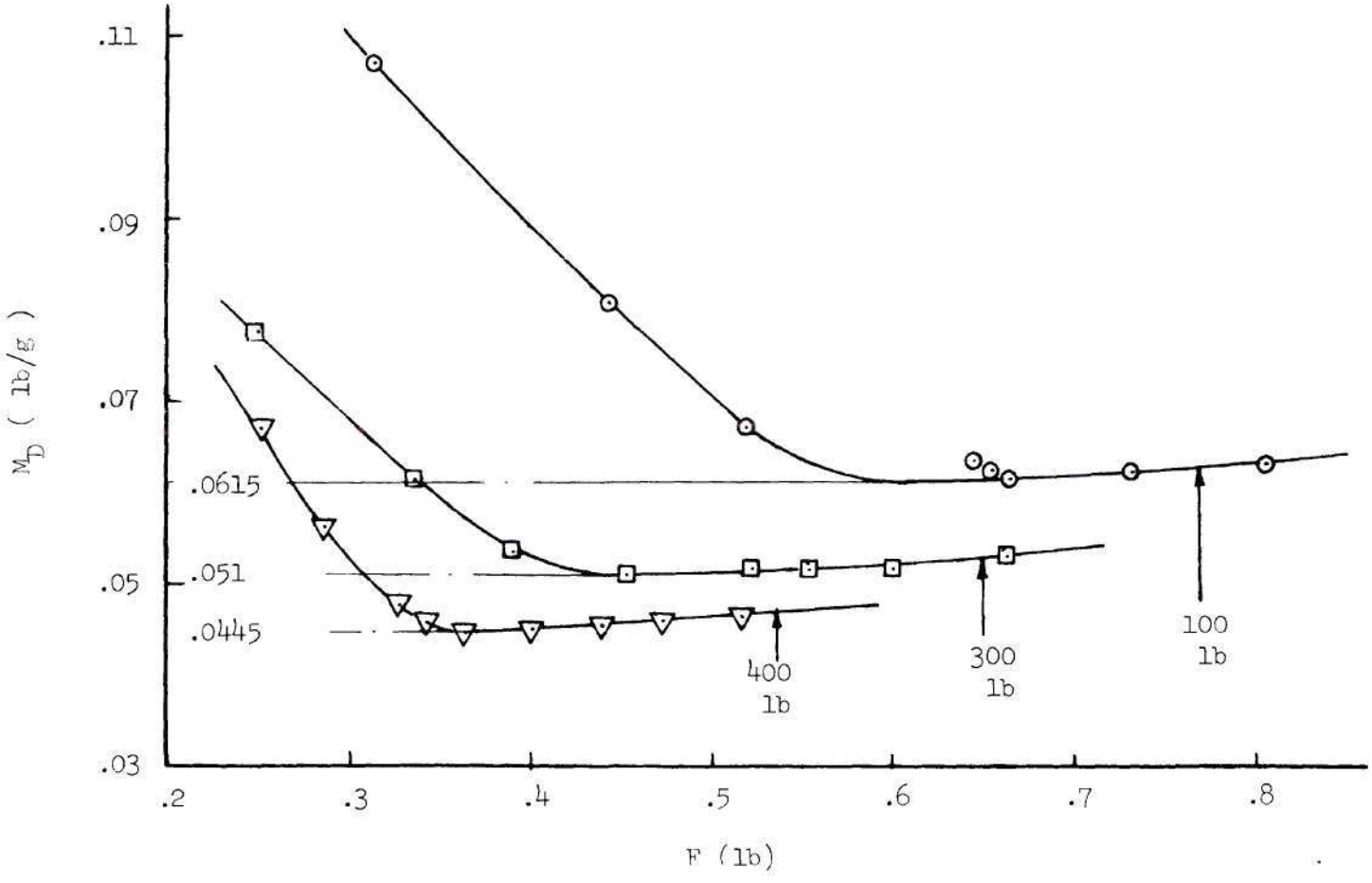

Figure 23. Circular Shell - M_D vs. F at 50 Hz.

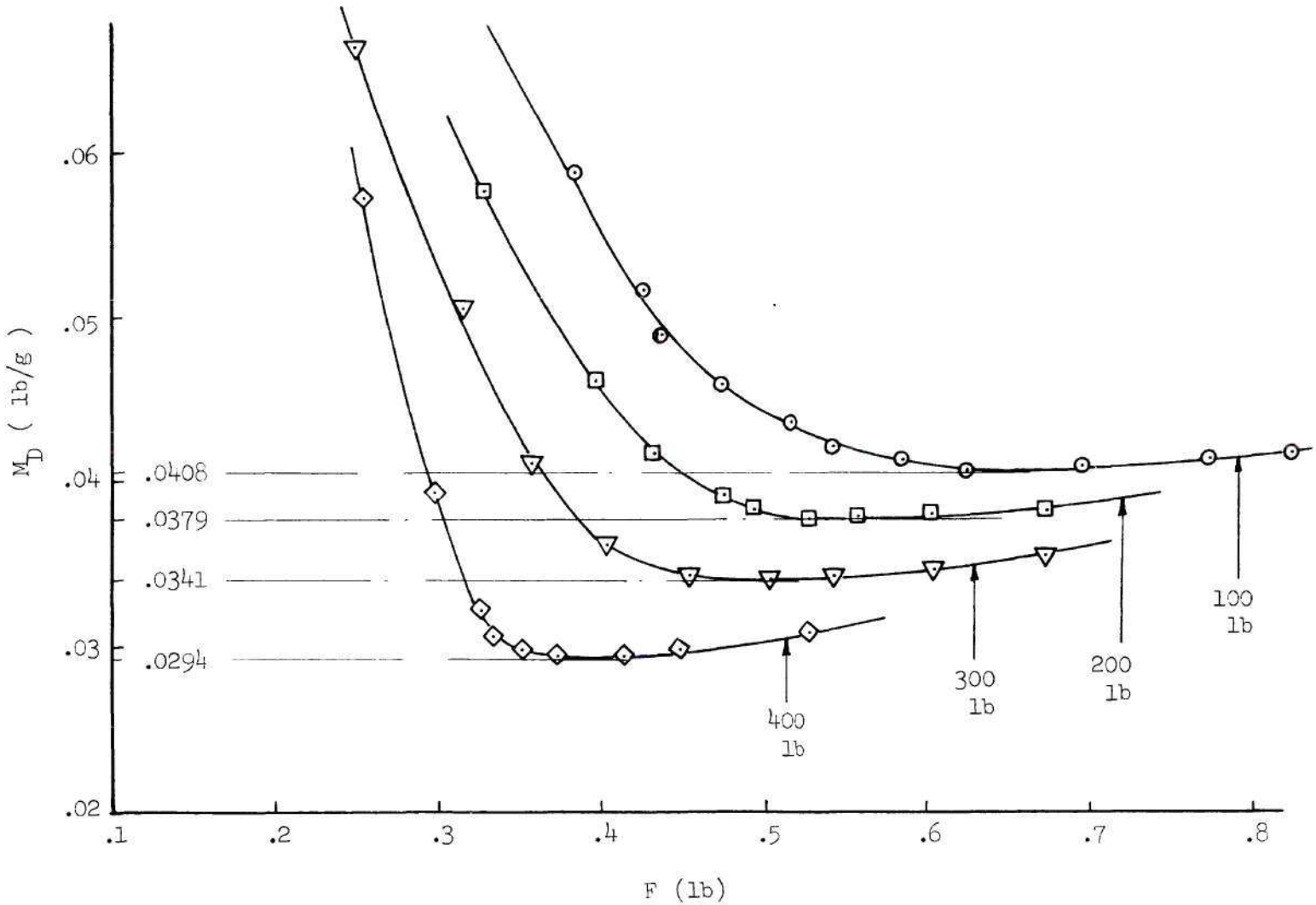

Figure 24. Circular Shell - M_D vs. F at 60 Hz.

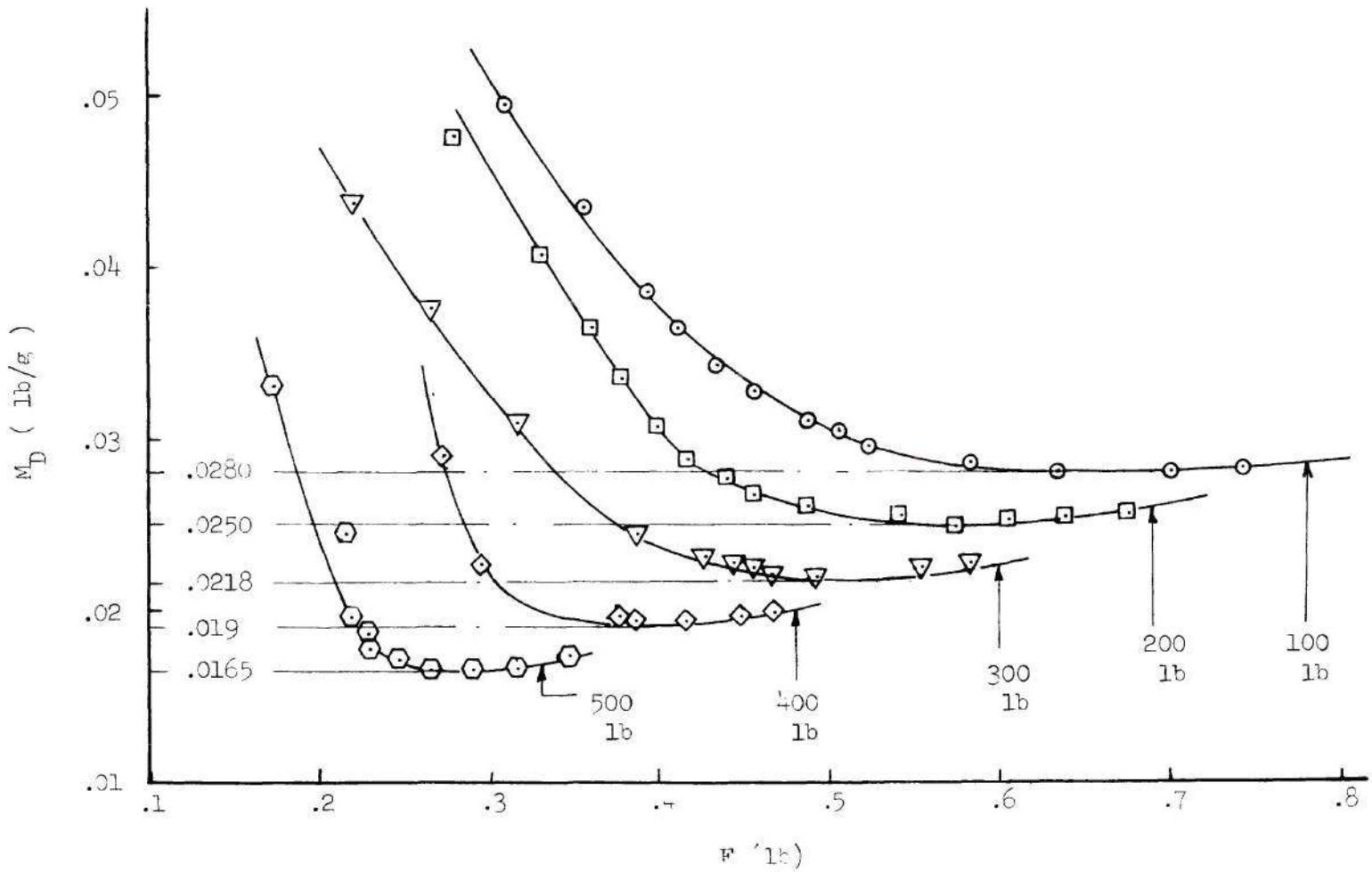

Figure 25. Circular Shell - M_D vs. F at 70 Hz.

where the minimum M_D is determined for each curve. Plots of those minima vs. the corresponding axial loads are given in Figure 26. The linear relationship is again clear for all frequencies. The intersections of those lines with the P-axis determined the buckling load of the shell to be between 1135 pounds and 1190 pounds.

The shell was later buckled and the pattern was observed to develop on the side of the shell where the dynamic mass distribution showed a depression (refer to Figure 20). The actual buckling load was observed to be 1195 pounds.

Rectangular Panel. The dynamic mass distribution was obtained at 1 inch intervals along the x and the y directions (refer to Table 21). Due to the geometric limitations the scan did not cover the lower 4 inches of the plate surface. The shaking force was 0.0783 pounds and was maintained constant within ± 0.4%. Figure 27 shows the M_D distribution at zero axial load and 40 Hz excitation frequency. In order to locate the region of least dynamic mass, the magnitude of M_D are compared at points symmetrically located with respect to the x and y axes. By doing this, it becomes immediately obvious that there are two regions of least M_D as indicated in Figure 27. These are indeed the two regions of buckling which were observed later when the axial load was increased and the panel failed in a two half-wave form.

The excitation force was then applied at the middle of the lower right region, namely at $(x,y) = (2.8, -2.6)$. Measurements of M_D were taken at several levels of the axial load and at excitation frequencies of 30 and 40 Hz. The results are plotted in Figures 28 and 29 and the least values of M_D are determined. These are plotted vs.

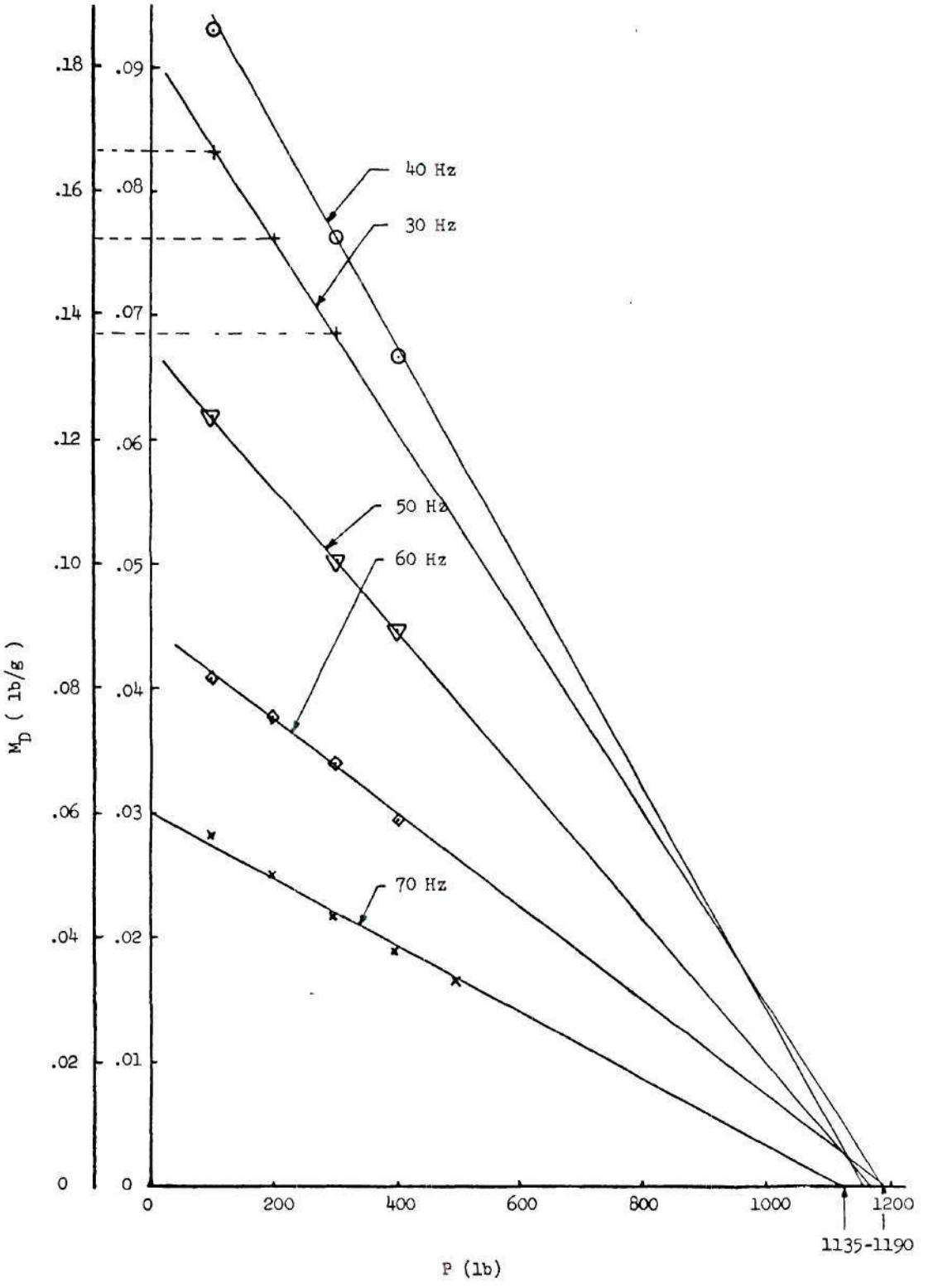

Figure 26. Circular Shell - Minimum M_D vs. Corresponding P.

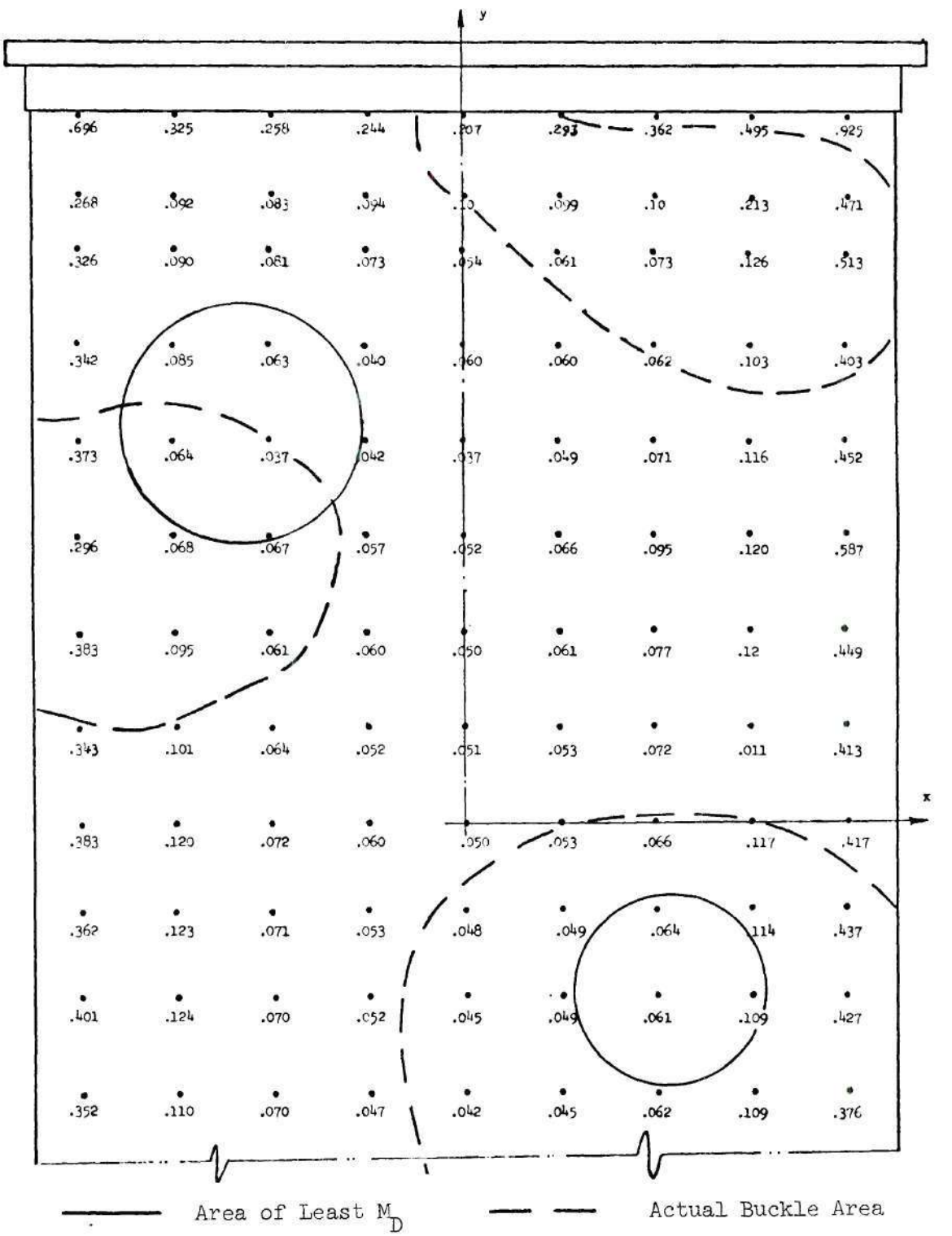

Figure 27. Rectangular Panel - M_D Distribution
(P = 0, f = 20 Hz and F = 0.0783 lb)

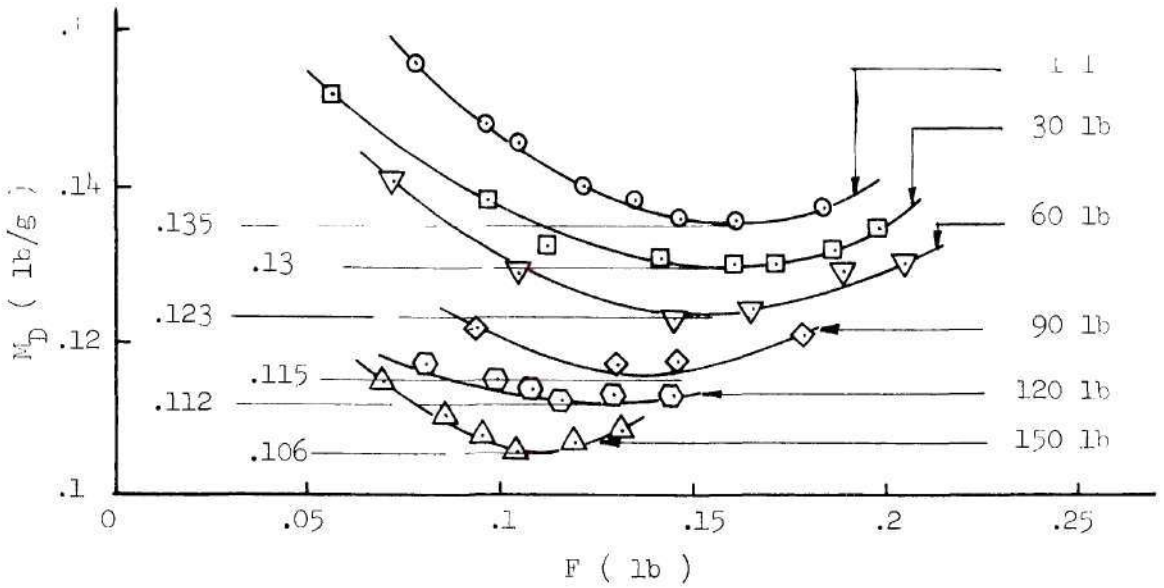

Figure 28. Rectangular Panel - M_D vs. F at 30 Hz.

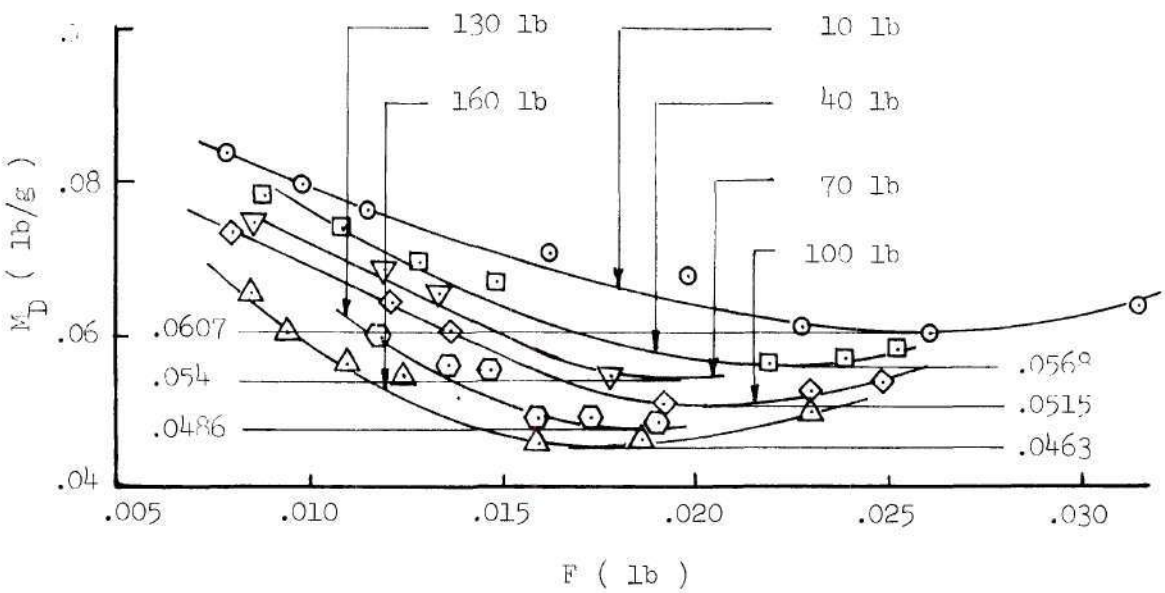

Figure 29. Rectangular Panel - M_D vs. F at 40 Hz.

the corresponding axial load in Figure 30. The resulting linear relations indicate that the critical load of the panel lies between 650 pounds and 675 pounds.

When the panel was axially loaded with the intension to determine its actual load carrying capability buckling was observed not to be of the sudden type. In fact the panel deflection kept growing steadily under axial load. The loading was stopped and it was decided to use the Southwell method to get a second estimate of the critical buckling load.

The locations of the two buckling regions were already known and therefore the observation point could be taken at either. The deflection measurements were taken by use of LVDT deflection transducer and the data are given in Table 22. The Southwell plot was produced as shown in Figure 31 and the critical load was determined to be 665 pounds.

Table 22. Panel Testing - Deflection Data

P (lb)	δ (Micro in)	δ/P
0	0	-
30	5	.167
60	9.6	.16
90	16	.178
120	22.2	.185
150	29.5	.1965
180	37.5	.208
210	45.5	.212
240	53.5	.223
270	59.5	.22
300	66	.22

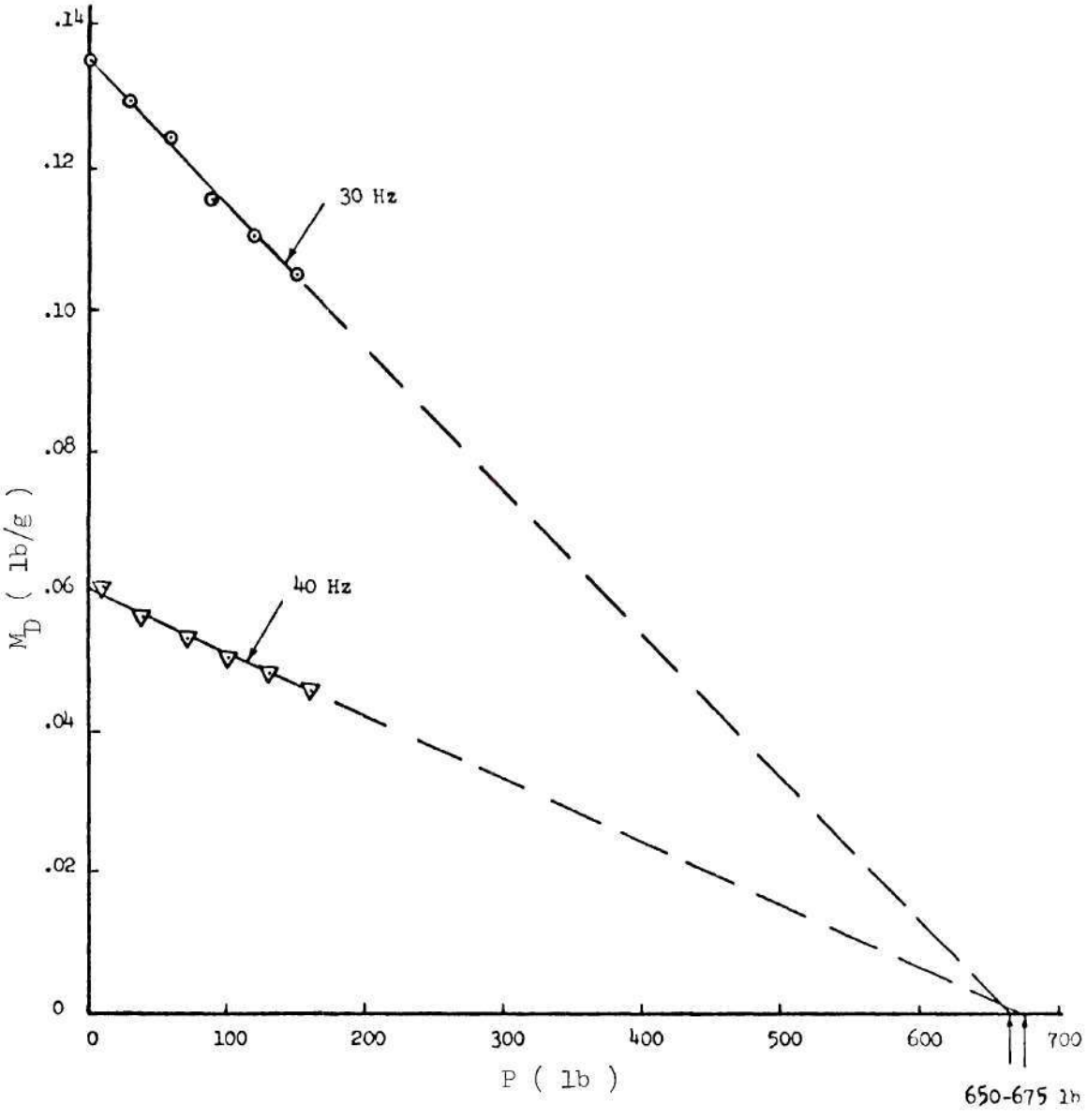

Figure 30. Rectangular Panel - Minimum M_D vs. Corresponding P.

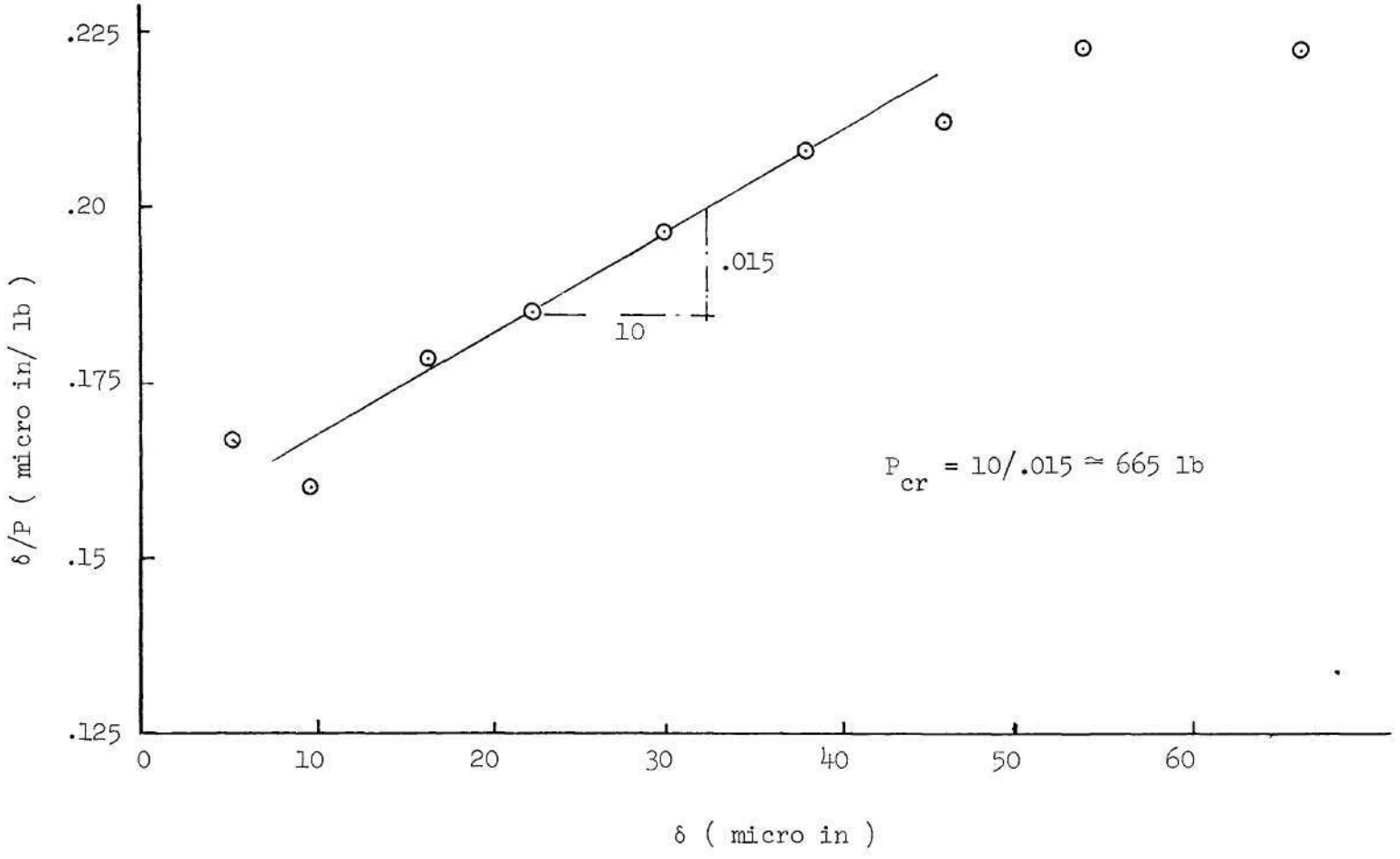

Figure 31. Rectangular Panel - Southwell Plot

Conclusion

This chapter describes an experimental technique which was used for the nondestructive determination of the critical axial loads on structures. The technique also succeeded in predicting, accurately, the locations of the regions where buckling developed first. The critical loads determined by the method for more than one structural configuration are in excellent agreement with the actual failing loads as observed in the laboratory. In cases where actual failings were not carried out the Southwell method was used to assess the actual capability of the structure.

In none of the tests conducted was it necessary to apply axial loads in excess of 1/3 of the critical value in order to generate the data required. In some cases axial loads were even as low as 1/4 of the critical. This strongly justifies the non-destructive rating of the method.

It is to be pointed out that there are limitations to the applicability of the technique. In order to succeed it is necessary for the buckling pattern to be geometrically similar to the induced vibrational pattern. For the kind of structures that have been tested these were of the diamond type. Similar tests were conducted on a spirally stiffened circular cylindrical shell but the method failed to determine the critical load. In fact the behavior of the dynamic parameters was completely different from that observed before. The reason became obvious when the shell was buckled and it was observed to fail in a ring type rather than diamond type.

APPENDIX A

A RATIONAL FUNCTION SOLUTION TO THE DEFLECTION SHAPE OF A LATERALLY LOADED BEAM WHOSE ENDS ARE ELASTICALLY RESTRAINED AGAINST ROTATION

Consider an elastically restrained beam under uniform lateral loading of intensity q, Figure 32. The deflection shapes, bending moments and slopes pertinent to the extreme end fixities are available in standard textbooks, e.g., reference [40]. For completeness these are listed in Table 23.

A rational function expression for the deflection shape will be taken as

$$W = \frac{a_1 + a_2 \beta_1 \beta_2 + a_3 \beta_1 + a_4 \beta_2}{b_1 + b_2 \beta_1 \beta_2 + b_3 \beta_1 + b_4 \beta_2} \qquad \text{(A-1)}$$

Compliance with the following four conditions

$$\beta_1 = \beta_2 = 0 \quad ; \quad W = W_{0\,0} = a_1/b_1$$

$$\beta_1 = \beta_2 = \infty \quad ; \quad W = W_{\infty\,\infty} = a_1/b_1$$

$$\beta_1 = \infty,\ \beta_2 = 0 \quad ; \quad W = W_{\infty\,0} = a_3/b_3$$

$$\beta_1 = 0,\ \beta_2 = \infty \quad ; \quad W = W_{0\,\infty} = a_4/b_4$$

reduces Equation (A-1) to

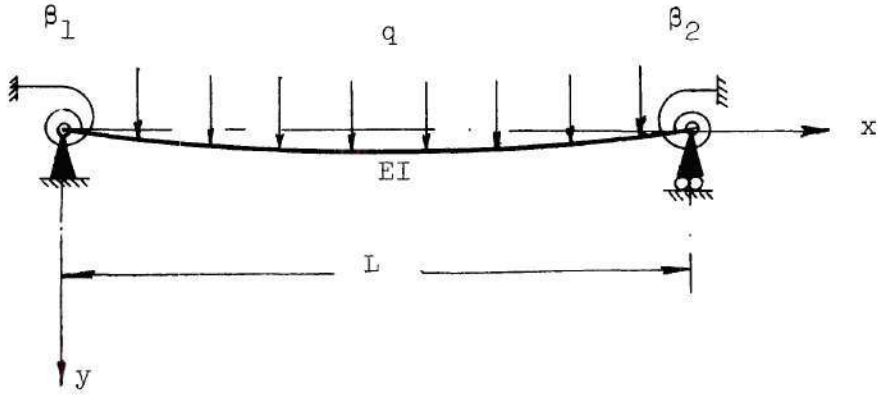

Figure 32. Elastically Restrained Beam Under Uniform Lateral Loading.

Table 23. Bending Characteristics of a Uniformly Loaded Beam

Case of End Fixity	W	W′		W″	
		x = 0	x = L	x = 0	x = L
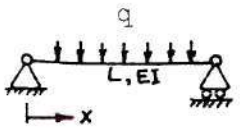	$\frac{qx}{24EI}\left(L^3 - 2Lx^2 + x^3\right)$	$\frac{qL^3}{24EI}$	$-\frac{qL^3}{24EI}$	0	0
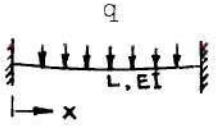	$\frac{qx^2}{24EI}\left(x^2 + L^2 - 2Lx\right)$	0	0	$\frac{qL^2}{12EI}$	$\frac{qL^2}{12EI}$
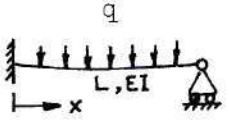	$\frac{q}{48EI}\left(L^3x + 2x^4 - 3Lx^3\right)$	0	$-\frac{qL^3}{48EI}$	$\frac{qL^2}{8EI}$	0
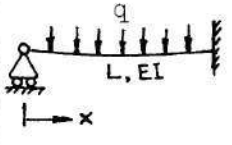	$\frac{q}{48EI}\left[L^3\left(L - x\right) + 2\left(L - x\right)^4 - 3L\left(L - x\right)^3\right]$	$\frac{qL^3}{48EI}$	0	0	$\frac{qL^2}{8EI}$

$$W = \frac{b_1 W_{0\,0} + b_2 \beta_1 \beta_2 W_{\infty\,\infty} + b_3 \beta_1 W_{\infty\,0} + b_4 \beta_2 W_{0\,\infty}}{b_1 + b_2 \beta_1 \beta_2 + b_3 \beta_1 + b_4 \beta_2} \qquad \text{(A-2)}$$

The ratio's of the four unknown quantities b_1, b_2, b_3 and b_4 can be determined by forcing the relation (A-2) to satisfy the three following conditions. The first condition is; when $\beta_1 = \beta_2 = \beta$ the deflection shape becomes symmetric with respect to a plane through the mid point of the beam. The second and third conditions are: at both ends of the beam the bending moment is always equal to the product of the angle of rotation by the stiffness of the torsional spring.

Applying the first condition to Equation (A-2) we get

$$W = \frac{b_1 W_{0\,0} + b_2 \beta^2 W_{\infty\,\infty} + \beta\left(b_3 W_{\infty\,0} + b_4 W_{0\,\infty}\right)}{b_1 + b_2 \beta^2 + \beta\left(b_3 + b_4\right)} \qquad \text{(A-3)}$$

which should be symmetric with respect to $x = \frac{L}{2}$. We know that both $W_{0\,0}$ and $W_{\infty\,\infty}$ are symmetric. We know also that $W_{\infty\,0}$ and $W_{0\,\infty}$ are not symmetric with respect to $x = \frac{L}{2}$, but, they are mirror immage of each other with respect to either end of the beam, i.e.,

$$W_{\infty\,0}(x) = W_{0\,\infty}(L-x) \qquad \text{(A-4)}$$

For the deflection W given by Equation (A-3) to be symmetric, the quantity $b_3 W_{\infty\,0} + b_4 W_{0\,\infty}$ have to be symmetric, i.e.,

$$b_3 W_{\infty\,0}(x) + b_4 W_{0\,\infty}(x) = b_3 W_{\infty\,0}(L-x) + b_4 W_{0\,\infty}(L-x)$$

but since

$$W_{\infty\,0}(L-x) = W_{0\,\infty}(x)$$

hence

$$b_3 W_{\infty\,0}(x) + b_4 W_{0\,\infty}(x) = b_3 W_{0\,\infty}(x) + b_4 W_{\infty\,0}(x)$$

or

$$W_{\infty\,0}(x)\left(b_3 - b_4\right) = W_{0\,\infty}(x)\left(b_3 - b_4\right)$$

Since $W_{\infty\,0}(x) \neq W_{0\,\infty}(x)$

we conclude that

$$b_3 = b_4 \tag{A-5}$$

hence

$$W = \frac{b_1 W_{0\,0} + b_2 \beta_1 \beta_2 W_{\infty\,\infty} + b_3\left(\beta_1 W_{\infty\,0} + \beta_2 W_{0\,\infty}\right)}{b_1 + b_2 \beta_1 \beta_2 + b_3\left(\beta_1 + \beta_2\right)} \tag{A-6}$$

Now, if we consider the bending moment - slope relation at the ends $x = 0$ and $x = L$ we write:

$$\left.\begin{aligned} \left.\frac{d^2W}{dx^2}\right|_{x=0} &= \frac{\beta_1}{L}\left.\frac{dW}{dx}\right|_{x=0} \\ \text{and at } x = L \qquad & \\ \left.\frac{d^2W}{dx^2}\right|_{x=L} &= -\frac{\beta_2}{L}\left.\frac{dW}{dx}\right|_{x=L} \end{aligned}\right\} \qquad \text{(A-7)}$$

Substituting for W from Equation (A-6) into Equation (A-7) and using Table 23 we get at x = 0,

$$b_2\,\beta_1\,\beta_2\,\frac{qL^2}{12EI} + b_3\,\beta_1\,\frac{qL^2}{8EI} = \frac{\beta_1}{L}\left[b_1\,\frac{qL^3}{24EI} + b_3\,\beta_2\,\frac{qL^3}{48EL}\right]$$

or

$$\frac{b_2\,\beta_2}{12} + \frac{b_3}{8} = \frac{b_1}{24} + \frac{b_3\,\beta_2}{48} \qquad \text{(A-8)}$$

Similarly at x = L we get,

$$\frac{b_2\,\beta_1}{12} + \frac{b_3}{8} = \frac{b_1}{24} + \frac{b_3\beta_1}{48} \qquad \text{(A-9)}$$

subtracting Equation (A-8) from (A-9) we get

$$b_3 = 4b_2$$

substituting into Equation (A-8) gives

$$b_1 = 3b_3 = 12b_2$$

hence the deflection shape becomes

$$W = \frac{12\, W_{0\,0} + \beta_1\, \beta_2\, W_{\infty\,\infty} + 4\left(\beta_1\, W_{\infty\,0} + \beta_2\, W_{0\,\infty}\right)}{12 + \beta_1\, \beta_2 + 4\left(\beta_1 + \beta_2\right)} \qquad \text{(A-10)}$$

By simple algebraic manipulation this expression can be shown to be equivalent to the exact expression which results from solving the differential equation subjected to the appropriate boundary conditions [41].

The same analysis was applied to several other lateral loading conditions as shown in Table 24. In each case it was found that the deflection shape can be expressed by the same formula (A-10) and in all cases this formula was identical to the exact solution as obtained by solving the differential equation of equilibrium.

It is to be emphasized that the prime purpose of the derivations herein made was the development of a process for representing the mode shapes of vibrating beams in terms of the edge restraint parameters and the modes corresponding to the limiting cases of edge fixities.

The success of the method of derivation as applied to the laterally loaded beams suggests its use for the stated purpose.

Table 24. General Expression for the Deflection of Laterally Loaded Beams

Loading case	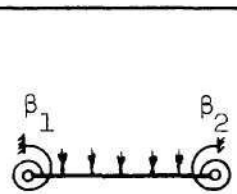	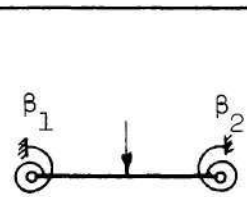	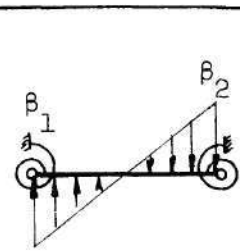	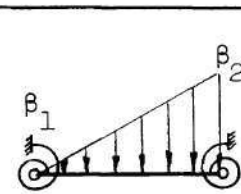	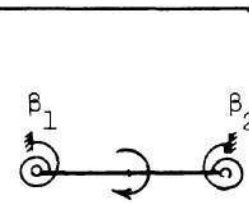
Deflection function*	$W = \dfrac{12\, W_{0\,0} + \beta_1\, \beta_2\, W_{\infty\,\infty} + 4\left(\beta_1\, W_{\infty\,0} + \beta_2\, W_{0\,\infty}\right)}{12 + \beta_1\, \beta_2 + 4\left(\beta_1 + \beta_2\right)}$				

where, $W_{0\,0}$, $W_{\infty\,\infty}$, $W_{\infty\,0}$ and $W_{0\,\infty}$ are the functions corresponding to the extreme cases of end fixity under the considered loading condition.

*The same form obviously applies to the derivatives of the deflection function.

APPENDIX B

THE VIBRATIONAL MODE SHAPE OF A BEAM WHOSE ENDS ARE LATERALLY SUPPORTED AND ELASTICALLY RESTRAINED AGAINST ROTATION

Consider the uniform homogeneous beam shown in Figure 33. The differential equation describing the vibrational shape is

$$\frac{d^4W}{dx^4} - \frac{\mu^4}{L^4} W = 0 \qquad \text{(B-1)}$$

where

$$\mu^4 = \omega^{*2} \frac{mL^4}{EI}$$

The general solution of Equation (B-1) is given by

$$W = A \cosh \mu \frac{x}{L} + B \sinh \mu \frac{x}{L} + C \cos \mu \frac{x}{L} + D \sin \mu \frac{x}{L} \qquad \text{(B-2)}$$

Referring to Figure 33 the boundary conditions are

$$\left[W\right]_{x = -\frac{L}{2}} = \left[W\right]_{x = \frac{L}{2}} = 0 \qquad \text{(B-3)}$$

$$\left[\frac{d^2W}{dx^2}\right]_{x = -\frac{L}{2}} = \frac{\beta_1}{L} \left[\frac{dW}{dx}\right]_{x = -\frac{L}{2}} , \quad \left[\frac{d^2W}{dx^2}\right]_{x = \frac{L}{2}} = -\frac{\beta_2}{L} \left[\frac{dW}{dx}\right]_{x = \frac{L}{2}}$$

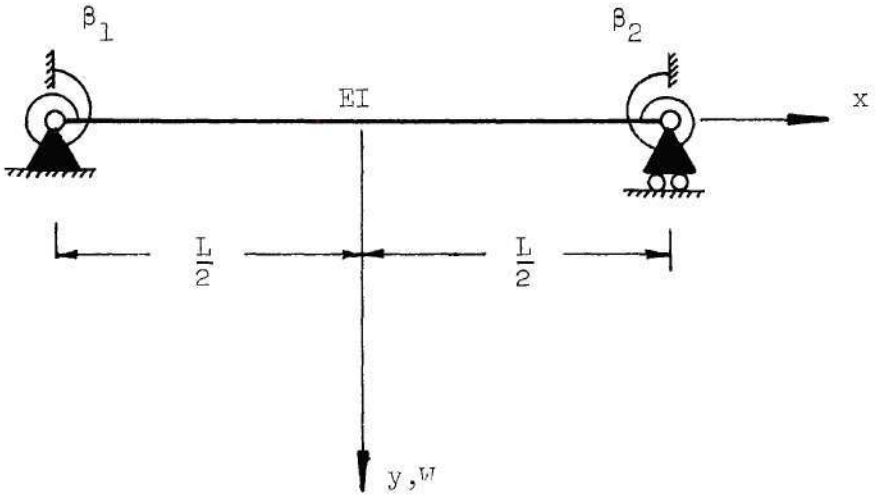

Figure 33. Beam with Elastic Rotational Restraints.

Substituting these boundary conditions into the general solution we get the following set of equations

$$A \cosh -\mu/2 + B \sinh -\mu/2 + C \cos -\mu/2 + D \sin -\mu/2 = 0 \qquad \text{(B-4)}$$

$$A \cosh \mu/2 + B \sinh \mu/2 + C \cos \mu/2 + D \sin \mu/2 = 0 \qquad \text{(B-5)}$$

$$\mu^2 \left[A \cosh -\mu/2 + B \sinh -\mu/2 - C \cos -\mu/2 - D \sin -\mu/2\right] \qquad \text{(B-6)}$$

$$= \beta_1 \mu \left[A \sinh -\mu/2 + B \cosh -\mu/2 - C \sin -\mu/2 + D \cos -\mu/2\right]$$

$$\mu^2 \left[A \cosh \mu/2 + B \sinh \mu/2 - C \cos \mu/2 - D \sin \mu/2\right] \qquad \text{(B-7)}$$

$$= - \beta_2 \mu \left[A \sinh \mu/2 + B \cosh \mu/2 - C \sin \mu/2 + D \cos \mu/2\right]$$

adding Equations (B-4) and (B-5) we get

$$2 A \cosh \mu/2 + 2 C \cos \mu/2 = 0$$

or

$$C = - A \frac{\cosh \mu/2}{\cos \mu/2} \qquad \text{(B-8)}$$

Subtracting Equation (B-4) from Equation (B-5) gives

$$2 B \sinh \mu/2 + 2 D \sin \mu/2 = 0$$

or

$$D = - B \frac{\sinh \mu/2}{\sin \mu/2} \tag{B-9}$$

Adding Equations (B-6) and (B-7) gives

$$A = - B \cdot F_1$$

where

$$F_1 = \frac{\left(\beta_2 - \beta_1\right)\left\{\cosh \mu/2 - \frac{\sinh \mu/2 \cos \mu/2}{\sin \mu/2}\right\}}{4 \mu \cosh \mu/2 + \left(\beta_1 + \beta_2\right)\left\{\sinh \mu/2 + \frac{\cosh \mu/2 \sin \mu/2}{\cos \mu/2}\right\}} \tag{B-10}$$

Also subtracting Equation (B-6) from Equation (B-7) gives

$$B = - A \cdot F_2$$

where

$$F_2 = \frac{\left(\beta_2 - \beta_1\right)\left\{\sinh \mu/2 + \frac{\cosh \mu/2 \sin \mu/2}{\cos \mu/2}\right\}}{4 \mu \sinh \mu/2 + \left(\beta_1 + \beta_2\right)\left\{\cosh \mu/2 - \frac{\cos \mu/2 \sinh \mu/2}{\sin \mu/2}\right\}} \tag{B-11}$$

Hence to summarize: the mode shape is given by Equation (B-2) and the coefficients A, B, C and D are given as follows

(a) for odd numbers of half waves

$$\left.\begin{aligned} A &= \sin \mu/2 \cos \mu/2 = \frac{1}{2} \sin \mu \\ B &= -\frac{1}{2} \sin \mu \cdot F_2 \\ C &= -\sin \mu/2 \cosh \mu/2 \\ D &= \cos \mu/2 \sinh \mu/2 \cdot F_2 \end{aligned}\right\} \quad \text{(B-12)}$$

(b) for even number of half waves A, B, C and D will be denoted as E, F, G, and H where:

$$\left.\begin{aligned} E &= -\frac{1}{2} \sin \mu \cdot F_1 \\ F &= \frac{1}{2} \sin \mu \\ G &= \sin \mu/2 \cosh \mu/2 \cdot F_1 \\ H &= -\cos \mu/2 \sinh \mu/2 \end{aligned}\right\} \quad \text{(B-13)}$$

where F_1 and F_2 are given in Equations (B-10) and (B-11) respectively.

APPENDIX C

ELASTICALLY RESTRAINED RECTANGULAR PLATES - SOLUTION NO. 1

This Appendix deals with the detailed algebra of solution No. 1. Table 25 summarizes the integrals that appear in the energy terms. The last two columns are code numbers given to the integrals for future use. With the aid of Table 25 the frequency is obtained as shown in Table 26. The expressions in Table 26 can be easily programmed for numerical calculation of the plate frequency at any combination of edge restraint parameters.

Table 25. Integrals in Solution No. 1

f(x)	$\int_{-a/2}^{a/2} f(x)\,dx$	Code Number for: $Q = \lambda_m$	Code Number for: $Q = \mu_n$
$\cosh^2 \frac{Qx}{a}$	$\frac{a}{2Q}\left(\sinh Q + Q\right)$	I_1	J_1
$\sinh^2 \frac{Qx}{a}$	$\frac{2}{2Q}\left(\sinh Q - Q\right)$	I_2	J_2
$\cos^2 \frac{Qx}{a}$	$\frac{a}{2}\left(1 + \frac{\sin Q}{Q}\right)$	I_3	J_3
$\sin^2 \frac{Qx}{a}$	$\frac{a}{2}\left(1 - \frac{\sin Q}{Q}\right)$	I_4	J_4
$\sinh \frac{Qx}{a} \cosh \frac{Qx}{a}$	0		
$\cos \frac{Qx}{a} \sinh \frac{Qx}{a}$	0		
$\sin \frac{Qx}{a} \cos \frac{Qx}{a}$	0		
$\sin \frac{Qx}{a} \cosh \frac{Qx}{a}$	0		
$\cos \frac{Qx}{a} \cosh \frac{Qx}{a}$	$\frac{a}{Q}\left[\sinh \frac{Q}{2} \cos \frac{Q}{2} + \cosh \frac{Q}{2} \sin \frac{Q}{2}\right]$	I_9	J_9
$\sin \frac{Qx}{a} \sinh \frac{Qx}{a}$	$\frac{a}{Q}\left[\cosh \frac{Q}{2} \sin \frac{Q}{2} - \sinh \frac{Q}{2} \cos \frac{Q}{2}\right]$	I_0	J_0

Table 26. Frequency Expression in Solution No. 1

$$\omega_{mn}^2 = \frac{\bar{D}}{\bar{m}b^4}\left[\frac{\lambda_m^4 R^4 U_2 U_3 + \mu_n^4 U_1 U_4 + 2\lambda_m \mu_n^2 R^2 U_5 U_6 + \lambda_m^2 R^4 U_2 U_7 + \mu_n^2 U_1 U_8}{U_1 U_2}\right]$$

where

$$R = \frac{b}{a} \quad , \quad 0 \le R \le 1$$

$$U_1 = E_n^2 J_1 + F_n^2 J_2 + G_n^2 J_3 + H_n^2 J_4 - 2 E_n G_n J_9 - 2 F_n H_n J_0$$

$$U_2 = E_n^2 J_1 + F_n^2 J_2 + G_n^2 J_3 + H_n^2 J_4 + 2 E_n G_n J_9 + 2 F_n H_n J_0$$

$$U_3 = A_m^2 I_1 + B_m^2 I_2 + C_m^2 I_3 + D_m^2 I_4 - 2 A_m C_m I_9 - 2 B_m D_m I_0$$

$$U_4 = A_m^2 I_1 + B_m^2 I_2 + C_m^2 I_3 + D_m^2 I_4 + 2 A_m C_m I_9 + 2 B_m D_m I_0$$

$$U_5 = A_m^2 I_1 + B_m^2 I_2 - C_m^2 I_3 - D_m^2 I_4$$

$$U_6 = E_n^2 J_1 + F_n^2 J_2 - G_n^2 J_3 - H_n^2 J_4$$

-continued-

Table 26. (continued)

$$U_7 = \beta_1 \left[- A_m \sinh \frac{\lambda_m}{2} + B_m \cosh \frac{\lambda_m}{2} + C_m \sin \frac{\lambda_m}{2} + D_m \cos \frac{\lambda_m}{2} \right]^2$$

$$+ \beta_2 \left[A_m \sinh \frac{\lambda_m}{2} + B_m \cosh \frac{\lambda_m}{2} - C_m \sin \frac{\lambda_m}{2} + D_m \cos \frac{\lambda_m}{2} \right]^2$$

$$U_8 = \beta_3 \left[- E_n \sinh \frac{\mu_n}{2} + F_n \cosh \frac{\mu_n}{2} + G_n \sin \frac{\mu_n}{2} + H_n \cos \frac{\mu_n}{2} \right]^2$$

$$+ \beta_4 \left[E_n \sinh \frac{\mu_n}{2} + F_n \cosh \frac{\mu_n}{2} - G_n \sin \frac{\mu_n}{2} + H_n \cos \frac{\mu_n}{2} \right]^2$$

$I_1, \ldots, I_0$ and $J_1, \ldots, J_0$ are given in Table 25.

$A_m, \ldots, D_m$ and $E_n, \ldots, H_n$ are given by Equations (B-12) and (B-13).

APPENDIX D

ELASTICALLY RESTRAINED RECTANGULAR PLATES - SOLUTION NO. 3

The integrals appearing in the energy terms are listed in Table 27 and numerically evaluated in Table 28. With the strain and kinetic energies being evaluated the frequency is obtained by use of the Rayleigh's quotient and the result is,

$$\omega^* = \sqrt{\frac{\bar{D}\left[\left(U_0U_1 + U_6 + U_7\right)R^4 + 2\,U_4U_5R^2 + U_2U_3 + U_8 + U_9\right]}{\bar{m}b^4\,U_1U_3}}$$

where

$$U_0 = I_1 + I_2\,\beta_1^2\,\beta_2^2 + I_3\left(\beta_1^2 + \beta_2^2\right) + I_4\,\beta_1\,\beta_2 + I_5\left(\beta_1 + \beta_2\right)$$

$$+ I_6\left(\beta_1^2\,\beta_2 + \beta_1\,\beta_2^2\right)$$

$$U_1 = I_7 + I_8\,\beta_3^2\,\beta_4^2 + I_9\left(\beta_3^2 + \beta_4^2\right) + I_{10}\,\beta_3\,\beta_4 + I_{11}\left(\beta_3 + \beta_4\right)$$

$$+ I_{12}\left(\beta_3^2\,\beta_4 + \beta_3\,\beta_4^2\right)$$

$U_2 \equiv U_0$ by replacing β_1 and β_2 by β_3 and β_4 respectively

$U_3 \equiv U_1$ by replacing β_3 and β_4 by β_1 and β_2 respectively

$$U_4 = I_{13} + I_{14}\,\beta_1^2\,\beta_2^2 + I_{15}\left(\beta_1^2 + \beta_2^2\right) + I_{16}\,\beta_1\,\beta_2 + I_{17}\left(\beta_1 + \beta_2\right)$$

$$+ I_{18}\left(\beta_1^2\,\beta_2 + \beta_1\,\beta_2^2\right)$$

$U_5 \equiv U_4$ by replacing β_1 and β_2 by β_3 and β_4 respectively

$$U_6 = \beta_1\,U_1\left[I_{19} + I_{20}\,\beta_2\right]^2$$

$$U_7 = \beta_2\,U_1\left[I_{19} + I_{20}\,\beta_1\right]^2$$

$$U_8 = \beta_3\,U_3\left[I_{19} + I_{20}\,\beta_4\right]^2$$

$$U_9 = \beta_4\,U_3\left[I_{19} + I_{20}\,\beta_3\right]^2$$

and I_i is given in Table 29 for $i = 1, \ldots, 20$.

Table 27. Integrals in Solution No. 3

$f(x)$	$\int_0^L f(x)\,dx$
$\cos^2 \frac{Qx}{L}$	$\left(\frac{1}{2} + \frac{1}{4Q} \sin 2Q\right)L$
$\sin^2 \frac{Qx}{L}$	$\left(\frac{1}{2} - \frac{1}{4Q} \sin 2Q\right)L$
$\cosh^2 \frac{Qx}{L}$	$\left(\frac{\sinh 2Q}{4} + \frac{Q}{2}\right)\frac{L}{Q}$
$\sinh^2 \frac{Qx}{L}$	$\left(\frac{\sinh 2Q}{4} - \frac{Q}{2}\right)\frac{L}{Q}$
$\cos \frac{Q_1 x}{L} \cos \frac{Q_2 x}{L}$, $Q_1 \neq Q_2$	$\left(Q_2 \cos Q_1 \sin Q_2 - Q_1 \sin Q_1 \cos Q_2\right)L \,/\, \left(Q_2^2 - Q_1^2\right)$
$\sin \frac{Q_1 x}{L} \sin \frac{Q_2 x}{L}$, $Q_1 \neq Q_2$	$\left(Q_1 \cos Q_1 \sin Q_2 - Q_2 \sin Q_1 \cos Q_2\right)L \,/\, \left(Q_2^2 - Q_1^2\right)$
$\cosh \frac{Q_1 x}{L} \cosh \frac{Q_2 x}{L}$, $Q_1 \neq Q_2$	$\left(Q_2 \cosh Q_1 \sinh Q_2 - Q_1 \sinh Q_1 \cosh Q_2\right)L \,/\, \left(Q_2^2 - Q_1^2\right)$

- continued -

Table 27. (continued)

$f(x)$	$\int_0^L f(x)\,dx$
$\sinh \frac{Q_1 x}{L} \sinh \frac{Q_2 x}{L}$, $Q_1 \neq Q_2$	$\left(Q_2 \sinh Q_1 \cosh Q_2 - Q_1 \cosh Q_1 \sinh Q_2\right)L \,/\, \left(Q_2^2 - Q_1^2\right)$
$\cos \frac{Q_1 x}{L} \sin \frac{Q_2 x}{L}$, $Q_1 \neq Q_2$	$\left(Q_2 - Q_2 \cos Q_1 \cos Q_2 - Q_1 \sin Q_1 \sin Q_2\right)L \,/\, \left(Q_2^2 - Q_1^2\right)$
$\cos \frac{Q_1 x}{L} \cosh \frac{Q_2 x}{L}$	$\left(Q_1 \cosh Q_2 \sin Q_1 + \cos Q_1 \sinh Q_2\right)L \,/\, \left(Q_1^2 + Q_2^2\right)$
$\cos \frac{Q_1 x}{L} \sinh \frac{Q_2 x}{L}$	$\left(Q_1 \sin Q_1 \sinh Q_2 - Q_2 + Q_2 \cos Q_1 \cosh Q_2\right)L \,/\, \left(Q_1^2 + Q_2^2\right)$
$\sin \frac{Q_1 x}{L} \cosh \frac{Q_2 x}{L}$	$\left(Q_1 - Q_1 \cos Q_1 \cosh Q_2 + Q_2 \sin Q_1 \sinh Q_2\right)L \,/\, \left(Q_1^2 + Q_2^2\right)$
$\sin \frac{Q_1 x}{L} \sinh \frac{Q_2 x}{L}$	$\left(Q_2 \sin Q_1 \cosh Q_2 - Q_1 \cos Q_1 \sinh Q_2\right)L \,/\, \left(Q_1^2 + Q_2^2\right)$

- continued -

Table 27. (continued)

$f(x)$	$\int_0^L f(x)\,dx$
$\cosh \frac{Q_1 x}{L} \sinh \frac{Q_2 x}{L}$, $Q \neq Q_2$	$\left(Q_2 \cosh Q_1 \cosh Q_2 - Q_2 - Q_1 \sinh Q_1 \sinh Q_2\right) L \,/\, \left(Q_2^2 - Q_1^2\right)$
$\cos \frac{Qx}{L} \sin \frac{Qx}{L}$	$\frac{L}{2Q} \sin^2 Q$
$\cosh \frac{Qx}{L} \sinh \frac{Qx}{L}$	$\frac{L}{2Q} \left(\cosh^2 Q - 1\right)$

Table 28. Numerical Evaluation of the Integrals in Solution No. 3

f(x)	$\frac{1}{a}\int_0^a f(x)^* dx$ when Q_1 and Q_2 take the values:						
	μ_1 & μ_1	μ_2 & μ_2	μ_3 & μ_3	μ_2 & μ_1	μ_3 & μ_1	μ_2 & μ_3	μ_3 & μ_2
$\cosh \frac{Q_1 x}{a} \cosh \frac{Q_2 x}{a}$	-	339.7146	82.4971	-	-	166.613	166.613
$\cosh \frac{Q_1 x}{a} \sinh \frac{Q_2 x}{a}$	-	339.16	81.9333	-	-	165.789	166.212
$\cosh \frac{Q_1 x}{a} \cos \frac{Q_2 x}{a}$	-	- 5.88223	- 4.5695	-	-	-9.175	- 3.13032
$\cosh \frac{Q_1 x}{a} \sin \frac{Q_2 x}{a}$	-	- 5.98649	0.12905	5.61742	3.27775	- 0.74652	- 2.56618
$\sinh \frac{Q_1 x}{a} \sinh \frac{Q_2 x}{a}$	-	338.715	81.4971	-	-	165.502	165.502

* The same values apply to $\frac{1}{b}\int_0^b f(y)\, dy$

- continued -

Table 28. (continued)

f(x)	$\frac{1}{a}\int_0^a f(x)^* dx$ when Q_1 and Q_2 take the values:						
	μ_1 & μ_1	μ_2 & μ_2	μ_3 & μ_3	μ_2 & μ_1	μ_3 & μ_1	μ_2 & μ_3	μ_3 & μ_2
$\sinh \frac{Q_1 x}{a} \cos \frac{Q_2 x}{a}$	-	-5.98699	-4.69682	-	-	-9.30029	-3.23172
$\sinh \frac{Q_1 x}{a} \sin \frac{Q_2 x}{a}$	-	- 6.09311	-0.00182	5.519	3.1511	- 0.085186	-2.69334
$\cos \frac{Q_1 x}{a} \cos \frac{Q_2 x}{a}$	-	0.49814	0.56366	-	-	0.48809	0.48809
$\cos \frac{Q_1 x}{a} \sin \frac{Q_2 x}{a}$	-	0.10568	0.063663	- 0.25569	0.16576	- 0.09088	0.289502
$\sin \frac{Q_1 x}{a} \sin \frac{Q_2 x}{a}$	0.50	0.50186	0.43634	0.25122	0.41004	0.40785	0.40785

Table 29. Numerical Values of I_i

i	I_i	i	I_i
1	4694.31	11	13.6
2	7.96357	12	0.2454
3	237.9	13	-475.633
4	250.9633	14	-0.193307
5	1319.06	15	- 11.55
6	58.366	16	- 32.79567
7	48.1918	17	- 66.9719
8	0.0159	18	-1.30913
9	1.00728	19	30.8426
10	3.55969	20	5.68135

LITERATURE CITED

1. Harris, C. M. and Crede, C. E., Shock and Vibration Handbook, Vol. 1, McGraw-Hill, 1961.

2. Newmark, N. M. and Veletsos, A. S., "A Simple Approximation for The Natural Frequencies of Partially Restrained Bars," J. Appl. Mech., Dec. 1952, Vol. 19, No. 4, p. 563.

3. Horton, W. H., "The Use of Rational Functions in Approximating Relationships of Significance in The Buckling and Vibration of Partially Restrained Beams," Lecture Notes, School of Aerospace Engineering, Georgia Institute of Technology, Atlanta, Georgia.

4. Horton, W. H., Singhal, M. K. and Nassar, E. E., "The Application of Rational Functions to Produce Simple Approximation of Significance in Structural Analysis," Unpublished, School of Aerospace Engineering, Georgia Institute of Technology, 1973.

5. Bank, M. H., "Some Discussions on the Stability of Structural and Mechanical Systems," Ph.D. thesis, Georgia Institute of Technology, Atlanta, Georgia, August 1971.

6. Newmark, N. M., "A Simple Approximate Formula for Effective End-Fixity of Columns," Journal of the Aeronautical Sciences, Vol. 16, Feb. 1949, p. 116.

7. Lundquist, E. E. and Stowell, E. Z., "Critical Compressive Stress for Flat Rectangular Plates Supported Along All Edges and Elastically Restrained Against Rotation Along the Unloaded Edges," N.A.C.A. Report No. 733, 1942.

8. Stowell, E. Z., "Critical Shear Stress of an Infinitely Long Flat Plate with Equal Restraints Against Rotation Along the Parallel Edges," U.S. National Advisory Committee for Aeronautics, Report 3K 12, 1943.

9. Hurty, W. C. and Rubinstein, M. F., Dynamics of Structures, Prentice-Hall, 1967.

10. Bisplinghoff, R. L., Ashley, H. and Halfman, R. L., Aeroelasticity, Addison-Wesley Publishing Company, Inc., 1957.

11. Strutt, J. W., 3rd Baron Rayleigh, The Theory of Sound, Vol. 1, London, 1877. (See also: Rayleigh, J. W. S., The Theory of Sound, Vol. 1, Second Edition, Dover Publications, 1945).

12. Timoshenko, S., Vibration Problems in Engineering, D. Van Nostrand Company, Inc., New York, N. Y., 1937.

13. Warburton, G. B., "The Vibration of Rectangular Plates," Proc. Inst. Mech. Eng., Ser. A., Vol. 168, No. 12, 1954, pp. 371-384.

14. Janich, R., "Die näherungsweise Berechung der Eigenfrequenzen von Rechteckigen Platten bei Verschiedenen Randbedingungen," Die Bautechnik, Vol. 3, Mar. 1962, pp. 93-99.

15. Iguchi, S., "Die Eigenwertprobleme für die Elastiche Rechteckige Platte," Mem. Fac. Eng., Hokkaido Univ., 1938, pp. 305-372.

16. Leissa, W., Vibration of Plates, NASA SP-160, 1970.

17. Ödman, S. T. A., "Studies of Boundary Value Problems. Part II. Characteristic Functions of Rectangular Plates," Proc. NR 24, Swedish Cement and Concrete Res. Inst., Roy. Inst. Tech., Stockholm, 1955, pp. 7-62.

18. Stokey, W. F., Zorowski, C. F., and Appl, F. C., "Prevention of Mechanical Vibrations in Electronic Chassis-Design Manual," Rept. to Rome Air Develop. Center, Contract AF30(602)-913, Sept. 1955.

19. Joga-Rao, C. V. and Kantham, C. L., "Natural Frequencies of Rectangular Plates with Edges Elastically Restrained Against Rotation," J. Aeron. Sci., Vol. 24, No. 4, Nov. 1957, pp. 855-856.

20. Carmichael, T. E., "The Vibration of a Rectangular Plate with Edges Elastically Restrained Against Rotation," Quart. J. Mech. Appl. Math., Vol. 12, Part 1, 1959, pp. 29-42.

21. Temple, G. and Bickley, W. G., Rayleigh's Principle and Its Applications to Engineering, Dover Publications 1956.

22. Ritz, W., "Theorie der Transversalschwingungen einer Quadratischen Platte mit Freien Rändern," Annalen der Physik, Vol. 28, 1909, p. 737.

23. Young, D., "Vibration of Rectangular Plates by the Ritz Method," J. Appl. Mech., Vol. 17, No. 4, Dec. 1950, pp. 448-453.

24. Kato, T., "On the Upper and Lower Bounds of Eigenvalues," Journal of the Physical Society of Japan, Vol. 4, 1949.

25. Temple, G., "The Accuracy of Rayleigh's Method of Calculating the Natural Frequencies of Vibrating Systems," Proceedings of the Royal Society of London, Series A Math. & Phys. Science, Vol. 4, 1949.

26. Southwell, R. V., "On the Analysis of Experimental Observations in Problems of Elastic Stability," Proceedings of the Royal Society, London, Series A. 135, 1932, pp. 601-616.

27. Horton, W. H., Cundari, F. L. and Johnson, R. W., "A Review of the Applicability of the "Southwell Plot" to the Interpretation of Test Data Obtained from Stability Studies of Elastic Column and Plate Structures," SUDAAR No. 296, Stanford University, Stanford, California, December 1967.

28. Horton, W. H. and Cundari, F. L., "On the Applicability of the Southwell Plot to the Interpretation of Test Data from Instability Studies of Shell Bodies," USAAVLABS Technical Report 68-77, March 1969.

29. Craig, J. I., "An Experimental Study of Wall Motions in Circular Cylindrical Shells under Combined Loading," Ph.D. Thesis, Stanford University, Stanford, California, August 1968.

30. Ford, J. S., "Parametric Studies on the Stability of Stringer and Ring Reinforced Circular Shells," Ph.D. Thesis, Georgia Institute of Technology, Atlanta, Georgia, Nov. 1970.

31. Flügge, W., Stresses in Shells, Springer-Verlag, Berlin, 1960.

32. Horton, W. H. and Durham, S. C., "The Effect of Restricting Buckle Depth in Circular Cylindrical Shells Repeatedly Compressed to the Buckling Limit," SUDAER No. 174, Stanford University, Stanford, California, Sept. 1963.

33. Horton, W. H. and Cox, J. W., "The Stability of Thin-Walled Unstiffened Circular Cylindrical Shells Under Non-Uniformly Distributed Axial Load," SUDAER No. 220, Stanford University, Stanford, California, 1965.

34. Gregory, M., Elastic Instability: Analysis of Buckling Modes and Loads of Framed Structures, E. and F. N. Spon. Ltd., London, 1967.

35. Singhal, M. K., "Studies on the Elastic Stability of Bodies," Ph.D. Thesis in course of preparation, Georgia Institute of Technology, Atlanta, Georgia.

36. Sommerfeld, A., "Eine Einfache Vorrichtung Zur Veranschaulichung des Knikungsvorganges," ZVDI 1905, pp. 1320-1323.

37. Massonnet, C., Les Relations entre les Modes Normaux de Vibration et la Stabilité des Systèmes Élastiques, Goemaere, Bruxelles, Belgium, 1940.

38. Lurie, H., "Lateral Vibrations as Related to Structural Stability," J. Appl. Mech., June 1952, pp. 195-204.

39. Massonnett, C., "Le Voilement des Plaques Planes Sollicitées dans leur Plan," Final Report of the Third Congress of the International Association for Bridge and Structural Engineering, Liege, Belgium, Sept. 1948.

40. Roark, R. J., Formulas for Stress and Strain, McGraw-Hill, 1965.

41. Iwamoto, T., "The Effect of End Fixity on the Stability of Structures," Ph.D. Thesis, Georgia Institute of Technology, Atlanta, Georgia, September 1970.

VITA

Esam Eldin M. Nassar, the son of Mahmoud Nassar and Neamat Abdu-Allah, was born in Cairo in 1943.

He obtained the High School Diploma in 1959 from Abbassia High School. He earned the Bachelor of Engineering from Cairo University in July 1964. During his undergraduate study he attended various engineering training programs in W. Germany and Switzerland.

In August 1964 he was employed by the Egyptian General Aero-Organization as an Aircraft Designer. In 1966 he was awarded a study leave during which he earned the Diploma of Aircraft Design from Cranfield Institute of Technology in England. He joined Georgia Institute of Technology in 1969.

Presently he is appointed as an Assistant Professor of Mechanics, Mechanical and Aerospace Engineering at Illinois Institute of Technology.

In 1967 he married Hanem Elshibini. They have one son, Ayman.